

**ISTANBUL TECHNICAL UNIVERSITY ★ GRADUATE SCHOOL OF SCIENCE**  
**ENGINEERING AND TECHNOLOGY**

**ASSESSMENTS ON SURFACE INTERPOLATION METHODS FOR LOCAL GEOID  
MODELLING**

**M.Sc. THESIS**

**Onur KARACA**

**Department of Geomatics Engineering**

**Geomatics Engineering Programme**

**JUNE 2016**



**ISTANBUL TECHNICAL UNIVERSITY ★ GRADUATE SCHOOL OF SCIENCE**  
**ENGINEERING AND TECHNOLOGY**

**ASSESSMENTS ON SURFACE INTERPOLATION METHODS FOR LOCAL GEOID  
MODELLING**

**M.Sc. THESIS**

**Onur KARACA**  
**(501141623)**

**Department of Geomatics Engineering**

**Geomatics Engineering Programme**

**Thesis Advisor: Assoc. Prof. Dr. Bihter EROL**

**Co-Advisor: Assist. Prof. Dr. Georgios S. VERGOS**

**JUNE 2016**



**İSTANBUL TEKNİK ÜNİVERSİTESİ ★ FEN BİLİMLERİ ENSTİTÜSÜ**

**YEREL GEOİD MODELİNİN BELİRLENMESİNDE YÜZEY İNTERPOLASYON  
YÖNTEMLERİNİN ARAŞTIRILMASI**

**YÜKSEK LİSANS TEZİ**

**Onur KARACA  
(501141623)**

**Geomatik Mühendisliği Bölümü**

**Geomatik Mühendisliği Programı**

**Tez Danışmanı: Doç. Dr. Bihter EROL**

**Eş Danışman: Yard. Doç. Dr. Georgios S. VERGOS**

**HAZİRAN 2016**



Onur KARACA, a M.Sc. student of ITU Graduate School of Science Engineering and Technology student ID 501141623, successfully defended the thesis/dissertation entitled “ASSESSMENTS ON SURFACE INTERPOLATION METHODS FOR LOCAL GEOID MODELLING”, which he prepared after fulfilling the requirements specified in the associated legislations, before the jury whose signatures are below.

**Thesis Advisor:**        **Assoc. Prof. Dr. Bihter EROL**  
Istanbul Technical University

**Co-Advisor:**            **Assist. Prof. Dr. Georgios S. VERGOS**  
Aristotle University of Thessaloniki

**Jury Members:**        **Prof. Dr. Cengizhan İPBÜKER**  
Istanbul Technical University

**Jury Members:**        **Assoc. Prof. Dr. Himmet KARAMAN**  
Istanbul Technical University

**Jury Members:**        **Assoc. Prof. Dr. D. Uğur ŞANLI**  
Yildiz Technical University

**Date of Submission : 9 May 2016**  
**Date of Defense : 6 June 2016**





## **FOREWORD**

First and foremost, I would like to express my deepest gratitude to my supervisor Dr. Bihter Erol for her support and guidance throughout my master study. With her enthusiastic teaching style, and motivational speeches, she endeared me to Geodesy and even teaching along this period. I always knew that her office was always open to knock the door whenever I had problem about my thesis.

A significant part of this thesis was carried out at the School of Rural and Surveying Engineering (SRSE) at Aristotle University of Thessaloniki. It was a very productive and unforgettable five months in Thessaloniki with the opportunity that my co-supervisor Dr. Georgios S. Vergos provided me. I would like to thank him for his supervision, valuable comments and encouragements that made me motivated to complete this thesis.

The Istanbul GPS Triangulation Network - GPS/leveling data that are used in the thesis research was provided by Geodesy Division of Istanbul Technical University.

I would like to thank my professors, colleagues and dear friends at the Department of Geomatics who were together with me all the time and support me even in the most difficult and tiring periods of my education life.

Last but not least, this thesis wouldn't have been possible without the love and patience of my family; Faruk Karaca, Meliha Karaca and Senem Güner. As in every stage of my life, their endless support and even sometimes a glance showing their belief in me, gave me the strength in this thesis period. I would like to thank them for reminding me one more time I am the luckiest to have this lovely family.

May 2016

Onur KARACA



## TABLE OF CONTENTS

	<b>Page No</b>
<b>FOREWORD</b> .....	<b>v</b>
<b>TABLE OF CONTENTS</b> .....	<b>vii</b>
<b>ABBREVIATIONS</b> .....	<b>ix</b>
<b>LIST OF SYMBOLS</b> .....	<b>xi</b>
<b>LIST OF TABLES</b> .....	<b>xiii</b>
<b>LIST OF FIGURES</b> .....	<b>xv</b>
<b>SUMMARY</b> .....	<b>xvii</b>
<b>ÖZET</b> .....	<b>xix</b>
<b>1. INTRODUCTION</b> .....	<b>1</b>
1.1 Overview of Interpolation Methods .....	1
1.2 Local Geoid Modelling .....	3
1.3 Objective .....	6
<b>2. HEIGHT SYSTEMS AND GEOID MODELING METHODS</b> .....	<b>7</b>
2.1 Introduction, Theoretical Background and Type of the Height Systems .....	7
2.1.1 Geopotential numbers .....	7
2.1.2 Dynamic height.....	8
2.1.3 Orthometric height.....	8
2.1.4 Ellipsoidal height .....	10
2.1.5 Normal height .....	11
2.1.6 Relationships between height systems.....	11
2.2 Geoid Modelling Methods.....	13
2.2.1 The astro-geodetic geoid determination .....	14
2.2.2 The gravimetric geoid determination.....	16
2.2.2.1 Stokes function.....	16
2.2.2.2 Fast fourier transformation (FFT) .....	16
2.2.2.3 Geoid determination using numerical density method .....	17
2.2.3 The geopotential approach.....	17
2.2.4 The hybrid methods (remove - restore) .....	18



2.2.5 The GPS/leveling methods .....	20
<b>3. SURFACE INTERPOLATION METHODS.....</b>	<b>23</b>
3.1 Deterministic Interpolation Method .....	29
3.1.1 Inverse distance weighting (IDW) .....	29
3.1.2 Nearest neighbor (NN) .....	30
3.1.3 Triangulation with linear interpolation .....	32
3.1.4 Natural neighbor .....	33
3.1.5 Polynomial regression.....	34
3.1.6 Local polynomial .....	35
3.1.7 Radial basis function.....	36
3.1.8 Modified Shepard's method.....	37
3.1.9 Minimum curvature .....	38
3.1.10 Moving average .....	39
3.1.11 Biharmonic spline interpolation.....	39
3.2 Geostatistical Interpolation Method .....	40
3.2.1 Kriging .....	40
<b>4. NUMERICAL TEST.....</b>	<b>45</b>
4.1 Data Description .....	45
4.2 Pre-Analysis of Data.....	48
4.3 Data Gridding and Interpolation Results .....	51
<b>5. CONCLUSION.....</b>	<b>59</b>
<b>BIBLIOGRAPHY .....</b>	<b>63</b>
<b>APPENDICES .....</b>	<b>67</b>
<b>CURRICULUM VITAE.....</b>	<b>95</b>



## **LIST OF ABBREVIATIONS**

<b>COMPASS</b>	: Global Navigation Satellite System
<b>DTM</b>	: Digital Terrain Model
<b>ED50</b>	: European Datum 1950
<b>EGM08</b>	: Earth Gravitational Model 2008
<b>EGM96</b>	: Earth Gravitational Model 1996
<b>FFT</b>	: Fast Fourier Transformation
<b>GALILEO</b>	: The European Navigation Satellite System
<b>GLONASS</b>	: Global Navigation Satellite System
<b>GNSS</b>	: Global Navigation Satellite System
<b>GPS</b>	: Global Positioning System
<b>GRACE</b>	: Gravity Recovery and Climate Experiment
<b>GRS80</b>	: Geodetic Reference System 1980
<b>IDW</b>	: Inverse Distance Weighting
<b>IGNA2005</b>	: Istanbul GPS Triangulation Network 2005
<b>ITRF</b>	: International Terrestrial Reference Frame
<b>LSC</b>	: Least Squares Collocation
<b>MSL</b>	: Mean Sea Level
<b>NN</b>	: Nearest Neighbor
<b>TG</b>	: Turkey Geoid
<b>TG03</b>	: Turkey Geoid 2003
<b>TG07</b>	: Turkey Geoid 2007
<b>TG76</b>	: Turkey Geoid 1976
<b>TG91</b>	: Turkey Geoid 1991
<b>TG99A</b>	: Turkey Geoid 1999A
<b>THG09</b>	: Turkey Hybrid Geoid 2009
<b>TUDKA</b>	: Turkish National Vertical Control Network (TNVCN)
<b>TUTGA</b>	: Turkish National Fundamental GPS Network (TNFGN)
<b>RMSE</b>	: Root Mean Square Error
<b>SLR</b>	: Satellite Laser Ranging

**SST** : Sea Surface Topography  
**VLBI** : Very Long Base Interferometry  
**WGS84** : World Geodetic System 1984  
**WNN** : Wavelet Neural Network  
**RBF** : Radial Basis Function  
**ANN** : Artificial Neural Network  
**ANFIS** : Adaptive Neuro Fuzzy Inference System



## LIST OF SYMBOLS

<b>N</b>	: Geoid height
<b>h</b>	: Ellipsoidal height
<b>H</b>	: Orthometric height
<b>C<sub>P</sub></b>	: Geopotential number at point P on the Earth's surface
<b>W</b>	: Gravity potential of the Earth
<b>W<sub>0</sub></b>	: Gravity potential of geoid
<b>U</b>	: Normal potential of the reference ellipsoid
<b>g</b>	: Gravity
<b><math>\bar{g}</math></b>	: Mean gravity
<b>P</b>	: Point of Earth's surface
<b>P<sub>0</sub></b>	: Corresponding point of P on the geoid surface
<b>dn</b>	: Vertical differential differences
<b>H<sub>P</sub><sup>dyn</sup></b>	: Dynamic heights of point P
<b><math>\gamma</math></b>	: Normal gravity
<b><math>\bar{\gamma}</math></b>	: Mean normal gravity
<b>dH</b>	: Orthometric height differences
<b>k</b>	: Newton's gravitational constant
<b><math>\rho</math></b>	: Nominal density value
<b><math>\frac{\partial \gamma}{\partial h}</math></b>	: Normal gravity gradient
<b>H<sub>P</sub><sup>*</sup></b>	: Normal height of point P
<b><math>\zeta</math></b>	: Height anomaly
<b><math>\Delta g</math></b>	: Gravity anomaly
<b><math>\Delta g_B</math></b>	: Bouguer gravity anomaly
<b>N<sub>model</sub></b>	: Geoid height obtained from the model
<b><math>\xi</math> and <math>\eta</math></b>	: Vertical deflection components
<b><math>\varphi</math></b>	: Geodetic latitude
<b><math>\lambda</math></b>	: Geodetic longitude

$\phi(r_i)$	: Radial basis function
$R$	: Mean radius
$S(\Psi)$	: Stokes function
$T$	: Disturbing potential
$F$	: Fast Fourier Transformation
$F^{-1}$	: Inverse Fast Fourier Transformation
$x, y$	: Cartesian coordinates
$GM$	: Gravitational constant
$a$	: The biggest radius of reference ellipsoid
$P_{nm}(\cos\theta)$	: Normalized Legendre function
$C_{nm}, S_{nm}$	: Normalized global harmonic coefficients
$\Phi$	: Potential of centrifugal force
$N_R$	: Residual geoid height derived from Stokes integral
$\hat{z}(x_0)$	: Estimated value at the point in region of interest
$n$	: Number of sampled points
$z$	: Observed value at sampled point
$P_i$	: Weight assigned to the sampled points
$k$	: Power parameter
$d_i$	: Distance between $x_0$ and $x_i$
$\nabla^2$	: Laplacian operator
$\nabla^4$	: Biharmonic operator
$\phi_m$	: Green function
$m(x)$	: Constructional component
$\varepsilon'(x)$	: Auto-correlated residual from $m(x)$
$\varepsilon''$	: Random noise
$\gamma(h)$	: Semivariance
$C$	: First order effect of the variogram
$C_0$	: Nugget effect (random noise)
$m$	: Root mean square error (RMSE)
$m_{avera}$	: Average RMSE
$\sigma$	: Standard deviation
$\mu_i$	: Mean value of the evaluated residuals

## LIST OF TABLES

	<u>Page No</u>
<b>Table 2.1:</b> The definitions and characteristics of the height systems .....	<b>13</b>
<b>Table 3.1:</b> The main characteristics of interpolation methods.....	<b>26</b>
<b>Table 3.2:</b> Various variogram models .....	<b>43</b>
<b>Table 4.1:</b> Description of local Istanbul GPS/leveling network (IGNA2005) ....	<b>47</b>
<b>Table A.1:</b> The Cross Validation statistics .....	<b>68</b>
<b>Table A.2:</b> Interpolation statistics of discrete benchmarks from the different reference grid data using Linear Interpolation Approach.....	<b>70</b>
<b>Table A.3:</b> Interpolation statistics of discrete benchmarks from the different reference grid data using Nearest Neighbor Interpolation Approach..	<b>72</b>
<b>Table A.4:</b> Interpolation statistics of discrete benchmarks from the different reference grid data using Cubic Interpolation Approach.....	<b>74</b>
<b>Table A.5:</b> Interpolation statistics of discrete benchmarks from the different reference grid data using Spline Interpolation Approach.....	<b>76</b>



## LIST OF FIGURES

	<u>Page No</u>
<b>Figure 2.1:</b> Equipotential surface and geopotential number .....	8
<b>Figure 2.2:</b> The difference in lengths along the curved plumb line and the straight ellipsoidal normal .....	10
<b>Figure 2.3:</b> Relationship between orthometric and ellipsoid heights.....	10
<b>Figure 2.4:</b> Normal height, height anomaly, telluroid and quasi-geoid .....	11
<b>Figure 2.5:</b> The reference surfaces and height systems .....	12
<b>Figure 2.6:</b> Astrogeodetic leveling.....	15
<b>Figure 2.7:</b> Turkey Geoid 1991 (TG91) .....	17
<b>Figure 2.8a:</b> Turkey Geoid 1999A (TG99A) .....	19
<b>Figure 2.8b:</b> Turkey Geoid 2003 (TG03) .....	19
<b>Figure 2.8c:</b> Turkey Hybrid Geoid 2009 (THG09) .....	20
<b>Figure 2.9a:</b> Istanbul 2005 local GPS/leveling geoid .....	21
<b>Figure 2.9b:</b> Sakarya 2002 local GPS/leveling geoid model .....	21
<b>Figure 2.9c:</b> Çankırı 2005 locally improved TG03 geoid model.....	21
<b>Figure 2.9d:</b> Izmir 2001 local GPS/leveling geoid .....	22
<b>Figure 2.9e:</b> Istanbul 1999 local GPS/leveling geoid .....	22
<b>Figure 2.10:</b> Turkey regional GPS/leveling geoid .....	22
<b>Figure 3.1:</b> Isotherm map of South Africa on 15 April, 2009 at 11 am.....	24
<b>Figure 3.2:</b> Categorization of spatial interpolation methods.....	24
<b>Figure 3.3:</b> Categorization of spatial interpolation methods.....	25
<b>Figure 3.4:</b> The sampling design types .....	27
<b>Figure 3.5:</b> Inverse Distance Weighting Interpolation.....	29
<b>Figure 3.6:</b> The graphical illustration of the effect of distance on relative weight	30
<b>Figure 3.7:</b> Voronoi diagram.....	31
<b>Figure 3.8:</b> Delaunay triangulation .....	31
<b>Figure 3.9:</b> Examples of classified post map (on the left) and the contour map (on the right) that represent the interpolated grid nodes derived using the nearest neighbor interpolation method.....	31

<b>Figure 3.10:</b>	Planar surface.....	<b>32</b>
<b>Figure 3.11:</b>	The classed post map and the contour map examples which shows the interpolated grid nodes using Triangulation technique.....	<b>33</b>
<b>Figure 3.12:</b>	The classed post map and the contour map examples which illustrates the natural neighbor interpolation method .....	<b>33</b>
<b>Figure 3.13:</b>	The classified map and the contour map example base on the local polynomial interpolation method.....	<b>35</b>
<b>Figure 3.14:</b>	Radial Basis Functions for different locations .....	<b>36</b>
<b>Figure 3.15:</b>	The classed post map and the contour map example that represents the interpolation result belongs to Radial Basis Function (RBF) method .....	<b>37</b>
<b>Figure 3.16:</b>	The classed post map that represents the scattered elevation data, and the contour map that illustrates the result of Kriging method .....	<b>41</b>
<b>Figure 3.17:</b>	Variogram models: (a) Gauss, (b) linear, (c) spherical and (d) exponential models .....	<b>42</b>
<b>Figure 3.18:</b>	Variogram models .....	<b>43</b>
<b>Figure 3.19:</b>	The interpolation outputs of different interpolation methods for an sample data set.....	<b>44</b>
<b>Figure 4.1:</b>	The processes of numerical tests (step by step) .....	<b>46</b>
<b>Figure 4.2:</b>	Distribution of Istanbul GPS/leveling points on topography .....	<b>48</b>
<b>Figure 4.3:</b>	Istanbul GPS/leveling surface with blundered benchmarks .....	<b>48</b>
<b>Figure 4.4:</b>	Istanbul GPS/leveling surface after removing the blundered benchmarks .....	<b>49</b>
<b>Figure 4.5:</b>	Istanbul GPS/leveling surface .....	<b>50</b>
<b>Figure 4.6:</b>	Distribution of 1151 geoid reference points .....	<b>50</b>
<b>Figure 4.7:</b>	Distribution of 50 test points .....	<b>50</b>
<b>Figure 4.8:</b>	Distribution of reference and test benchmarks depending on topography .....	<b>51</b>
<b>Figure 4.9:</b>	The contour maps of Istanbul GPS/leveling geoid based on various gridding methods .....	<b>52</b>
<b>Figure B.1:</b>	The distribution of geoid undulation residuals at the test benchmarks depending on Linear Interpolation Algorithm .....	<b>78</b>
<b>Figure B.2:</b>	The distribution of geoid undulation residuals at the test benchmarks depending on Nearest Neighbor Interpolation Algorithm .....	<b>82</b>
<b>Figure B.3:</b>	The distribution of geoid undulation residuals at the test benchmarks depending on Cubic Interpolation Algorithm.....	<b>86</b>
<b>Figure B.4:</b>	The distribution of geoid undulation residuals at the test benchmarks depending on Spline Interpolation Algorithm .....	<b>90</b>

# **ASSESSMENTS ON SURFACE INTERPOLATION METHODS FOR LOCAL GEOID MODELLING**

## **SUMMARY**

The height information is crucial in many fields such as engineering surveying, flood management, coastal research, navigation, management of water sources, and risk analysis for earthquakes, etc. In parallel with the developments on satellite technology, obtaining ellipsoidal height using Global Navigation Satellite Systems (GNSS) provides practical, precise and quick solution in many applications and becomes widespread everyday. The ellipsoidal height does not answer the purposes for the applications that require spatial information. The height information, which has physical and uniquely defined, is used instead of ellipsoidal height. In this regard, orthometric height, which is defined according to geoid surface, is used in many countries. Geoid undulation is a connection while obtaining orthometric height information from ellipsoidal height.

Within the scope of this study, local geoid models are determined by using different interpolation techniques in order to obtain geoid height information with high accuracy that directly affects the precision of transformed orthometric height through GNSS. Although there is no regional geoid model within cm in Turkey yet, local GPS/leveling geoid is computed in limited areas based on Large Scale Map and Spatial Data Production Regulation (2005, article 42). In computing a local geoid models; beside the distribution, quality and density of the reference data, the employed surface interpolation technique has critical role in obtained accuracy of the model. Hence different interpolation algorithms are implemented in Istanbul area using Istanbul GPS Triangulation Network 2005 for determining grid based local geoid model.

In the content of research, the cross validation results belonging to the 12 interpolation techniques (Inverse Distance Weighting, Nearest Neighbor, Triangulation with Linear Interpolation, Natural Neighbor, Polynomial Regression, Local Polynomial, Radial Basis Function, Modified Shepard's Method, Minimum Curvature, Moving Average, Biharmonic Spline Interpolation, Kriging) are investigated in order to test the consistence of computed grid values within themselves. In the light of obtained results, it can be stated that linear interpolation results for all of the gridding methods except minimum curvature, polynomial regression (simple planar surface, bilinear saddle) and moving average reveal the best performance with a standard deviation of 5.5 cm and 6.0 cm. The performances of the determined grids are examined at the reference benchmarks and test benchmarks, respectively by employing linear, nearest neighbor, cubic and spline interpolation methods. As a linear interpolation result of these testing processes of grids, biharmonic spline interpolation method draws the attention as the most accurate method, whose standard deviation is 1.2 cm at the reference benchmarks and 3.2 cm at test benchmarks. This results show that generated geoid model data

can be used in all kind of engineering projects that require height information within cm accuracy.

In the evaluation of nearest neighbor interpolation at test points, the grid data that is obtained through natural neighbor method gives the most accurate result while moving average method gives the worst result. When considering cubic interpolation results, this can be said that triangulation with linear interpolation gives the best result; on the contrary, moving average gives the worst result. In the evaluation of spline interpolation results at test points, point Kriging (linear drift) and point Kriging (quadratic drift) give the best results. On the other hand, moving average has the worst standard deviation value.

As a result, this study proved that local GPS/leveling geoids, which are performed with available interpolation algorithms, can be used in order to obtain high accuracy geoid undulation. Combining this research with different data sets except geoid and computation algorithms such as finite element and soft computing methods is one of the main goals in the planned studies in future. Local GPS/leveling geoids provide short-term and limited solution for height transformation problem. Therefore, having a 1-2 cm accuracy regional geoid across the country is more viable solution for height control in GNSS applications.



## YEREL GEOİD MODELİNİN BELİRLENMESİNDE YÜZEY İTERPOLASYON YÖNTEMLERİNİN ARAŞTIRILMASI

### ÖZET

Mühendislik ölçmeleri, taşkın analizi ve planlama, kıyı araştırmaları, su kaynaklarının yönetimi, doğal afetler için risk analizi gibi alanlarda yükseklik bilgisi hayati önem taşımaktadır. Uydu teknolojilerindeki gelişmeler ile birlikte, hızlı ve pratik çözüm sağlayan Küresel Seyrüsefer Uydu Sistemleri'nden (GNSS) elipsoit yüksekliklerinin elde edilmesi, günden güne yaygın hale gelmektedir. Konumsal veriyle ilgili birçok uygulamada elipsoid yükseklikler ihtiyacı karşılayamamakta, bunun yerine fiziksel ve tek anlamlı olan nokta yükseklik bilgisine ihtiyaç duyulur. Bu bağlamda birçok ülkede geoid yüzeyine göre tanımlanan ortometrik yükseklikler kullanılmaktadır. Geoid interpolasyonları, elipsoit yüksekliklerinden ortometrik yüksekliklerin elde edilmesinde kullanılan bir bağlantıdır.

Bu çalışma kapsamında, ortometrik yüksekliklerin doğruluğunu etkileyen prezyonlu geoid yüksekliklerini elde etmek için farklı interpolasyon tekniklerini kullanarak yerel geoid modelleri oluşturulmuştur. Türkiye'de santimetre (cm) doğrulukta bölgesel bir geoid modeli henüz mevcut olmadığından dolayı, Büyük Ölçekli Harita ve Harita Bilgileri Üretim Yönetmeliği'ne dayanarak (2005, madde 42), sınırlı alanlarda GPS/Nivelman geoidi hesaplanarak kullanılabilir. Yüksek doğruluklu yerel geoid modelleri hesaplamak için; verinin dağılımı, yoğunluğu ve kalitesinin yanında modelin doğruluğunu etkileyen faktörlerden biri olan farklı interpolasyon yöntemleri, bu çalışma kapsamında İstanbul GPS/Nivelman 2005 (IGNA 2005) verilerini kullanarak geoid modelleme amacıyla uygulanmıştır.

Sayısal testlerde, üretilen grid değerlerinin kendi içlerindeki tutarlılığını test etmek için 12 interpolasyon tekniğine ait çapraz test sonuçları değerlendirilmiştir. Bu çalışmalar ışığında belirtilebilir ki; en küçük eğrilikli yüzey interpolasyonu (minimum curvature), polinomlarla regresyon (polynomial regression- simple planar surface, bilinear saddle) ve hareketli ortalama (moving average) yöntemleriyle oluşturulan gridler hariç tüm gridlerin lineer interpolasyon sonuçlarına ait standart sapma değerleri 5.5 cm ile 6.0 cm arasında değişmektedir. Lineer (linear), en yakın komşu (nearest), kübik (cubic) ve spline interpolasyon yöntemlerini kullanarak, gridlerin referans ve test noktalarındaki performansları sırayla test edilmiştir. Bu test çalışmalarının sonucunda lineer interpolasyon sonuçları değerlendirildiğinde, referans noktalarında 1.2 cm ve test noktalarında 3.2 cm doğruluğa sahip biharmonic spline interpolasyon yöntemi, en doğruluklu yöntem olarak dikkat çekmektedir. Bu sonuçlar, üretilen modelin 5 cm'nin altında doğruluklu yükseklik bilgisi gerektiren mühendislik uygulamalarında da kullanılabileceğini göstermektedir.

Test noktalarında en yakın komşu (nearest neighbor) metodu ile elde edilen interpolasyon verilerinin istatistikleri değerlendirildiğinde, hareketli ortalama (moving average) yöntemi en kötü sonucu verirken, en yakın komşuluk (nearest neighbor) yöntemi en iyi sonucu vermektedir. Test noktalarında kübik interpolasyon sonuçları değerlendirildiğinde, üçgenlemeye dayalı doğrusal interpolasyon

(triangulation with linear interpolation) metodunun en iyi sonucu verdiđi söylenebilir. Buna karşılık, hareketli ortalama (moving average) en kötü sonucu vermektedir. Test noktalarında yapılan spline interpolasyon sonuçları değerlendirildiğinde, en iyi sonucu noktasal Kriging- doğrusal drift (linear drift) ve noktasal Kriging- kuadratik drift (quadratic drift) yöntemleri vermektedir. Diğer taraftan, hareketli ortalama en yüksek standart sapma değerine sahiptir.

Sonuç olarak, bu çalışma uygun interpolasyon algoritmalarıyla yüksek doğruluklu (bir kaç santimetre doğruluklu) geoit ondülasyonlarının elde edilmesi için uygun sıklıkta ve dağılımda yerel GPS/Nivelman geoitlerinin kullanılabileceğini kanıtlamıştır. Bu çalışmanın geoit yüksekliklerinin dışında da farklı mekansal veri gruplarıyla ve esnek hesaplama, sonlu elemanlar gibi farklı hesaplama yaklaşımları ile birleştirilmesi, gelecekte gerçekleştirilmesi planlanan çalışmalardır. Yerel GPS/Nivelman geoitleri yükseklik dönüşümü sorununa sınırlı ve kısa süreli çözüm sağlamaktadır. Bu nedenle tüm ülkeyi kapsayan prezisyonlu bölgesel bir geoit modelinin hesaplanması ve kullanıma sunulması gerekmektedir.

# 1. INTRODUCTION

## 1.1 Overview of Interpolation Methods

The importance and urgency of spatial information, which states location, size etc. of an object in space, is increasing everyday in many fields such as engineering, management and risk analysis parallel to the technological progresses. Although this is hard to obtain spatial continuous data at every point in region of interest; due to restrictions of time, money, and geological conditions etc., spatial interpolation techniques are required and performed. Interpolation process can be described as an assumption of obtaining approximate values at unknown unsampled locations for any geographic point by using known sample data (Robeson, 1997).

Spatial interpolation has been applied in many disciplines such as, geodesy, geophysics, civil engineering, water resources, meteorology, mathematics, marine science and agriculture etc. Specific applications under those disciplines are many such as mine exploration, climate change investigation, crustal deformation monitoring, classification of soil properties, population density modelling, digital terrain model (DTM) generation and use, chemical concentration modelling, soil Ph or moisture estimation and so on (Li and Heap, 2008).

There are many spatial interpolation methods and those methods are classified in different ways in the literature. Siu and Lam (1983) classifies interpolation methods as Point and Areal Interpolation. Sen and Srivastava (1990) states that interpolations are grouped into three methods as *i-*) point wise, *ii-*) global and *iii-*) piece wise. Mitas and Mitsova (1999) classifies interpolation methods as local neighborhood, geostatistical and variational approaches.

Interpolation methods are grouped into three as non-geostatistical methods, geostatistical methods and combined methods, by Li and Heap (2008). Some features that are used to distinguish interpolation methods can be described as follows:

In *global* interpolation, all of the spatial data in application area are used to obtain information about unknown point. Contrary to global interpolation, small samples around point being estimated are used in *local* interpolation. In *exact* interpolation, the estimated value of the point is the same value as its known value. On the contrary, the estimated value of the point and its known value are different from each other in *inexact* interpolation method.

There is no error computations belong to estimated value in *deterministic* methods, whereas there is error computations in *stochastic* methods belong to estimated value.

According to Olea (1999), the “*Geostatistics* can be regarded as a collection of numerical techniques that deal with the characterization of spatial attributes, employing primarily random models in a manner similar to the way in which time series analysis characterizes temporal data”.

If the techniques employ secondary information in geostatistics, they are described as *multivariate*; if not, they are described as *univariate* geostatistical techniques. The general name of this category is referred as Kriging method. In *combined* procedure, spatial interpolation methods and other statistical approaches are used together (Li and Heap, 2008). The details of the methods that are used in this study are described with details in following chapters.

It is crucial to perform an optimal method for data interpolation in an application. Furthermore, while choosing an optimal methods, the factors that affect the performance of the spatial interpolation methods should be considered. These factors include data density, surface type, sample size and design, data quality, scale, variance and accuracy of the data (Li and Heap, 2008). Most of the methods give the same results if the data is sufficiently dense. On the other hand, deciding an appropriate interpolation method becomes crucial when the data has low density. Otherwise, interpolation methods give better results when the data get dense.

When the surface types are taken into consideration, it can be said that discontinuity in the surface causes poor results in interpolation. As mentioned before, the sample size and design are crucial for the type of spatial interpolation methods. The low data noise decreases the grid size (scale) and hence may cause better result for interpolation process. The performance of the interpolation methods decreases when the variation of data increases (Li and Heap, 2008). As a last factor which affects the

performance of spatial interpolation can be described as its sampling within the region of interest. The sampling can be regular, random, stratified random, cluster, transect and contour type.

## 1.2 Local Geoid Modelling

In parallel to technological development, Global Navigation Satellite Systems (GNSS) have significant role in geodetic and surveying applications. The observable data from GPS, leveling and geoid information have significant role for geodetic height control (Kavzoglu and Saka, 2005). The height of a point can be obtained with traditional leveling measurements but height transformation using GPS and a geoid model is faster, easier, cheaper and practical in order to obtain orthometric height.

The heights are described as the geometrical and physical relation in vertical between the point position and a reference surface. Ellipsoid is the geometrical shape of the Earth while Geoid is formed under topographical density and molar dispersal of ground irregularity. According to Heiskanen and Moritz (1967), “the *geoid* is a surface of a constant gravity potential and coincides with the mean sea level after removing the effect of sea surface topography over the oceans “.

There is a simple geometrical relationship between the heights, which refer different reference surfaces, ignoring the vertical deflection of plumbline;

$$h - H - N = 0 \quad (1.1)$$

where  $H$  is the orthometric height,  $h$  is the ellipsoidal height, which is the vertical distance between the point on the Earth and the ellipsoid that can be obtained from GPS, and  $N$  is the geoid height that is the distance between geoid and ellipsoid along ellipsoidal normal. Ellipsoidal height is a geometrical value and may not serve in practical purposes adequately. Therefore, in most high precision surveying and engineering applications, orthometric height, which is the distance from the point on Earth to the geoid along plumb line, is employed. The first way of obtaining orthometric height is performing geometric leveling measurements based on a control point, which has known height information, and applying the gravimetric corrections on that measurement results. Second way is transforming ellipsoidal height derived from GPS to orthometric height by using geoid height. Since geoid height affects the accuracy of orthometric height, determination of geoid model has a

key role in surveying applications (Yıldız, 2012). It can be said under these statements above that the local geoid model with higher accuracy means higher accurate geoid height and thus the orthometric height via GNSS.

It is hard to make measurements for obtaining heights in whole region of interest, therefore; interpolation methods, which are used to perform geoid model, are effective tools for estimation of heights belong to unknown points. The distribution of the reference data, topographical character of region and interpolation method affect directly the accuracy of the derived height from the geoid model (Erol, 2007).

Geoid models are mainly divided into three groups such as global (EGM96, OSU91, etc.), regional (TG03, TG07, etc.) and local (Istanbul 1999 local GPS/leveling geoid, etc). Global geoid models do not provide high accuracy for surveying applications - accuracy is around 0.5 meter in Turkey - while local models may give results with higher accuracy (Ayar, 2009). Evaluating the geoid models in Turkey constitutes the initial objective of this study, therefore, a brief history of the geoid modelling studies in Turkey are given following (Erol, 2007; Yıldız, 2012). 1976 is the starting date of the studies of geoid determination in Turkey. For this preliminary study, Ayan (1978) and Gürkan (1978) performed Astrogeodetic Geoid (TG-76) by using astrogeodetic deflection at ED50 datum. After that South-Western Anatolia Doppler Geoid was performed in 1987 with developments in GNSS technology (Ayhan et al., 1987). In 1991, General Command of Mapping employed Turkish Gravimetric Geoid (TG-91), which was estimated with remove-restore technique, by using earth geopotential model, DTM (digital terrain model) and gravity observations.

Due to the fact that there are differences between orthometric heights which were derived from TG-91 Geoid and geometric leveling based on Turkish National Vertical Control Network (TUDKA or TNVCN). Therefore, 197 Turkish National Fundamental GPS Network (TUTGA-99 or TNFGN-99) benchmarks were connected to Turkish National Vertical Control Network 1999 (TUDKA-99 or TNVCN-99) via leveling measurements. Consequently, GPS/leveling geoid was determined (Ayar, 2009). It was investigated that there are differences such as slope and offsets in long wavelength between TG-91 Geoid and GPS/leveling geoid. In order to solve datum discrepancies, Turkey Geoid 1999A (TG99A) were employed by combining TG-91 and GPS/leveling geoid. The internal accuracy of TG99A is 10 cm while external accuracy is 15 cm (Direnç et al., 2012). Relying on the assessment

results in small areas, the General Command of Mapping reported that the accuracy of TG99A Geoid model is sufficient for small scale mapping applications.

As the updated version of TG99A geoid, the new geoid, which is named as Turkey Geoid 2003 (TG03), was released. For this purpose, EGM96 global geopotential model, 62 500 gravity measurements, which were used in the computation of TG91 gravimetric model, and gravity anomalies derived from altimetry data were operated via least squares collocation (LSC). Although the geoid heights of GPS/leveling benchmarks are different, the accuracy of this geoid is in decimeter level (Yıldız, 2012; Erol, 2007). By using a geopotential model which was derived from the combination of EGM96 global geopotential model and GRACE GGM02S global geopotential model, digital elevation model derived from SRTM-3 (Shuttle Radar Topography Mission-3) and KMS02 gravity anomalies; Turkey Geoid 2007 (TG07) were computed that has  $\pm 8.8$  cm accuracy (Yıldız, 2012). Finally, Turkish Hybrid Geoid 2009 (THG-09), which has  $\pm 9$  cm accuracy, were performed by using surface gravity observations, DTM (Digital Terrain Models) and EGM08 earth gravitational model and satellite altimetry (URL-1).

The accuracy of recent geoid model in Turkey (THG-09) is still not good enough ( $\pm 9$  cm), therefore; local geoid models are required and determined with higher accuracy in limited area. For this purpose, appropriate corrections are done by using leveling points in densification area. This procedure leads to determine GPS/leveling points in region of interest to determine geoid heights. Currently vertical control is provided relying on the Turkish National Vertical Control Network (TUDKA). However, the TUDKA benchmarks disappear due to structuring, enlargement works on roads and tectonic motions on crust. Considering all of these, it can be said that height system in Turkey needs to be modernized. The term of modernization means identifying new viable vertical datum. Modernization process can be realized by using three methods which are stated below (Türkezer et al., 2011).

- Regeneration of whole leveling network
- Recovering geoid and regeneration of some leveling network
- Recovering geoid and using that as a vertical datum

Even if regeneration of the whole leveling networks, which requires much time and money, are chosen for modernization process, the determination and use of local

geoid continues to provide the optimal solution until re-establishment of height system is constituted all over the country.

### **1.3 Objective**

The aim of this thesis is performing an optimal local geoid model with 1204 GPS/leveling points by using different interpolation methods in order to obtain high accurate geoid heights. As stated in overview of introduction chapter, ellipsoidal heights derived from GPS are transformed to orthometric heights via geoid heights. Since the accuracy of Turkey Geoid is not sufficient, developing and employing local geoid model has a significant role in many geodetic applications require centimeter accuracy in heights.

This thesis consists of five chapters. In Chapter 1, mainly, the preliminary information about geodetic terms, theoretical background, and the aim of the thesis are asserted. In order to give this chapter more explicitly; definitions, methods and examples of spatial interpolation methods are given. Identification of geoid, ellipsoidal and orthometric heights, history of geoid determination studies in Turkey, ongoing modernization of height systems, the importance of local geoid models for vertical control in Turkey are realized in details.

Height systems and geoid modelling methods are identified in Chapter 2. The first part of this chapter starts with the definition of height systems and vertical datum. In the second part of the chapter, geoid modelling methods in general are provided.

In Chapter 3, surface interpolation methods, which are specifically Biharmonic Spline, Inverse Distance to a Power, Kriging, Minimum Curvature, Modified Shepard's Method, Natural Neighbor, Nearest Neighbor, Polynomial Regression, Radial Basis Function in addition to Triangulation with Linear Interpolation, Moving Average and Local Polynomial, are described and explained.

The experiment set-up and numerical tests are described in Chapter 4. Istanbul 2005 GPS/leveling data is used in the study and defined briefly under the chapter. Data descriptions, pre-processes of data such as blunder detection procedure are explained and the numerical results of data interpolation processes are described in Chapter 4. In the last part, which is Chapter 5, the results of the numerical tests and interpolations are assessed and interpreted.



## 2. HEIGHT SYSTEMS AND GEOID MODELLING METHODS

### 2.1 Introduction, Theoretical Background and Type of the Height Systems

The height information is crucial in many applications such as engineering survey, flooding management, coastal research, navigation, management of water sources, and risk analysis for earthquakes. The height of a point with respect to a reference surface can be described relying on different height systems. The reference surface for describing the height of a point is called as vertical datum and these can be geoid, quasi-geoid, ellipsoid and mean sea level (MSL). The level surface of the gravity field of earth (such as geoid) and mean sea level do not fit each other. Furthermore; the difference between MSL and geoid is called as sea surface topography (SST). The mean sea level is obtained via the average level of ocean surface (Torge, 2001; Erol, 2007).

As stated in the beginning of this chapter, there are different height systems based on chosen reference surface in order to obtain height information. The height systems that are geopotential numbers, dynamic heights, orthometric heights, ellipsoidal heights normal heights; and relationship among them are identified and illustrated in the following.

#### 2.1.1 Geopotential numbers

Due to the fact that height differences, which are obtained from leveling, are dependent to the path; gravity potential can be used since the potential differences between points are independent from the leveling path, consistent and only one surface with  $W$  potential passes from a point. The difference in potential among geoid and equipotential surface is defined as geopotential number, furthermore; the geopotential of the point  $P$  on the Earth's surface  $C_P$  is identified below;

$$C_P = W_0 - W_P = \int_{P_0}^P g dn \quad (2.1)$$

where  $W_0$  is the constant potential value at geoid, P is the point at the Earth's surface and  $W_P$  is its potential,  $P_0$  is the point on the geoid (Erol, 2007; Ince, 2011).

The unit of geopotential number is  $m^2/sn^2$ . Leveling equipotential surfaces are illustrated in Figure 2.1.

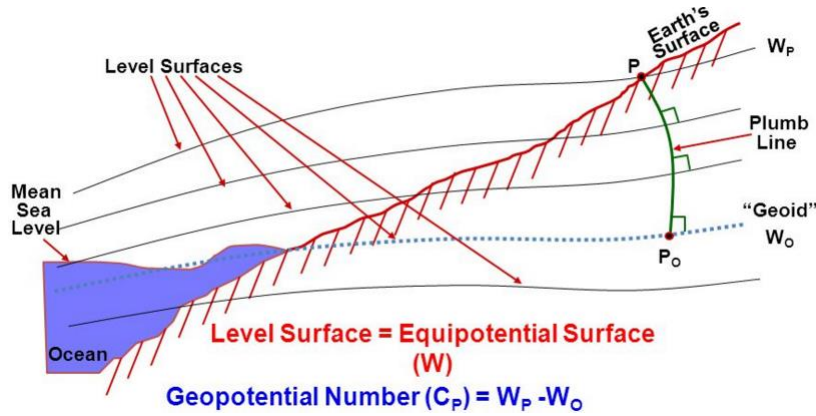


**Figure 2.1:** Equipotential surface and geopotential number (Roman, 2007).

### 2.1.2 Dynamic height

Owing to the fact that the unit of geopotential number  $m^2/sn^2$  is not coherent with length unit, dynamic heights whose formula is given in 2.2 are performed.

$$H_P^{dyn} = \frac{C_P}{\gamma_0} \quad (2.2)$$

where  $\gamma_0$  is normal gravity for fixed latitude which is usually taken as  $45^\circ$ . Dynamic height does not have precise geometric clarification. Moreover, dynamic heights on the same equipotential surfaces are the same but geometrical distances are different from each other (Torge, 2001).

### 2.1.3 Orthometric height

The orthometric height is the distance between geoid and the point located on the Earth's surface along plumb line, and described by;

$$H_P = \frac{C_P}{\bar{g}_P} \quad (2.3)$$

where  $\bar{g}_P$  is the average value of the gravity through plumb line and obtained by the following formula below;

$$\bar{g}_P = \frac{1}{H_P} \int_{P_0}^P g dH \quad (2.4a)$$

Practically, this is not possible to obtain  $\bar{g}_P$  since the mass density along plumb line is unknown. Therefore, orthometric heights are linked to approximation on calculation of the mean value of gravity. Furthermore, the value of  $\bar{g}_P$  is obtained by using different models such as Helmert that is the most popular method and based on Poincaré Prey reduction model (Erol, 2007).

In practice, the mean gravity value is performed as follows;

$$\bar{g}_P = g_P - 2\pi k\rho H_P + \frac{1}{2} \frac{\partial \gamma}{\partial h} H_P \quad (2.4b)$$

where nominal density value is  $\rho = 2.67 \text{ g/cm}^3$ , normal gravity gradient is:

$$\frac{\partial \gamma}{\partial h} = 0.3086 \text{ mGal/m} \quad (2.4c)$$

and  $k$  is the Newton's gravitational constant ( $66.7 \times 10^{-9} \text{ cm}^3 \text{ g}^{-1} \text{ sec}^{-2}$ ). When these values are replaced in the formula, the recent view takes place as below;

$$\bar{g}_P = g_P + 0.0424 H_P \quad (2.4d)$$

By combining the formula above and the formula belongs to orthometric height, Helmert orthometric heights are performed as stated below;

$$H_P = \frac{C_P}{g_P + 0.0424 H_P} \quad (2.5)$$

The given equation is solved via iterations since  $H_P$  is a necessity in order to obtain mean gravity through plumb line (Hofmann-Wellenhof and Moritz, 2005; Jekeli, 2000).

As asserted so far, the distance between geoid and the point on the Earth's surface through plumb line is referred as orthometric height (Pizetti's projection). On the other hand, the distance through ellipsoidal normal instead of plumb line stated as orthometric height in order to obtain orthometric height simpler (Helmert's projection). This simplification process leads to errors and these errors are ignored

for the topographic heights on the Earth's surface (Jekeli, 2000; Erol, 2007). The vertical deflection between plumb line and ellipsoidal normal referred as  $\theta$  can be seen in the Figure 2.2.

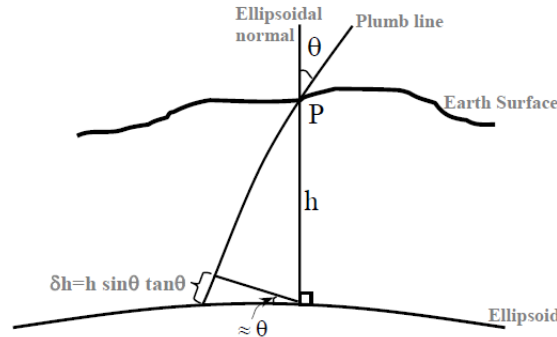


**Figure 2.2:** The difference in lengths along the curved plumb line (orthometric height,  $H$ ) and the straight ellipsoidal normal (Erol, 2007).

#### 2.1.4 Ellipsoidal height

Ellipsoidal height ( $h$ ) is the distance from a point on the Earth's surface to the ellipsoid along ellipsoid normal. Nowadays, ellipsoidal heights can be employed from different ways that are satellite laser ranging (SLR), very long base interferometry (VLBI), global navigation satellite systems (GNSS) (Erol, 2007).

The Figure 2.3 shows the relationships between ellipsoidal, orthometric and geoid heights.

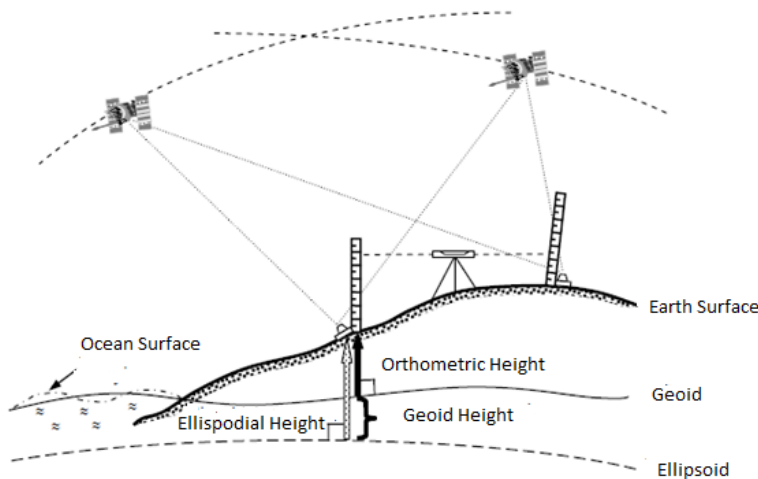


**Figure 2.3:** The relationship between orthometric and ellipsoidal heights (Yılmaz and Arslan, 2006).

### 2.1.5 Normal height

Normal height is the distance between the point on the Earth's surface and quasi-geoid. That is employed led by Molodensky with the thought that orthometric height cannot be employed theoretically. The normal height is obtained by using following equation;

$$H_p^* = \frac{C_p}{\bar{\gamma}_p} \quad (2.6)$$

where  $\bar{\gamma}_p$  is the mean normal gravity value along plumb line, R is the point on the telluroid where  $U_R = W_p$  (see Figure 2.5).  $H^*$  is the normal height of the point P on Earth's surface, and  $\zeta_p$  is the height anomaly at point P which is the difference between ellipsoidal height and normal height. The surface that is  $\zeta_p$  upside of the ellipsoid is referred as quasi-geoid. (Hofmann-Wellenhof and Moritz, 2005; Jekeli, 2000; Ince, 2011). Figure 2.4 shows the components of normal height.

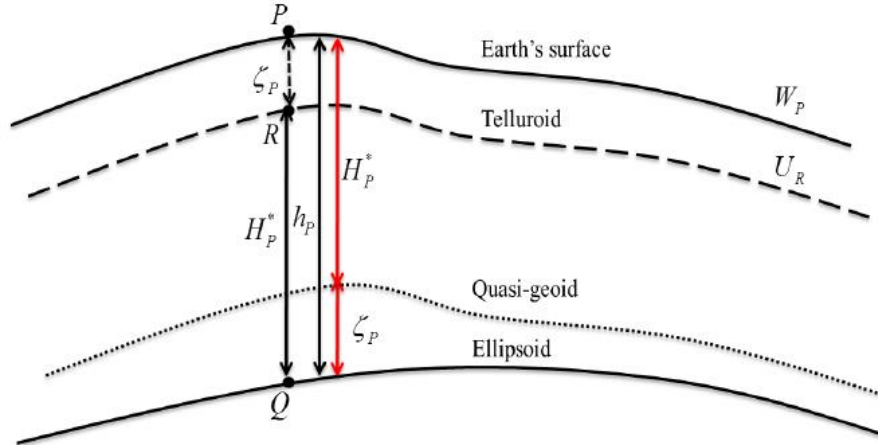


**Figure 2.4:** Normal height, height anomaly, telluroid and quasi-geoid (Ince, 2011).

### 2.1.6 Relationships between height systems

There is a connection between height systems via geopotential number. By using equations belong to Helmert orthometric heights  $H_p = \frac{C_p}{g_p + 0.0424H_p}$  and orthometric heights  $H_p^* = \frac{C_p}{\bar{\gamma}_p}$ , the following equations can be computed;

$$h_p = H_p + N = H_p^* + \zeta_p \quad (2.7)$$

and

$$N - \zeta_P = H_P^* - H_P = \frac{\bar{g} - \bar{\gamma}}{\bar{\gamma}} H_P \approx \frac{\Delta g_B}{\bar{\gamma}} H_P \quad (2.8)$$

where  $\Delta g_B$  represents the Bouguer gravity anomaly. Although both of the orthometric and normal heights are stated geometrically; computation of normal height can be employed by using information about mass density while orthometric height cannot be employed. In contrast to dynamic heights, all other height systems don't have physical meaning (Ince, 2011).

The reference surfaces and height systems are given in the Figure 2.5 following.

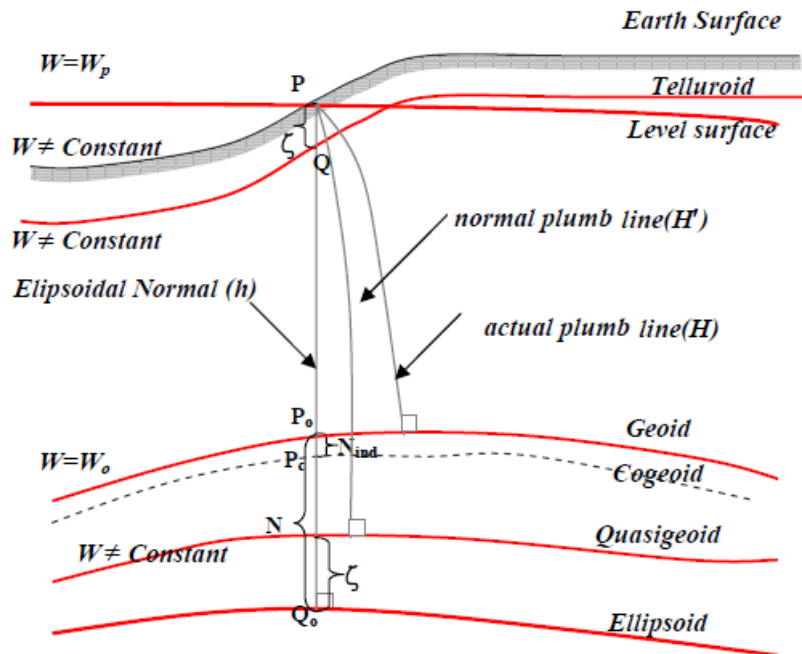


**Figure 2.5:** The reference surfaces and height systems (Erol, 2007).

In the light of the foregoing information mentioned so far, the definitions and characteristics of the height systems are summarized in Table 2.1 following.

**Table 2.1:** The definitions and characteristics of the height systems (Ince, 2011).

Height Type	Definition	Meaning	Usage/ Characteristic
Ellipsoidal height	$h_p$	Geometrically meaningful.	Geometrically defined along the perpendicular to the ellipsoid.
Dynamic height	$H_p^{\phi^n} = \frac{C_p}{\gamma_0}$	Physically meaningful and associates with a value computed at a fixed latitude.	Indicates the direction of water flow.
Orthometric height	$H_p = \frac{C_p}{\bar{g}_p}$	Geometrically meaningful and cannot be determined exactly.	The distance along the plumb line between the geoid and point on the Earth's surface. The calculation requires the complete knowledge of the mass density of the crust.
Normal height	$H_p^* = \frac{C_p}{\bar{\gamma}_p}$	Geometrically meaningful and can be determined exactly.	The distance between the quasi-geoid and the point on Earth's surface. There is no need to make approximations for the density of the Earth's crust.
Normal-orthometric height	$H_p^{no} = \frac{C^n}{\bar{\gamma}}$	Approximates to either orthometric or normal heights.	Makes use of normal geopotential number. It is not compatible with geoid or quasi-geoid.
Geoid height	$h_p - H_p = N_p$	The separation between the geoid and the reference ellipsoid.	Used in the conversion of the geometrically defined heights into physical heights.
Height anomaly	$h_p - H_p^* = \zeta_p$	The separation between the quasi-geoid and the reference ellipsoid.	Approximation of the geoid undulation according to the Molodensky's theory.

## 2.2 Geoid Modelling Methods

The aim of the geoid determination is obtaining geoid heights (N), which are natural connection between orthometric heights obtained from leveling and ellipsoidal heights derived from satellite positioning technologies. The geoid heights have lower accuracy than ellipsoidal heights, therefore; determining a precise geoid model is critical to get orthometric heights using global positioning satellite system hence the satellite positioning system is used more efficiently. Geoid models can be used in local, global and regional areas. Furthermore, the accuracy of model is dependent to topography, characteristics (density and distribution) of the reference data and modelling technique. The validation of regional geoid models can be controlled with geoid height differences that are derived from GPS/leveling and model at co-located benchmarks (see equation below) (Erol, 2007).

$$\Delta N = h - H - N_{\text{model}} \quad (2.9)$$

Geoid determination methods are classified below based on the computation method and data used in calculations (Yılmaz and Arslan, 2006):

- I) The Astro-Geodetic Geoid Determination
- II) The Gravimetric Geoid Determination
  - a) Stokes Function
  - b) Fast Fourier Transformation
    - 1 Dimensional (1D-FFT)
    - 2 Dimensional (2D-FFT)
    - Geoid Determination According to Numerical Density Method
- III) The Geopotential Approach
- IV) The Hybrid Method (Remove - Restore)
- V) The GPS/Leveling Methods
  - a) The polynomials method
  - b) The fuzzy logic method
  - c) The artificial neural network
  - d) Etc. (interpolation methods used in numerical test of the thesis)

### 2.2.1 The astro-geodetic geoid determination

Geoid height can be obtained by using vertical deflections. Ellipsoidal latitude and longitude have to be in a reference geodetic datum (e.g ITRF96 datum referring to GRS80 ellipsoid) in order to define astro-geodetic geoid. The change on geoid height in ds distance can be calculated as following;

$$dN = -\varepsilon ds \quad (2.10)$$

where  $\varepsilon$  is deflection and calculated with the equation below;

$$\varepsilon = \xi \cos\alpha + \eta \sin\alpha \quad (2.11)$$



$\xi$  and  $\eta$  are components of deflection and  $\alpha$  is the azimuth. The figure 2.6 belongs to Astrogeodetic Leveling can be seen below.

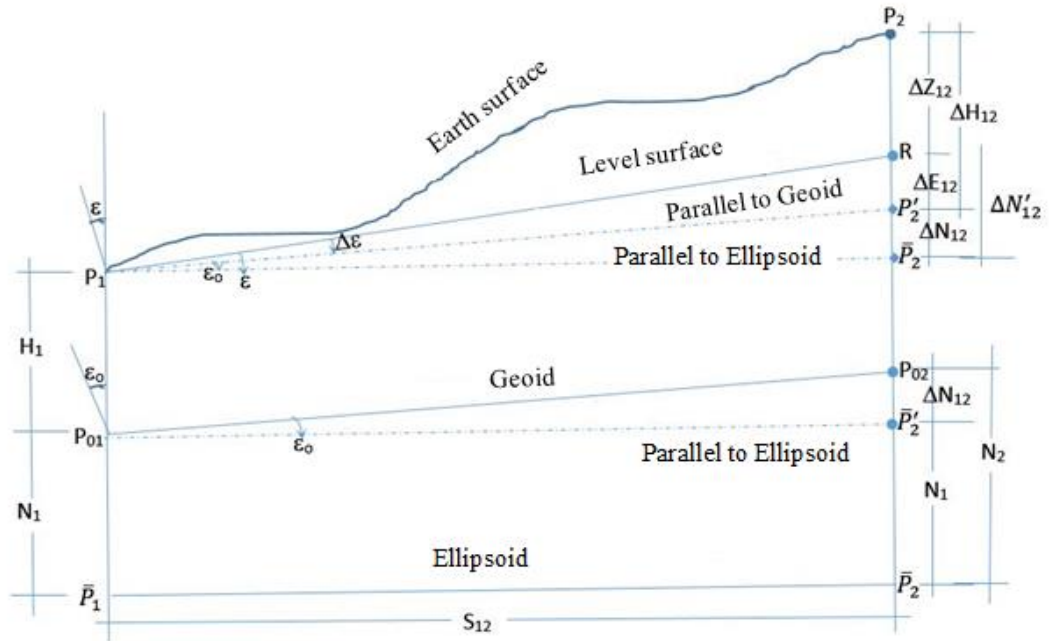


**Figure 2.6:** Astrogeodetic Leveling (Deniz and Ayan, 2002)

The formula to calculate deflection components are given following.

$$\xi = \Phi - \varphi, \eta = (\Lambda - \lambda)\cos\varphi \quad (2.12)$$

In the equation above,  $\Phi$  and  $\Lambda$  are astronomic coordinates while  $\varphi$  and  $\lambda$  are geodetic latitude and longitude. The change of geoid heights in a distance between A and B points can be calculated if the geoid height at starting point A is known. Furthermore, the geoid height at B can also be calculated with the integral below;

$$N_B = N_A - \int_A^B \epsilon ds \quad (2.13)$$

As can be seen in the formulas above, astronomic and geodetic coordinates are used together in order to identify geoid, that's why this method is referred as astrogeodetic.

Sparse data requirement to determine high precision geoid model in astrogeodetic levelling makes this method more efficient and economical. Determining a geoid that

has 2-5 cm accuracy, 50-500 gravity points in 1000 km<sup>2</sup> are required while only 5-15 astronomic points are enough (Yılmaz and Arslan, 2005).

## 2.2.2 The gravimetric geoid determination

### 2.2.2.1 Stokes function

Geoid heights can be computed by using Stokes integral which is the way to transform gravity data collected at the Earth's surface to geoid heights. It based on an assumption that there is no any mass outside of the geoid; therefore the Earth's surface is eliminated mathematically. The disturbing potential (T), as the difference between the normal potential of the reference ellipsoid (U) and the gravity potential of the Earth (W):

$$T = \frac{R}{4\pi} \iint_{\sigma} \Delta g S(\Psi) d\sigma \quad (2.14a)$$

where R is the mean radius,  $\sigma$  is Earth's surface, S( $\Psi$ ) is the Stokes function. If the same normal potential is chosen for reference ellipsoid (U) and gravity potential on Earth (W), the relationship between disturbing potential (T), normal gravity on reference ellipsoid ( $\gamma$ ) and geoid height (N) can be created as following (Yılmaz and Arslan, 2005);

$$T = \gamma \cdot N \quad (2.14b)$$

Hence the geoid height can be obtained through the following formula of Bruns;

$$N = \frac{T}{\gamma} = \frac{R}{4\pi} \iint_{\sigma} \Delta g S(\Psi) d\sigma \quad (2.15)$$

### 2.2.2.2 Fast fourier transformation (FFT)

FFT is a productive evaluation of convolution integrals in contrast to classical numerical integration and decrease the time of computation for large dataset. The geoid height (N) can be obtained by using global geopotential model and residual gravity anomalies ( $\Delta g$ ) as shown below (Yılmaz and Arslan, 2005; Ghanem and Jiancheng, 2000).

$$N^{\Delta g}(x_k, y_l) = \frac{\Delta x \Delta y}{2\pi y} F^{-1} \{ F \{ \Delta g(x_k, y_l) \} F \{ 1_N(x_k, y_l) \} \}$$

$$= \frac{\Delta x \Delta y}{2\pi y} F^{-1} \{ \Delta G(u_m, v_n) L_N(u_m, v_n) \} \quad (2.16)$$

where  $F$  is 2D Fast Fourier Transformation,  $F^{-1}$  is inverse Fast Fourier Transformation and  $u$ - $v$  are the frequencies corresponding to  $x$ - $y$ .

The Turkey Geoid 1991 (TG-91) can be given as an example that was calculated using gravimetric method and FFT computations (see the TG-91 in Figure 2.7).

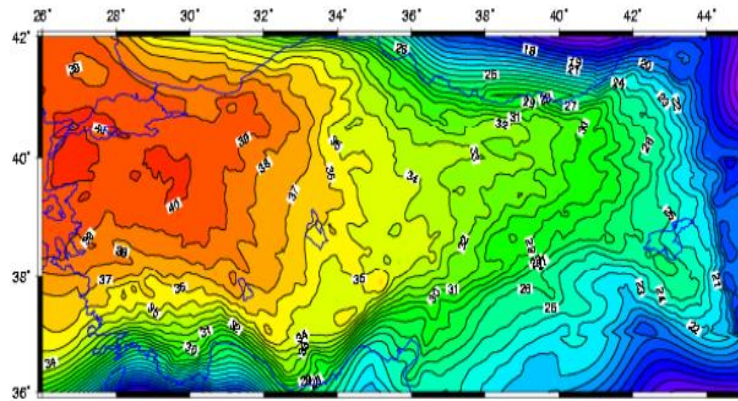


**Figure 2.7:** Turkey Geoid 1991 (TG91) (Direnç et al., 2012).

### 2.2.2.3 Geoid determination using numerical density method

Geoid determination relies on Newton's law of attraction and distribution of internal mass of the Earth. Therefore instead of adopting constant  $\rho=2.67 \text{ gr/cm}^3$  mass density in Gravimetric geoid modelling, the topographic density models can be employed in order to provide more rigorous computations (Deniz and Ayan, 2002; Yılmaz and Arslan, 2005).

### 2.2.3 The geopotential approach

Geopotential models have a significant role to combine national height systems and promote vertical datum modernization based on GPS positioning. This model was used to determine the gravity potential of the Earth and computing the satellite orbits, but now, it has a significant role to determine geoid heights by using equations below (Erol, 2007);

$$W(r, \vartheta, \lambda) = \frac{GM}{r} \left\{ 1 + \sum_{n=1}^{\infty} \left( \frac{a}{r} \right)^n \sum_{m=0}^n (C_{nm} \cos m\lambda + S_{nm} \sin m\lambda) P_{nm}(\cos \vartheta) \right\} + \Phi \quad (2.17)$$

where  $r$ ,  $\theta$ ,  $\lambda$  are the polar coordinates of the gravity field of Earth ( $W$ ),  $GM$  is the gravitational constant,  $a$  is the major radius of reference ellipsoid,  $P_{nm}(\cos\theta)$  is normalized Legendre function,  $C_{nm}$ ,  $S_{nm}$  are the normalized global harmonic coefficients and  $\Phi$  is the centrifugal potential. Gravity anomalies are calculated using the spherical harmonic expansion model;

$$\Delta g(r, \vartheta, \lambda) = \frac{GM}{r^2} \left\{ \sum_{n=2}^{\infty} (n-1) \left( \frac{a}{r} \right)^n \sum_{m=0}^n (\Delta C_{nm} \cos m\lambda + \Delta S_{nm} \sin m\lambda) P_{nm}(\cos \vartheta) \right\} \quad (2.18)$$

and geoid heights can be obtained as;

$$N(r, \vartheta, \lambda) = \frac{GM}{r\gamma} \left\{ \sum_{n=2}^{\infty} \left( \frac{a}{r} \right)^n \sum_{m=0}^n (\Delta C_{nm} \cos m\lambda + \Delta S_{nm} \sin m\lambda) P_{nm}(\cos \vartheta) \right\} \quad (2.19)$$

where  $\gamma$  is the normal gravity value at point  $P(r, \theta, \lambda)$ .

The accuracy of the model is getting higher when there are more coefficients due to the fact that the Earth has information about shorter wavelengths (Erol, 2007).

#### 2.2.4 The hybrid method (remove - restore)

According to this method, which is one of the commonly applied technique for regional geoid determination, the geoid model is calculated with the combination of the global geopotential model and terrestrial gravity measurements. In this method, short wavelength and long wavelength components are subtracted that is called as “Remove”. After applying Stokes integral using residual gravity anomalies, the original signal in the region of interest are restored by replacing topography and geopotential model back. Therefore, this process is called as “Restore”. The advantage of this method is easy detection of ill-matched data in the region whereas the restricted dataset sufficiency in the limited area can be considered as its

disadvantage (Deniz and Ayan, 2002). Geoid heights are obtained with following equations;

$$N = N_{model} + N_{Res.} + N_{tc} \quad (2.20)$$

where  $N_{model}$  is geoid height obtaining from geopotential model,  $N_{tc}$  is the terrain correction of topography on the geoid height,  $N_{Res.}$  is the residual geoid height derived from Stokes integral that is given below.

$$N_R = \frac{R}{4\pi\gamma} \iint_{\sigma} \Delta g_{RFA} S(\Psi) d\sigma \quad (2.21)$$

where  $\Delta g_{RFA}$  is the residual FAYE anomaly.

The hybrid geoids in Turkey, which were derived from remove-restore technique after fitting to GPS/leveling surface, are exemplified below (see Figures 2.8 - a, b, c).

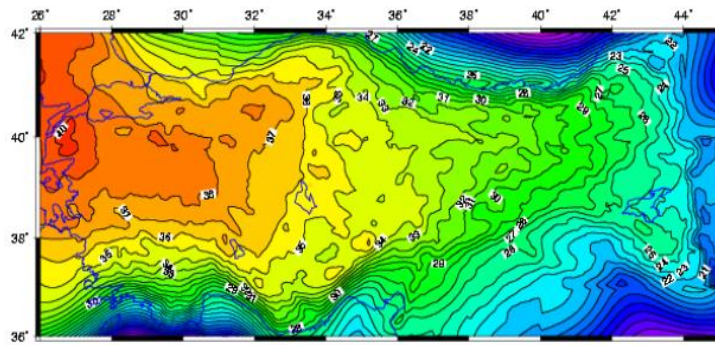


**Figure 2.8a:** Turkey Hybrid Geoid 1999A (TG99A) (Direnç et al., 2012).

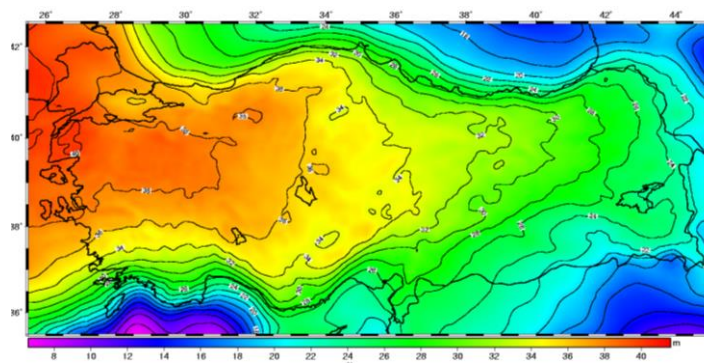


**Figure 2.8b:** Turkey Hybrid Geoid 2003 (TG03) (Direnç et al., 2012).

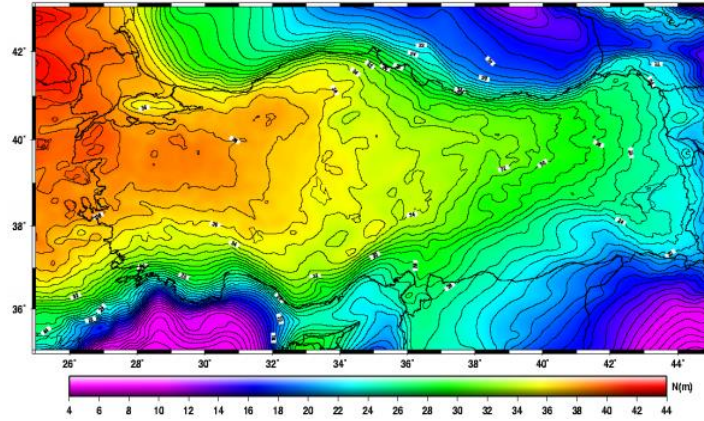


**Figure 2.8c:** Turkey Hybrid Geoid 2009 (THG09) (Direnç et al., 2012).

Although these regional geoids in Turkey were determined in different years sequentially, there is no improvement in accuracy among them (Yıldız, 2012).

### 2.2.5 The GPS/leveling methods

The global positioning system has wide range of application today, and determining precise geoid GPS is getting more important day by day in parallel to the progress in satellite positioning systems. Beside the ellipsoidal heights obtained through the GPS in the datum of World Geodetic System 1984 (WGS84), the orthometric heights, derived from leveling, are required for most of the geodetic applications. Geoid heights can be employed with the combination of ellipsoidal and orthometric heights. The equation belong to relationship between three different height is given below;

$$N_{\text{GPS/Lev.}} = h_{\text{GPS}} - H_{\text{Leveling}} \quad (2.22)$$

In order to determine the geoid via GPS/leveling method, a geodetic network is required which consists of collocated geoid reference points with known ellipsoidal and orthometric heights (see equation 22). These reference points should be selected in watershed lines, peaks and hills etc. in order to represent the topographic mass variations well (Deniz and Çelik, 2005). GPS/leveling geoids in Turkey are exemplified below (see Figures 2.9 - a,b,c,d,e and 2.10) (Ayan et al., 2006; Erol, 2007).

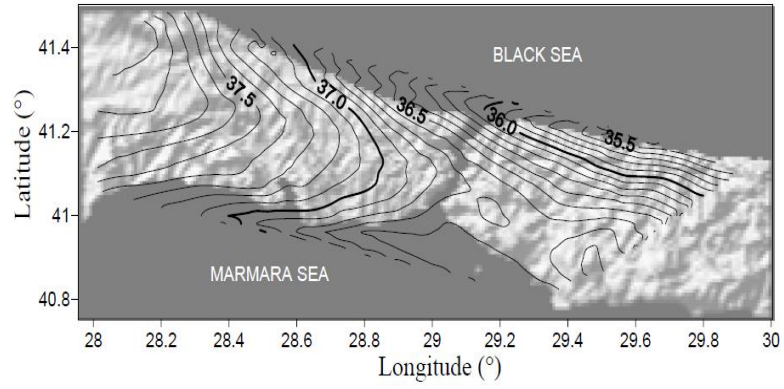


**Figure 2.9a:** Istanbul 2005 local GPS/leveling geoid (Erol, 2007).

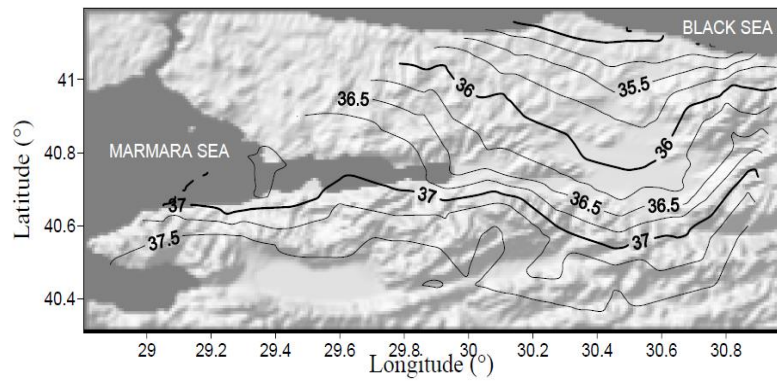


**Figure 2.9b:** Sakarya 2002 local GPS/leveling geoid model (Erol, 2007).

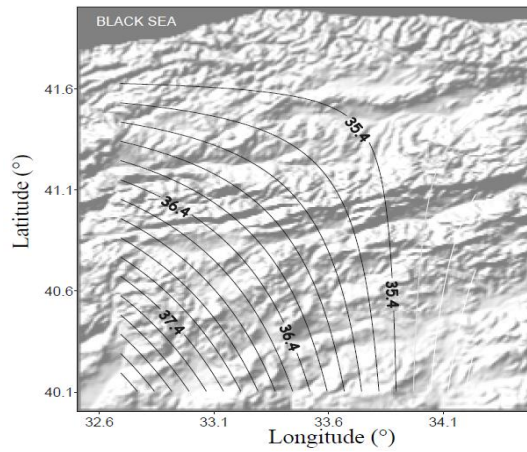


**Figure 2.9c:** Çankırı 2005 locally improved Turkey Geoid 2003 geoid model (Erol, 2007).

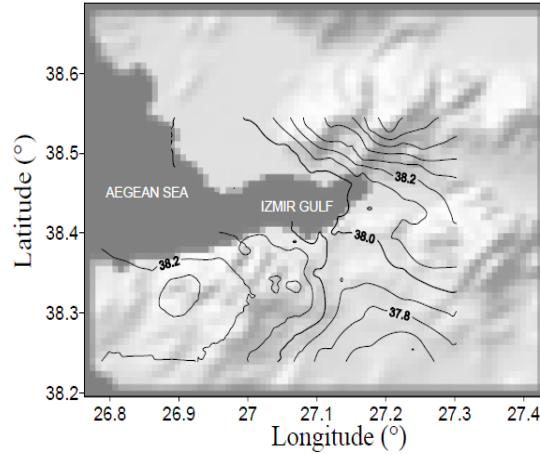


**Figure 2.9d:** Izmir 2001 local GPS/leveling geoid model (Erol, 2007).

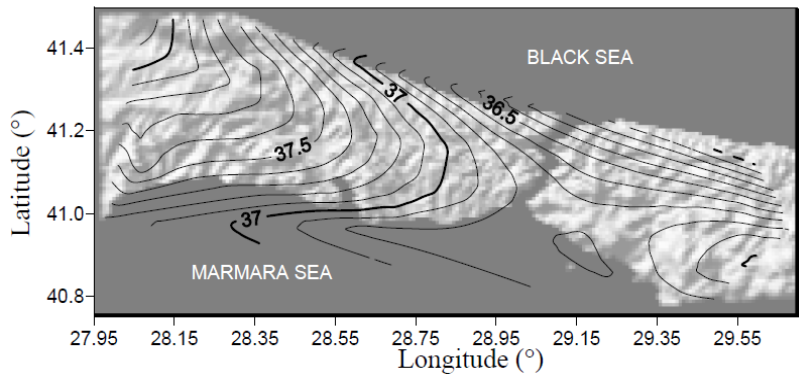


**Figure 2.9e:** Istanbul 1999 local GPS/leveling geoid (Erol, 2007).

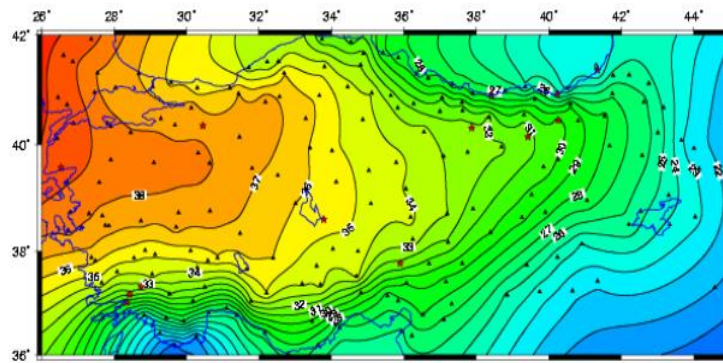


**Figure 2.10:** Turkey GPS/leveling geoid surface (Direnç et al., 2012).

The geoid model can be served as a parametric model as well as the produced grid data having geoid undulations. Local GPS/leveling geoid models constitute an alternative to the regional geoids of Turkey today with higher accuracy advantage in applications where transformation of GNSS ellipsoidal heights into regional vertical datum are required. However, the limited area where the local geoid model is available, is the main disadvantage of these modes (Erol, 2007).



### 3. SURFACE INTERPOLATION METHODS

In most of geodetic, scientific and engineering applications, spatial information is required. However, there is no continuous spatial data in every point of interested area. GPS/leveling data is used in case study and numerical tests of this thesis, and if the statements above are considered within the context of GPS/leveling method, this can be said that there is no possibility to have geoid height information, which is a connection between ellipsoidal height derived from GPS and orthometric height derived from leveling, for infinite number of points in the region of interest. In order to obtain geoid heights of unknown points, geoid models are performed by using several techniques such as (Soycan and Soycan, 2003);

- Linear Interpolation
- Polynomial regression equations
- Least Squares Collocation
- Finite Element Methods
- Artificial Neural Network based models such as ANN, WNN, ANFIS

In this thesis, 12 interpolation methods are used to determine geoid model in grid form. Basically interpolation is the process of estimating the data at unknown points by using the data at known points. There are wide range application areas for spatial interpolations like geophysical exploration, climate research, geodynamic (i.e. estimating the crustal velocities), hydrologic studies (investigating soil properties), population density research, DTM analysis (obtaining elevations from DTM), environmental studies (mapping chemical concentrations, estimating soil Ph or moisture) and geology (predicting haddock of ages) (Li and Heap, 2008).

Isotherm map is provided as an example for interpolated temperatures in South African Weather Stations for April 15, 2009 at 11 am can be seen in Figure 3.1.

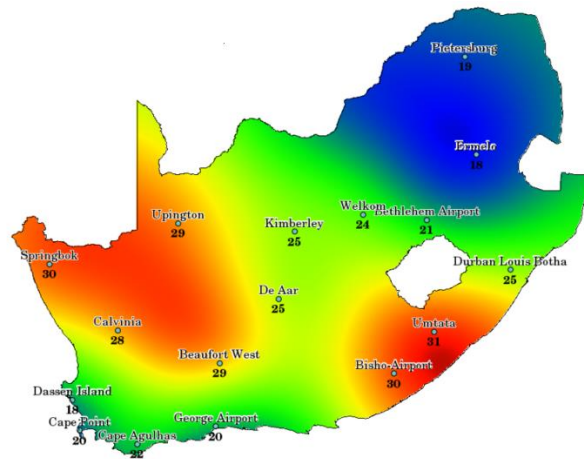


**Figure 3.1:** Isotherm map in South Africa (Sutton et al., 2009).

As stated in the introductory part, there are numerous interpolation methods in literature and the classifications of interpolation methods vary according to different references. Siu and Lam (1983) describes interpolation methods as point and areal Interpolation that can be seen in Figure 3.2 below.

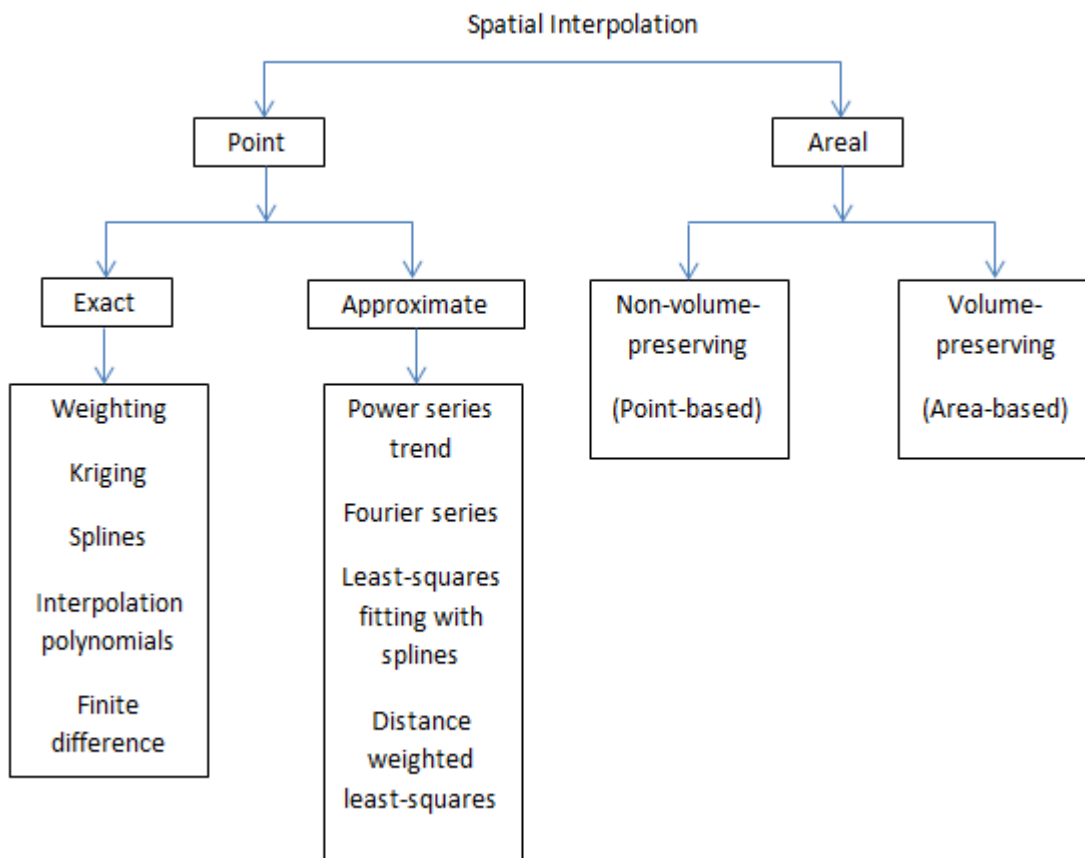


**Figure 3.2:** Categorization of spatial information methods according to Siu and Lam (1983).

Interpolation methods are grouped into three as: *i-*) point wise *ii-*) global and *iii-*) piece wise methods in Sen and Srivastava (1990). Mitas and Mitasova (1999) makes a categorization of the interpolation methods as local neighborhood approach, geostatistical approach and variational approach. Li and Heap (2008) provides a review of spatial interpolation methods for environmental science and cathegorize the methods into three as non-geostatistical methods, geostatistical methods and combined methods that can be seen in the Figure 3.3.

Non-geostatistical	Geostatistical		Combined method
	Univariate	Multivariate	
Nearest neighbors			Classification combined other interpolation methods
Triangular irregular network related interpolations	Simple kriging	Universal kriging	Trend surface analysis combined with kriging
Natural neighbors	Ordinary kriging	SK with an external drift	Lapse rate combined with kriging
Inverse distance weighting	Block kriging	Simple cokriging	Linear mixed model
Regression models	Factorial kriging	Ordinary cokriging	Regression trees combined with kriging
Trend surface analysis	Dual Kriging	Standardized OCK	Residual maximum likelihood-empirical best linear unbiased predictor
Splines and local trend surfaces	Indicator Kriging	Principal component kriging	Regression kriging
Thin plate splines	Model-based Kriging	Colocated cokriging	Gradient plus inverse distance squared
Classification	Simulation	Kriging within strata	
Regression tree		Multivariate factorial kriging	
Fourier series		Indicator kriging	
Lapse rate		Indicator cokriging	
		Probability kriging	
		Simulation	

**Figure 3.3:** The spatial interpolation methods according to Li and Heap (2008).

The categorization of non-geostatistical interpolation methods is provided by de Smith (2015) and can be seen in the Table 3.1.

**Table 3.1:** The main characteristics of interpolation methods (de Smith et al., 2015).

Method	Speed	Type	Comments
Inverse distance weighting (IDW)	Fast	Exact, unless smoothing factor specified	Tends to generate bull's eye patterns. Simple and effective with dense data. No extrapolation. All interpolated values between data points lie within the range of the data point values and hence may not approximate valleys and peaks well
Natural neighbor	Fast	Exact	A weighted average of neighboring observations using weights determined by Voronoi polygon concepts. Good for dense datasets. Typically implementations do not provide extrapolation
Nearest-neighbor	Fast	Exact	Most useful for almost complete datasets (e.g. grids with missing values). Does not provide extrapolation
Kriging - Geostatistical models	Slow/ Medium	Exact if no nugget (assumed measurement error)	Very flexible range of methods based on modelling variograms. Can provide extrapolation and prediction error estimates. Some controversy over aspects of the statistical modelling and inference. Speed not substantially affected by increasing number of data points. Good results may be achieved with <250 data points
Radial basis	Slow/ Medium	Exact if no smoothing value specified	Uses a range of kernel functions, similar to variogram models in Kriging. Flexible, similar in results to Kriging but without addition assumptions regarding statistical properties of the input data points
Modified Shepard	Fast	Exact, unless smoothing factor specified	Similar to inverse distance, modified using local least squares estimation. Generates fewer artifacts and can provide extrapolation
Triangulation with linear interpolation	Fast	Exact	A Delaunay triangulation based procedure. Requires a medium-large number of data point to generate acceptable results.
Minimum curvature	Medium	Exact/Smoothing	Generates very smooth surfaces that exactly fit the dataset
Spline functions	Fast	Exact (smoothing possible)	Available as a distinct procedure and incorporated into a number of other methods. Bicubic and biharmonic splines are commonly provided
Local pol.	Fast	Smoothing	Most applicable to datasets that are locally smooth
Polynomial regression	Fast	Smoothing	Provides a trend surface fit to the data points. Most effective for analyzing 1 <sup>st</sup> -order (linear) and 2 <sup>nd</sup> -order (quadratic) patterns, and residuals analysis/trend removal. Can suffer from edge effects, depending on the data.

Deciding the optimal interpolation method has a significant role in local geoid modelling since the accuracy of the model is strictly connected to the performance and capabilities of interpolation methods. The factors such as data density, surface type, sample size and design, data quality, scale, variance and accuracy of the data; should be considered for the choice of interpolation methods (Li and Heap, 2008). The Figure 3.4 belongs to the types of sampling design, which are regular, random, stratified random, cluster, transect and contour samplings, are represented below.

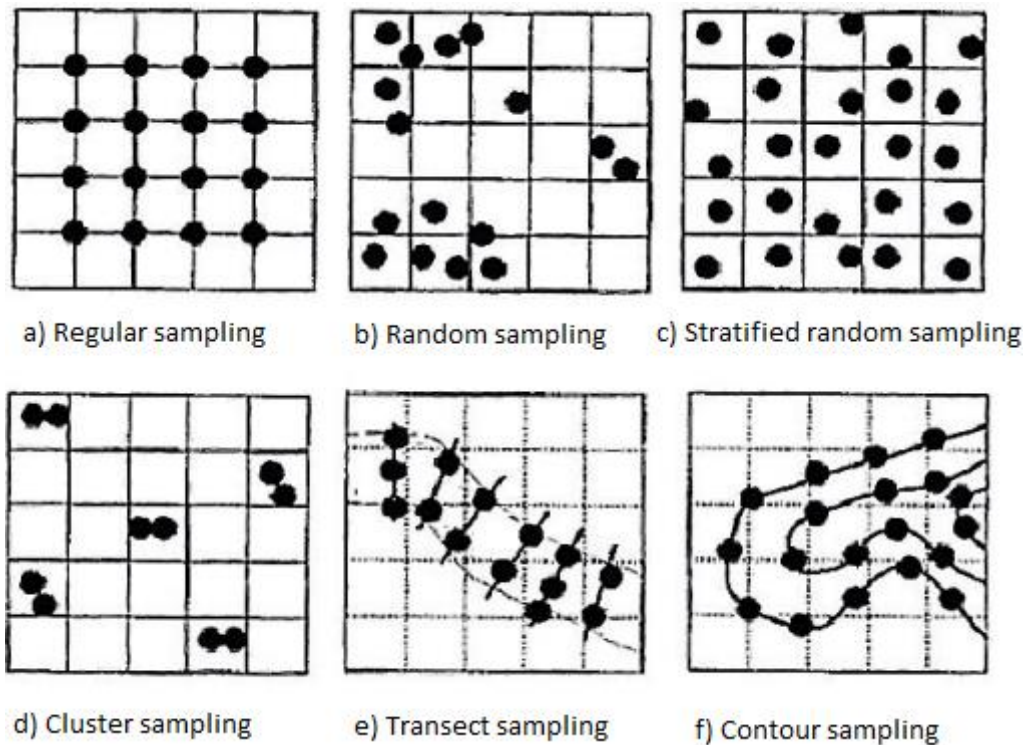


**Figure 3.4:** Data sampling examples (URL-2).

The effects of all another factors on the performance of spatial interpolation are already mentioned in introduction chapter.

The list of interpolation methods evaluated in this thesis is given below;

- Inverse Distance Weighting (IDW)
- Nearest Neighbor
- Triangulation with Linear Interpolation
- Natural Neighbor
- Polynomial Regression
  - Simple Planar Surface
  - Bi-linear Saddle

- Quadratic Surface
- Cubic Surface
- Local Polynomial
  - First Order Polynomial
  - Second Order Polynomial
  - Third Order Polynomial
- Radial Basis Function
  - Inverse Multiquadratic
  - Multilog
  - Multiquadratic
  - Natural Cubic Spline
  - Thin Plate Spline
- Modified Shepard's Method
- Minimum Curvature
- Moving Average
- Biharmonic Spline Interpolation
- Kriging
  - Point Kriging
  - Block Kriging

The basic idea of the spatial interpolation methods can be described by the following closed formula;

$$\hat{z}(x_0) = \sum_{i=1}^n P_i z(x_i) \quad (3.1)$$

where  $\hat{z}(x_0)$  is the estimated value at the interpolation point in region of interest ( $x_0$ ),  $n$  is the number of sampled points,  $z$  is the observed value at the reference point,  $P_i$  is weight assigned to the reference point (Li and Heap, 2008).

Considering the adopted interpolation algorithms in this thesis, it is possible to categorize the methods as deterministic and geostatistical as well.

### 3.1 Deterministic Interpolation Methods

In this technique, surfaces are performed from measured points by using the smoothing degree or extend of similarity. Deterministic interpolation method is also divided into two groups like local and global interpolation. In global technique, all of the data in region of interest are used whereas discrete data are used in local technique. Last but not least, deterministic methods do not give illustrations about the degree of possible errors (URL-3). Deterministic interpolation methods are explained in details below.

#### 3.1.1 Inverse distance weighting (IDW) method

In Inverse distance weighting method, which is one of the simplest and practice methods, the value at an unsampled point is estimated by using weighted average of sampled point within a certain cut-off distance. The relevant figure (see Figure 3.5) and the equation of IDW (Li and Heap, 2008) are illustrated below.

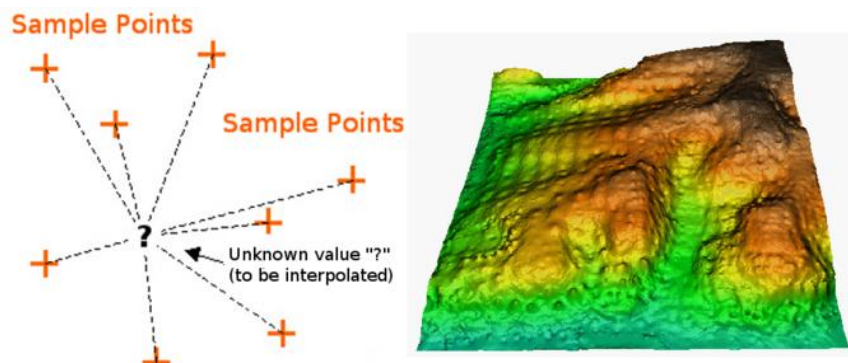


**Figure 3.5:** Inverse distance weighting interpolation (Sutton et al., 2009).

The equation of IDW is given below (Li and Heap, 2008);

$$N_0 = \frac{\sum_{i=1}^m N_i P_i}{\sum_{i=1}^m P_i}, \quad P_i = \frac{1}{d_i^k}, \quad d_i = \sqrt{(x_i - x_0)^2 + (y_i - y_0)^2} \quad (3.2)$$

where  $N_0$  is the geoid height at the new point to be estimated,  $N_i$  is the geoid height at the new point,  $k$  is the power parameter,  $m$  is the number of sampled points used,  $d_i$  is the distance between the reference and interpolation point  $(x_0, x_i)$ . The power parameter “ $k$ ” is the main factor that affects the accuracy of IDW. When the power parameter “ $k$ ” decreases, weight for distance data increases. Similarly, weight

decreases when the distance is increased between reference point and interpolation point which will be predicted. The relationship between relative weight and distance is illustrated in Figure 3.6 below.

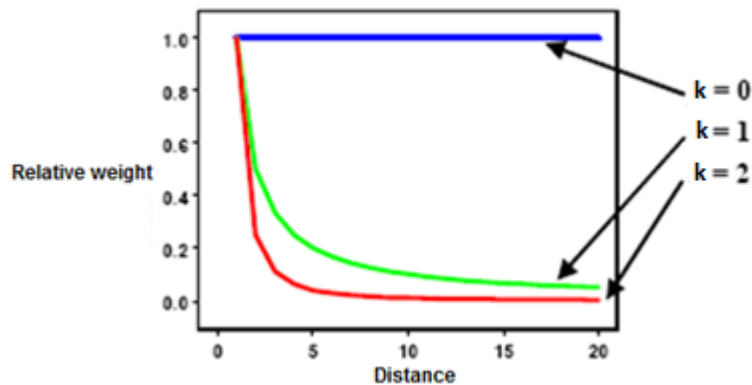


**Figure 3.6:** The graphics on the effect of distance on relative weight (URL-3).

The power parameter is mostly chosen as 2 ( $k=2$ ). Power parameter is also affect smoothness of the estimated surface directly: The higher power parameter, the better surface smoothness. When  $k$  is equal to zero, IDW is called as “moving average”. If  $k$  is equal to 1, IDW is referred as “linear interpolation”. IDW is also referred as “weighted moving average” when  $p$  is not equal to 1 (Li and Heap, 2008).

### 3.1.2 Nearest neighbor (NN) method

In this method, geoid height of unsampled point is obtained from nearest sampled points by using bisector between sampled points ( $n$ ) like Voronoi (Thiessen) polygons ( $V_i, i=1,2,3,\dots,n$ ) that are established by lining between neighbor points. Each sample has one polygon and samples are located in the center of these polygons (see Figure 3.7). The points within the same polygon are described with the same value. In another words, each points and its nearest sample points have the same value. This method can be used when the surface is not regular and sampling is not homogenous (Li and Heap, 2008; URL-2).

The lines that are used to establish Thiessen polygons are the sides of Delaunay triangles. In Delaunay triangle, a circle is formed along its three corners that never involve another sample points. There are several methods to form polygons like pycnophylactic interpolation which was developed by Waldo Tobler. In this



technique, the volume of the data is preserved, but moved inside the area in order to generate a continuous surface (URL-2).

The Figures 3.7, 3.8 and 3.9 belong to Voronoi diagram, Delaunay triangulation and an example of nearest neighbor are given below. Similar to Figure 3.9, a relation can be established between the reference data distribution that is applied in numerical tests in Figure 4.8 and interpolation surface that is calculated using Nearest Neighbor algorithm that is given in Figure 4.9(e).

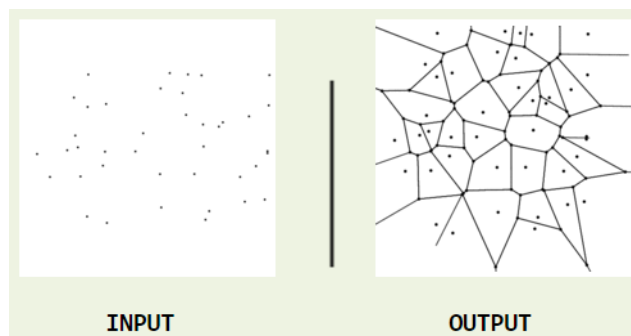


**Figure 3.7:** Voronoi diagram (Skiena, 2008).

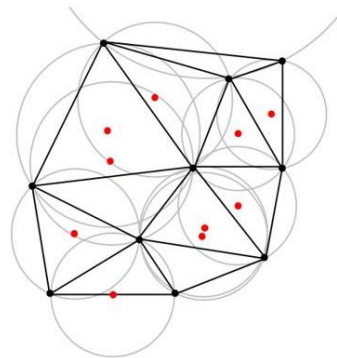


**Figure 3.8:** Delaunay triangulation (URL-4).

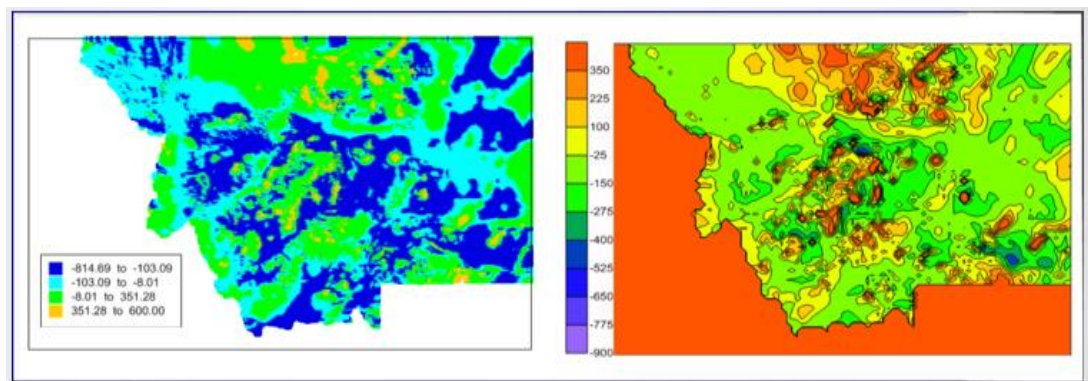


**Figure 3.9:** Examples of classified post map (on the left) and the contour map (on the right) that represent the interpolated grid nodes derived using the nearest neighbor interpolation method (URL-5).

### 3.1.3 Triangulation with linear interpolation method

This exact interpolation method works best when the data is distributed homogenously over the region of interest. In this method, triangles are generated by drawing lines between data points. Moreover, these triangles never intersect each other. The outputs are always within the data limits and obtained rapidly (URL-5).

The figure (see Figure 3.10) and equations of planar linear surface are provided below (Soycan and Soycan, 2003);

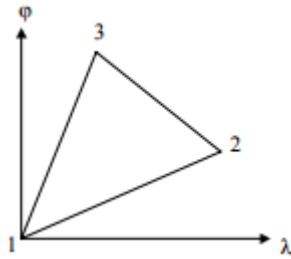


**Figure 3.10:** Planar Surface.

$$N_1 = a_0 + a_1\varphi_1 + a_2\lambda_1$$

$$N_2 = a_0 + a_1\varphi_2 + a_2\lambda_2, \varphi_1, \lambda_1 = 0, \quad \underline{N} = \begin{vmatrix} N_1 \\ N_2 \\ N_3 \end{vmatrix} = \begin{vmatrix} 1 & 0 & 0 \\ 1 & \varphi_2 & \lambda_2 \\ 1 & \varphi_3 & \lambda_3 \end{vmatrix} \begin{vmatrix} a_0 \\ a_1 \\ a_2 \end{vmatrix} \quad (3.3a)$$

$$N_3 = a_0 + a_1\varphi_3 + a_2\lambda_3$$

where  $a_0, a_1, a_2$  coefficients are estimated from following equations;

$$a_0 = N_1$$

$$a_1 = \frac{[(\lambda_2 - \lambda_3)N_1 + \lambda_3N_2 - \lambda_2N_3]}{(\varphi_2\lambda_3 + \varphi_3\lambda_2)} \quad (3.3b)$$

$$a_2 = \frac{[(\varphi_3 - \varphi_2)N_1 + \varphi_3N_2 - \varphi_2N_3]}{(\varphi_2\lambda_3 + \varphi_3\lambda_2)}$$

An example belongs to triangulation with linear interpolation is given in Figure 3.11. Similar relation that is provided between the data points and interpolation surface according to Triangulation with Linear Interpolation method, the used reference data and interpolation surface is valid when the Figure 4.8 and Figure 4.9(f) are taken into account.

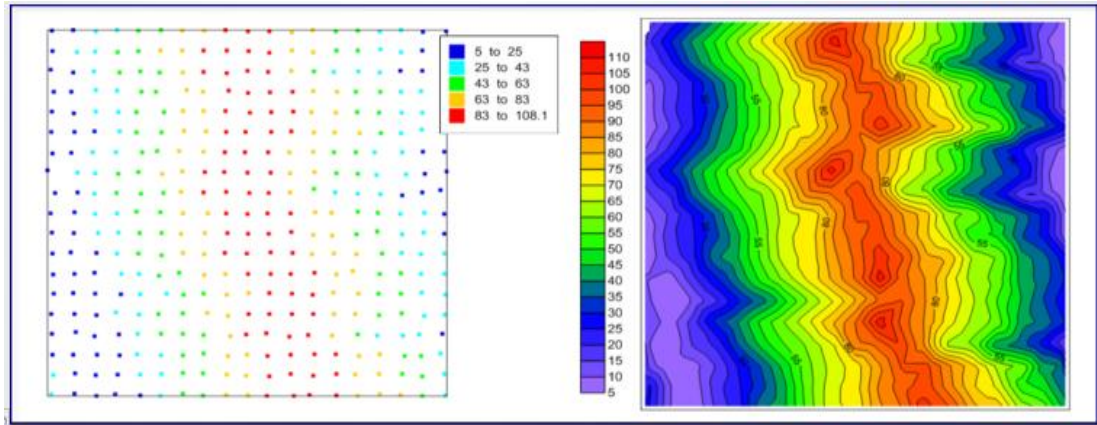


**Figure 3.11:** The classed post map (on the left).and the contour map (on the right) show the interpolated grid nodes using Triangulation with Linear Interpolation technique (URL-5).

### 3.1.4 Natural neighbor method

The natural neighbor interpolation method is used when the dense and sparse data exist in region of interest. Weighted averages of local data are obtained from natural neighbor coordinates that are derived from Thiessen polygons and polyhedral. Weighted average of nearest neighbor values, whose weights are dependent on volume of the data, is obtained from unsampled points. The number of sampled points, which are used in estimations of unsampled points, vary and dependent on the spatial construction of the data. The application areas of this method are mainly topography, bathymetry and geophysics (Mitas and Mitasova, 1999).

An example of natural neighbor interpolation is given below (see Figure 3.12). Please find the similar comparison considering Figure 4.8 and Figure 4.9(d) that shows the interpolation surface that is generated using Natural Neighbor method.

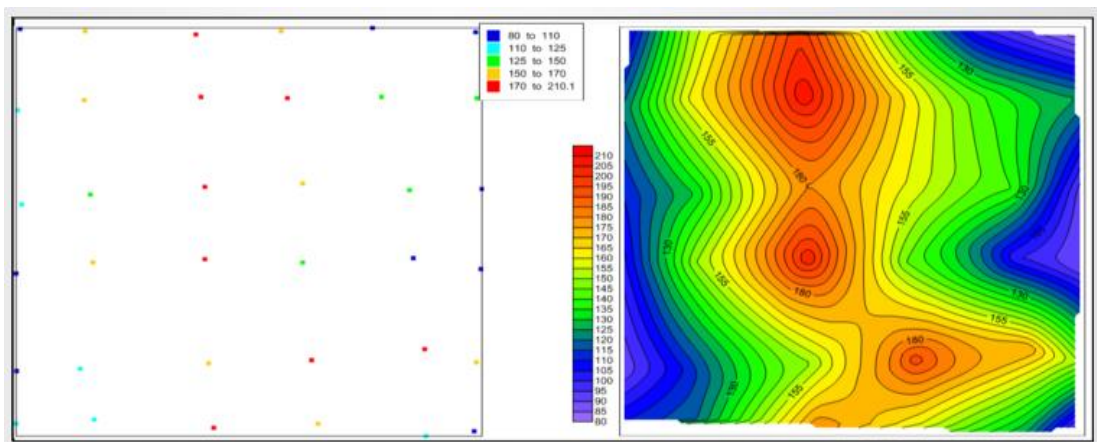


**Figure 3.12:** The classed post map is on the left. The contour map, which is on the right, illustrates the natural neighbor interpolation result (URL-5).

### 3.1.5 Polynomial regression method

Polynomial regression is used to identify large-scale trends and patterns in the data. Thus, it cannot directly estimate unknown  $Z$  values but is used for trend surface determination. The main idea of this method is representing the working area with a function. The closed formula belongs to polynomial regression is illustrated below.

$$N = (\varphi, \lambda) = \sum_{i=0}^n \sum_{j=0}^m a_{ij} \varphi^i \lambda^j \quad (3.4)$$

where  $a_{ij}$  is the unknown coefficients of polynomial,  $n$  is the surface degree,  $i$  and  $j$  are the positive integers of powered numbers of  $x$  and  $y$  coordinates.

There are different types of regression methods depend on surface definition such as simple planar surface, bi-linear saddle, quadratic surface, cubic surface, etc. The equations belong to these methods are given below (Soycan and Soycan, 2003);

- Simple planar surface

$$N_0 = a_0 + a_1\varphi + a_2\lambda \quad (3.5)$$

- Bi-linear saddle

$$N_0 = a_0 + a_1\varphi + a_2\lambda + a_3\varphi\lambda \quad (3.6)$$

- Quadratic surface

$$N_0 = a_0 + a_1\varphi + a_2\lambda + a_3\varphi^2 + a_4\lambda^2 + a_5\varphi\lambda \quad (3.7)$$

- Cubic surface

$$N_0 = a_0 + a_1\varphi + a_2\lambda + a_3\varphi^2 + a_4\lambda^2 + a_5\varphi\lambda + a_6\varphi^3 + a_7\lambda^3 + a_8\varphi^2\lambda + a_9\varphi\lambda^2 \quad (3.8)$$

Higher degree polynomials can be computed based on first equation. When the degree of polynomial increases, the number of required sampled data also increases. The reality and suitability of the surface depend on the selection of polynomial degree and coefficients.

The distribution of the sample data (in Figure 4.8) and calculated interpolation surface map using Polynomial Regression (in Figure 4.9 - h.1, h.2, h.3) can be considered for the visualization of the Polynomial Regression model.

### 3.1.6 Local polynomial method

In local polynomial, samples are located equally on a grid by using weighted least squares. Likewise, the data values, within the searching neighborhood, are distributed normally. Local polynomial method uses varying degrees of polynomials (first, second, third, etc.) within a defined neighborhood. The single order local polynomial performs a plane through the data, the second order local polynomial performs a surface with a bend while third order local polynomial performs two bends. The local polynomial equations based on polynomial degree are given below;

$$\begin{aligned}
 1: N(\varphi, \lambda) &= a + b\varphi + c\lambda \\
 2: N(\varphi, \lambda) &= a + b\varphi + c\lambda + d\varphi\lambda + e\varphi^2 + f\lambda^2 \\
 3: N(\varphi, \lambda) &= a + b\varphi + c\lambda + d\varphi\lambda + e\varphi^2 + f\lambda^2 + g\varphi^2\lambda + \\
 &\quad h\varphi\lambda^2 + i\varphi^3 + j\lambda^3
 \end{aligned}
 \tag{3.9}$$

The accuracy of surface is higher when the multiple planes are described. The computation speed is independent from data size; therefore, this method can be used for large data. If the data is getting closer to the grid nodes, the higher weight is obtained. The Figure 3.13 belongs to local polynomial is illustrated below;

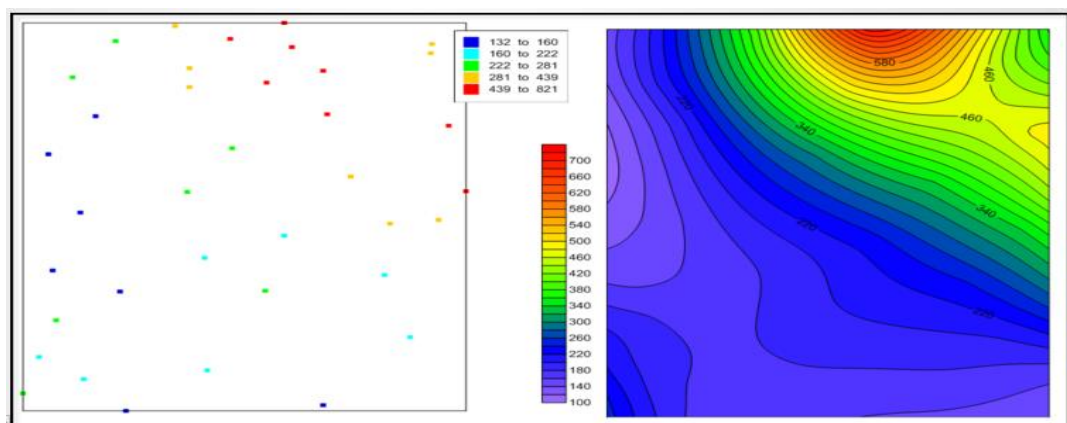


**Figure 3.13:** The classified map (on the left) was created with the data points. The contour map (on the right) represents the local polynomial interpolation result (URL-5).

### 3.1.7 Radial basis function method

Radial basis function, which is the special case of spline, is basically a distance from the location of each points and it generates a reverse cone over each location. Radial basis function is an exact interpolation method and used for performing smooth surfaces from a large dataset. The technique is not suitable when there are extreme changes in the surface within short distance (URL-3 and URL-5). The figure 3.14 belongs to radial basis function for different location and general equations are given below.

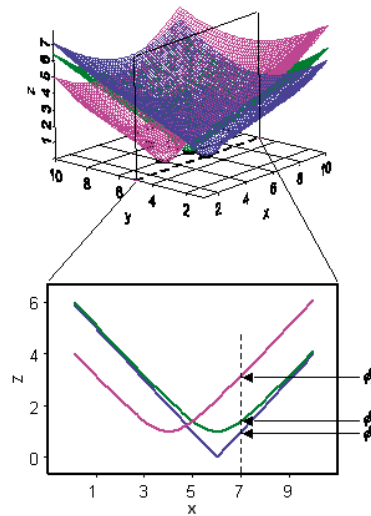


**Figure 3.14:** Radial basis functions for different locations (URL-3).

$$z_p = \sum_{i=1}^n P_i \phi(r_i) + m \quad (3.10)$$

where  $z_p$  is  $z$  value at point,  $P_i$  is weight for  $i^{\text{th}}$  point,  $\phi(r_i)$  is radial basis function for radius  $r_i$  and  $m$  is the bias or offset value.

This method is like Kriging method due to the fact that the result of radial basis function performs an accurate data. There are five types of radial basis function (RBF) which are listed below;

- Inverse Multiquadratic
- Multilog
- Multiquadratic
- Natural Cubic Spline
- Thin Plate Spline

Each method has different equations and their interpolated surfaces differ from each other. If the parameters have high value, the occurred map is smooth except inverse multiquadratic (the case is vice versa for inverse multiquadratic) (URL-3).

Thin plate spline, whose performance is illustrated in Figure 3.15, is widely used in geodetic applications. The result of the application using Thin Plate Spline with geoid reference data can be seen in Figure 4.9(i.5).

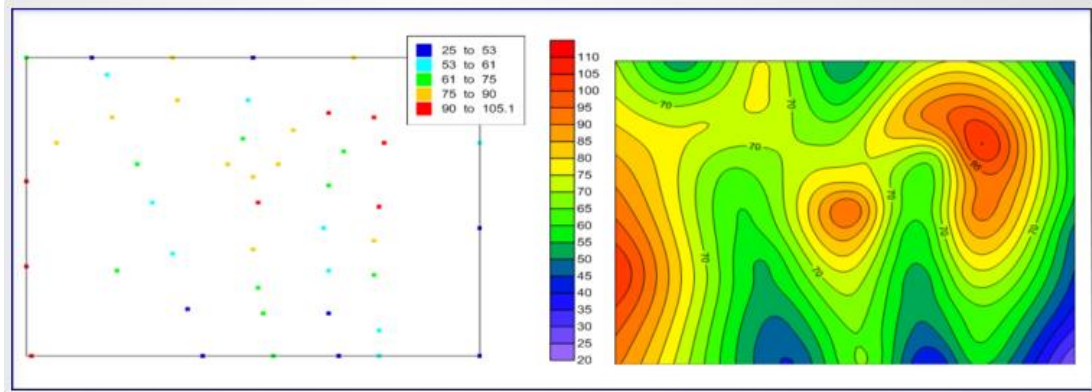


**Figure 3.15:** The classed post map on the left was created with the data points. The contour map on the right represents the interpolation result belongs to radial basis function (URL-5).

### 3.1.8 Modified Shepard's method

Modified Shepard's method, which is an exact interpolation method and reveals rather smooth surface pattern, works similar to inverse distance weighting, and the "bull's eye" effect is eliminated by using least squares adjustment. This method bases on a weighted average of the values at the points and is formulated by (Thacker, et al., 2009) as;

$$f(x) = \frac{\sum_{k=1}^n P_k(x) Z_k(x)}{\sum_{k=1}^n P_k(x)} \quad (3.11)$$

$P_k(x)$  is the weight function,  $Z_k(x)$  is a local approximant to the function  $f(x)$  centered at  $x^{(k)}$  and with weight function;

$$P_k(x) = \left[ \frac{R_w^{(k)} - d_k(x)}{R_w^{(k)} d_k(x)} \right]^2 \quad (3.12a)$$

where  $d_k(x)$  is the Euclidean distance between  $x - x^{(k)}$ ,

$$d_k(x) = \|x - x^{(k)}\|_2 \quad (3.12b)$$

$R_w^{(k)}$  is a radius of influence for point  $x^{(k)}$  and  $Z_k$  is the polynomial function. This is possible to work in n-dimensional space in modified Shepard's method and it can be used to interpolate the distributed data.

### 3.1.9 Minimum curvature method

The minimum curvature interpolation method performs a surface which is analog to a thin, linearly elastic plate for the data values with minimum blending. This method is not an exact interpolation method, and it performs a smoothest surface as far as possible (Yang et al., 2012).

The formula of minimum curvature interpolation method based on the modified biharmonic differential equation is given below (Dressler, 2009).

$$(1 - T)\nabla^4 f(x, y) - (T)\nabla^2 f(x, y) = 0 \quad (3.13)$$

with three boundary condition;

$$\begin{aligned} 1. \quad & \frac{(1 - T) \partial^2 f}{\partial n^2} + \frac{(T) \partial f}{\partial n} = 0 \\ 2. \quad & \frac{\partial(\nabla^2 f)}{\partial n} = 0 \quad \text{on the edges} \\ 3. \quad & \frac{\partial^2 f}{\partial x \partial y} = 0 \quad \text{at the corners} \end{aligned} \quad (3.14)$$

where

$T \in \langle 0, 1 \rangle$  is a tensioning parameter,  $\nabla^2$  is the Laplacian operator;

$$\nabla^2 f = \partial^2 f / \partial x^2 + \partial^2 f / \partial y^2 \quad (3.15a)$$

$\nabla^4 = (\nabla^2)^2$  is the biharmonic operator;

$$\nabla^4 f = \partial^4 f / \partial x^4 + \partial^4 f / \partial y^4 + 2 \partial^4 f / \partial x^2 \partial y^2 \quad (3.15b)$$

and  $n$  is the boundary normal. The biharmonic differential equation is solved when  $T=0$ . On the other hand, if  $T=1$ , the Laplace differential equation is solved. In this



method, estimation speed is high and the effect of the data increase is less on that speed. However, the algorithm is complex and required computer usage (Dressler, 2009).

### 3.1.10 Moving average method

In this method, averages of the values are used by forming search ellipse that is defined by the user. The large number of data is required in order to obtain reasonable results. By locating the search ellipse to the center of the node, the neighboring data are determined. The output value is assigned the same as the arithmetic average of the determined neighboring data. The grid node is blanked if the output grid node value is less than the amount of minimum specified data in the neighborhood. In another words, the range of interpolated values is limited by the range of the data (Yang et al., 2012). The main equation of simple moving average is given below (URL-6).

$$s_i = \frac{1}{n} \sum_{i=i}^n a_i \quad (3.16)$$

where  $s_i$  is the interpolated value of the point with moving average method,  $a_i$  is the value of the each sampled point being averaged and  $n$  is the number of the points.

### 3.1.11 Biharmonic spline interpolation method

Biharmonic Spline Interpolation is a linear combination of Green function that is located at the center of the data. This method is very flexible, but relatively unaffected and unsteady. The data belong to slope measurements can be used in this method which is useful for some remote sensing applications when the accuracy of slopes are higher than heights. Another benefit of this method is that the degree of Green functions can be less than the number of data. Therefore, interpolating surface can be independent from inaccurate sample points. The degree of this differentiation can be high, but not useful if it is more than 4. In this thesis, This method is used as two dimensional. The equation of the method is described as follow (Sandwell, 1987);

$$\nabla^4 f(x) = \sum_{j=i}^N a_j \delta(x - x_j), \quad w(x_i) = w_i \quad (3.17)$$

where  $N$  is the number of data points in  $m$  dimensions,  $\nabla^4$  is the biharmonic operator and  $x$  is the position in  $m$  dimensions.

$$f(x) = \sum_{j=i}^N a_j \phi_m(x - x_j) \quad (3.18)$$

where  $a_j$  is found by solving linear system.

$$f_i = \sum_{j=i}^N a_j \phi_m(x_i - x_j) \quad (3.19)$$

where  $\phi_m$  is Green function. As stated before, slope data can be used in this method whose equation is illustrated below;

$$s_i = (\nabla f * n)_i = \sum_{j=i}^N a_j \nabla \phi_m(x_i - x_j) * n_i \quad (3.20)$$

## 3.2 Geostatistical Interpolation Method

Geostatistics is a branch of statistic which is used to perform continuous surface by estimating and evaluating the spatial attributes of sampled points. Kriging is one of the main techniques of geostatistical interpolation (Isaaks and Srivastava, 1989).

### 3.2.1 Kriging method

This method, which is local, exact and stochastic, is founded by a mining engineer named D.G. Krige and a geostatistician named Georges Matheron, and estimates the values at unsampled points by using sampled points at surrounding locations. This method is one of the commonly used methods for interpolation since it is based on the statistical illustration of the best linear unbiased estimate. In another word, the variance of the observations is minimized (best) and the true expected value of data is matched (unbiased) in Kriging method that is a linear estimator (URL-7). The Figure 3.16 describes the Kriging interpolation result on sample scattered elevation

data. Also a similar comparison is valid in Figure 4.8 and 4.9(k.1-k.6) using the numerical data of this study.

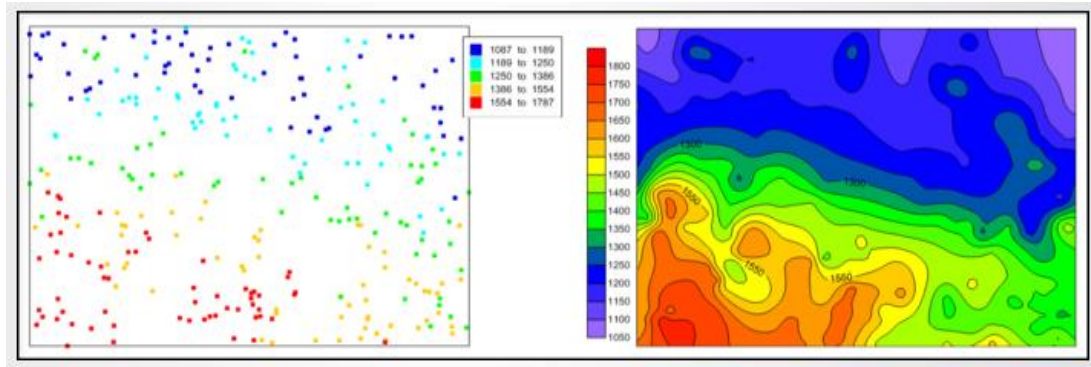


**Figure 3.16:** The classed post map on the left represents the scattered elevation data. The contour map on the right illustrates the result of Kriging method using the given sample discrete data (URL-5).

In order to describe the variation on the surface, a spatial correlation, which is expressed by the distance between sampled points, is used. This method has a multistage process that involves exploratory statistical analysis of the data, variogram modelling, performing the surface, and exploring a variance surface arbitrarily. The variogram model is a mathematical illustration of spatial variability of data. When there is a directional bias in the data or spatially correspond distance, Kriging is one of the most useful interpolation technique. (URL-8).

The Kriging process starts by defining the variation on spatial data that is usually too complicate to be modeled mathematically with a simple function. Therefore, that variation of spatial data is modeled as a stochastic surface or random field. The equation belongs to Kriging method is given below (URL-2);

$$Z(x) = m(x) + \varepsilon'(x) + \varepsilon'' \quad (3.21)$$

where  $Z(x)$  is a random variable at  $x$ ,  $m(x)$  is a constructional component,  $\varepsilon'(x)$  is auto-correlated residual from  $m(x)$  and  $\varepsilon''$  is random noise.

The expected differences in the value of two points  $x$  and  $x+l$  is zero since the mean value of  $m(x)$  is the mean value in the sampled area.

$$E[Z(x) - Z(x + l)] = 0 \quad (3.22)$$

where  $l$  is the distance between points. The variance of the differences can be stated as distance between points like:

$$E[\{Z(x) - Z(x + l)\}^2] = E[\{\varepsilon'(x) - \varepsilon'(x + l)\}^2] = 2\gamma(h) \quad (3.23)$$

where  $\gamma(l)$  is referred as the semivariance. Under the statements above when the semivariance is substituted to the auto-correlated residual in Eq. (3.21), the model can be described as;

$$Z(x) = m(x) + \gamma(l) + \varepsilon'' \quad (3.24)$$

Semivariance can be estimated by using the equation below;

$$\hat{\gamma}(h) = \frac{1}{2n} \sum_{i=1}^n \{z(x_i) - z(x_i + l)\}^2 \quad (3.25)$$

The number of pairs of sample points is described by  $n$  in the equation above. According to different  $l$  values, semivariance can be estimated. Experimental variogram is the name of the plot for the semivariance that uses  $l$  values. There are various variogram models, which are spherical, exponential, Gaussian, linear, and suitable model is determined considering the shape of the experimental variogram. If the shape of the variogram is classic (a), a spherical model is used. When the spherical model is smooth, estimations for correlations are zero. However, there may be small correlations for large distance, and this property is modeled with exponential variogram (b). If there is no sill within the region of interest, linear model can be used (c). When there is small nugget and very smooth variation, Gaussian model can be used (d). The Figure 3.17 belongs to various variogram models, which are described so far, is given below.

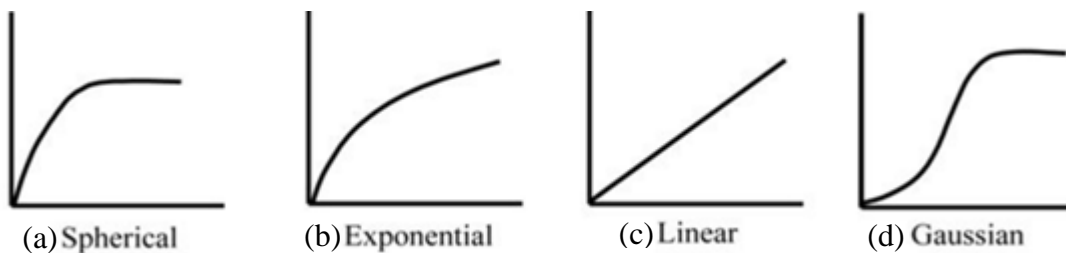


**Figure 3.17:** Various variogram models: (a) Gaussian, (b) linear, (c) spherical and (d) exponential models (Chang, 2008).

Spherical, exponential and linear variograms are illustrated together on the same figure that can be seen below (see Figure 3.18).

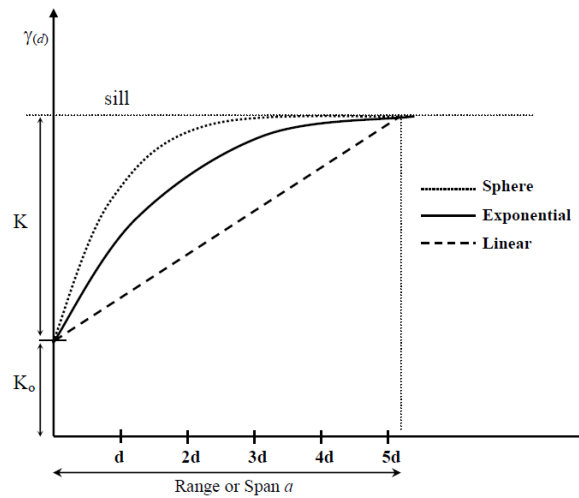


**Figure 3.18:** Variogram Models (Erol, 2007).

The expressions and conditions of the various variogram models are illustrated in the Table 3.2.

**Table 3.2:** Various variogram models (Isaaks and Srivastava, 1989).

name of the model	expression	condition
Gaussian	$\gamma(d) = K_0 + K \left( 1 - e^{-d^2/a^2} \right)$	none
Exponential	$\gamma(d) = K_0 + K \left( 1 - e^{-d/a} \right)$	none
Spherical	$\gamma(d) = K_0 + K \left[ \left( \frac{3d}{2a} \right) - \left( \frac{d^3}{2a^3} \right) \right]$	$0 \leq d \leq a$
	$\gamma(d) = K_0 + K$	$d > a$
Linear	$\gamma(d) = K_0 + K d$	none

K is the first order effect of the variogram. And  $K_0$  is the nugget effect (random noise) which is corresponding semivariance value at  $d=0$ . The intersection point of the vertical axis and variogram curve referred as nugget (see Figure 3.18).  $a$  is the horizontal distance at range (top limit). Horizontal distance between the samples is illustrated with  $d$ . The top limit of the variogram ( $K_0 + K$ ) is stated as the sill (Isaaks and Srivastava, 1989).

There are two Kriging types commonly applied that are point and block Kriging. In point Kriging, the value of a point is simply estimated from neighbor values. Block Kriging calculates the mean value of the rectangular blocks that are located on the center of the grid nodes. The drift type can be chosen as linear, quadratic or the drift

may not be applied as optional. If there is no drift adopted, the method is preserved as ordinary Kriging. On the other hand, the linear or quadratic drift type choices reveal to universal Kriging. Ordinary Kriging is a linear prediction considering stationary mean structure. In another words, the mean is constant within region of interest. However, universal Kriging is a linear prediction considering non-stationary mean structure which means linear or higher order trend in values of the data are fitted. The data can be predicted easier in ordinary Kriging. In contrast to ordinary Kriging, the universal Kriging method relies on more complicate predicting algorithm (URL-5). An example belongs to outputs of some interpolation methods is given below in order to discriminate differences (see Figure 3.19).

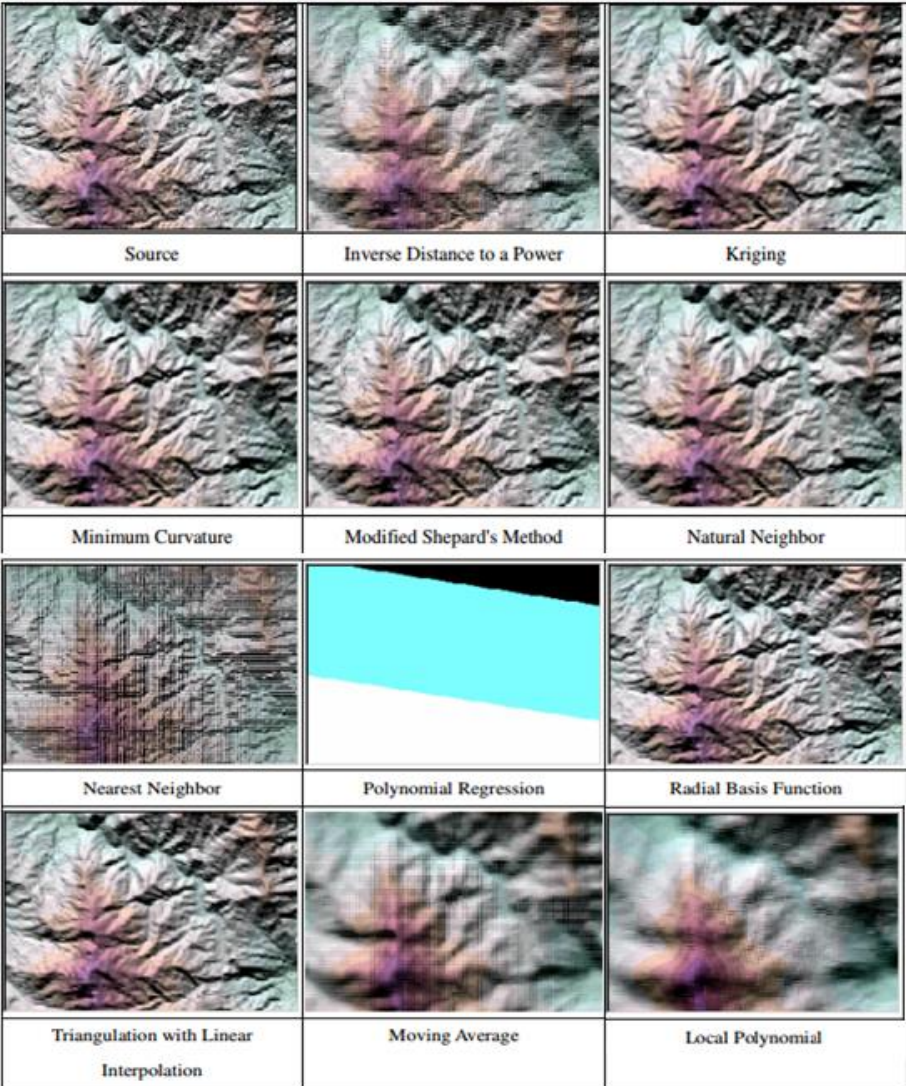


**Figure 3.19:** The output of different interpolation algorithms (Yang et al., 2012).

The shadow and color change can be seen on the figure above. For more information see Yang et al., (2012).

## **4. NUMERICAL TEST**

The orthometric heights can be derived from GPS ellipsoidal heights and geoid heights that are derived from geoid model. It has to be considered that the accuracy of geoid heights affects directly the accuracy of orthometric heights during the transformation process. The performance and efficiency of GPS technique in geodetic and surveying applications increases with a high accurate geoid model. The Turkish regional geoid does not have sufficient accuracy (approximately 10 cm); therefore, performing local geoids has an important role for GPS/leveling applications (Deniz and Çelik, 2005). The aim of this study is to determine precise local GPS/leveling geoid for Istanbul by using different interpolation methods (e.g., Inverse Distance to a Power, Kriging, Minimum Curvature, Modified Shepard's Method, Nearest Neighbor). In order to determine the optimal geoid solution in the study area, the accuracy and practicability of the local geoids, which are calculated via different interpolation algorithms, are assessed and compared. Finally, local geoid models are provided that can be embedded into regional geoid model for Turkey (TG03) in future works. IGNA 2005 data, is used for numerical evaluations and the processes of numerical test are identified step by step in Figure 4.1.

### **4.1 Data Description**

In this thesis, 1204 Istanbul GPS Leveling Network 2005 (IGNA 2005) data, which is established to realize the height systems as geodetic infrastructure of Istanbul, is operated. The location of Istanbul is between 40°30' N - 42°00' N latitudes, 27°30' E - 30°00' E longitudes, and topographic heights change between sea level and 650 meter. IGNA network is established in 1999, however the measurements are renewed in 2005 due to earthquakes in Kocaeli (August 17, 1999) and Düzce (November 12, 1999). The GPS observations are performed by using dual frequency GPS receivers and the recording interval is at most 15 second. The observation time for C1 degree network is at least 2 hours while that is 45 – 60 minutes for C2 degree network (Deniz and Çelik, 2005).

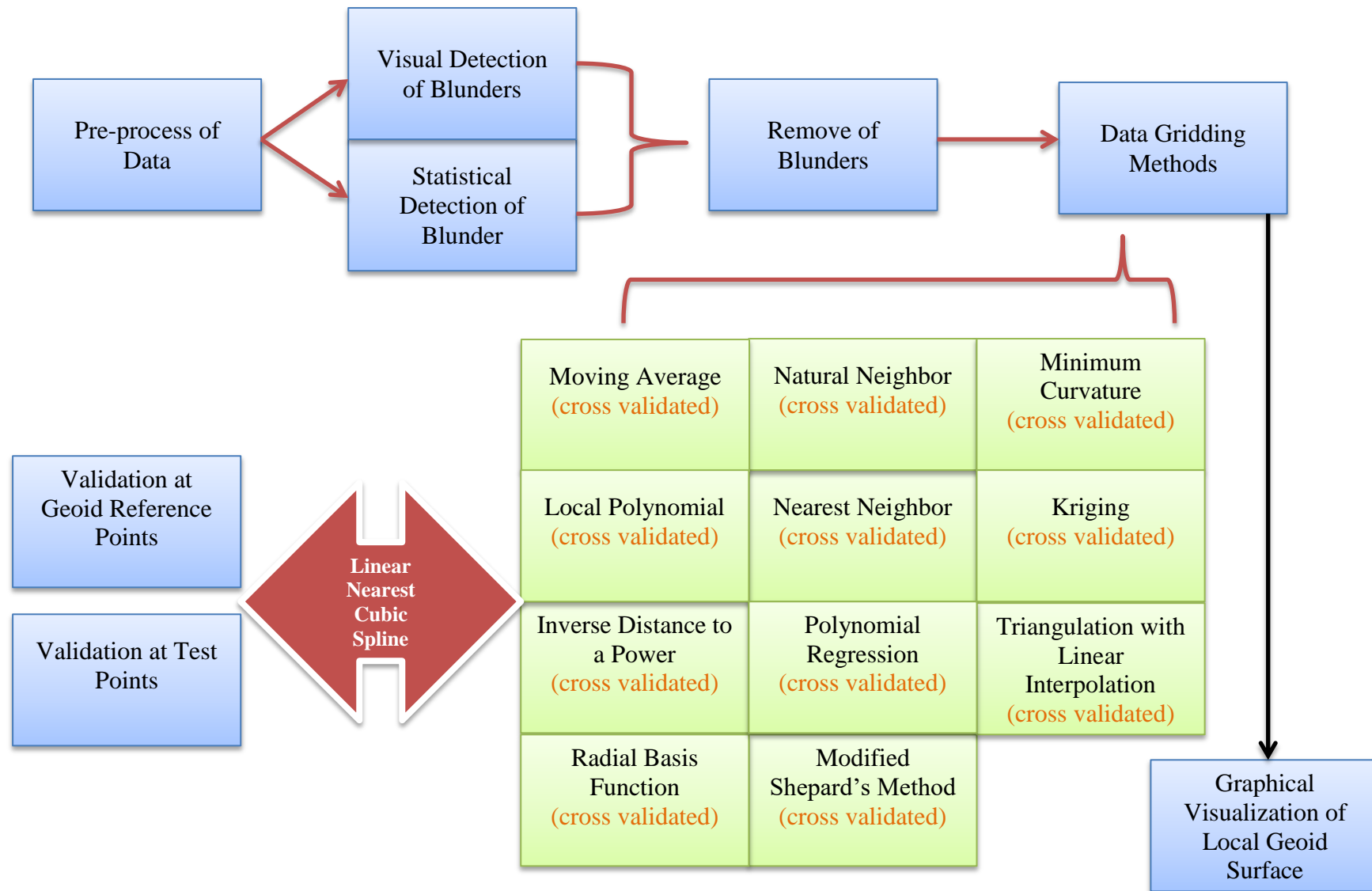


**Figure 4.1:** Processes of numerical tests step by step.



The coordinates of IGNA 2005 data is obtained in ITRF96 datum and orthometric heights of the C order densification points are obtained in TUDKA99 (Turkey National Vertical Control Network Datum 1999) through adjustment of leveling observations in the network (Ayan et al., 2006).

The density of GPS/leveling benchmarks in IGNA2005 is “1 benchmark per 20 km<sup>2</sup>” which means 1 benchmark in every 4-5 km. The description of local GPS/leveling networks is given as a table below.

**Table 4.1:** The description of local Istanbul GPS/leveling network (IGNA 2005) (Ayan et al., 2006).

	<i>Description</i>	<b>İstanbul (2005)</b>
<b>Network &amp; Topography</b>	Area, km <sup>2</sup>	110 x 220
	number of GPS/levelling BMs *	1206 (-23)
	density, BM per km <sup>2</sup>	1 / 20
	Elevation between, m	1 – 608
<b>GPS observations</b>	GPS receiver type	dual frequency
	number of sessions & duration	2 & 30 min
	coordinate datum	ITRF96
	2D coordinate accuracy, cm	±1.5
	h-accuracy, cm	±2.5
<b>Levelling</b>	levelling method	geometric
	H-accuracy, cm	±2.5
	vertical datum**	TUDKA99
<b>Geometry</b>	network geometry	good
	density of BMs	dense
	distribution of BMs	homogenous

The distribution of GPS/leveling data is illustrated on SRTM 30 plus data (±16 cm reported accuracy) for Istanbul region in order to determine how well the density and distribution of GPS/leveling points on topography (see Figure 4.2).

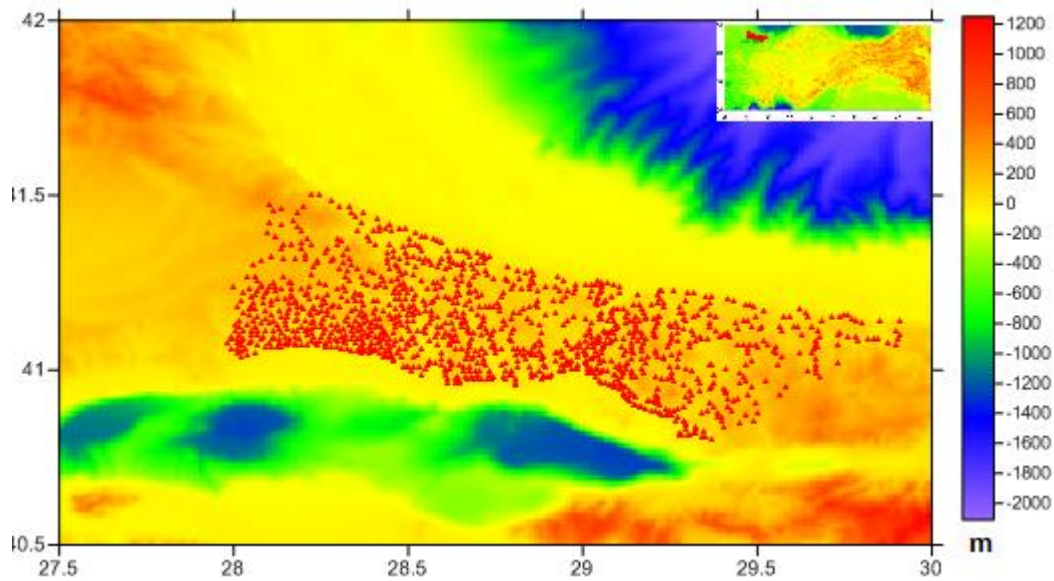


**Figure 4.2 :** Istanbul GPS/leveling points on topography (SRTM30 plus) (URL-9).

#### 4.2 Pre-Analysis of Data

Using 1204 GPS/leveling points having the ITRF coordinates and orthometric heights in TUDKA99, firstly; geoid heights are calculated as the difference of ellipsoidal heights and orthometric heights ( $h - H = N$ ) and these points are plotted with wireframe and postmap for visual detection of possible blunders in the data (see Figure 4.3).

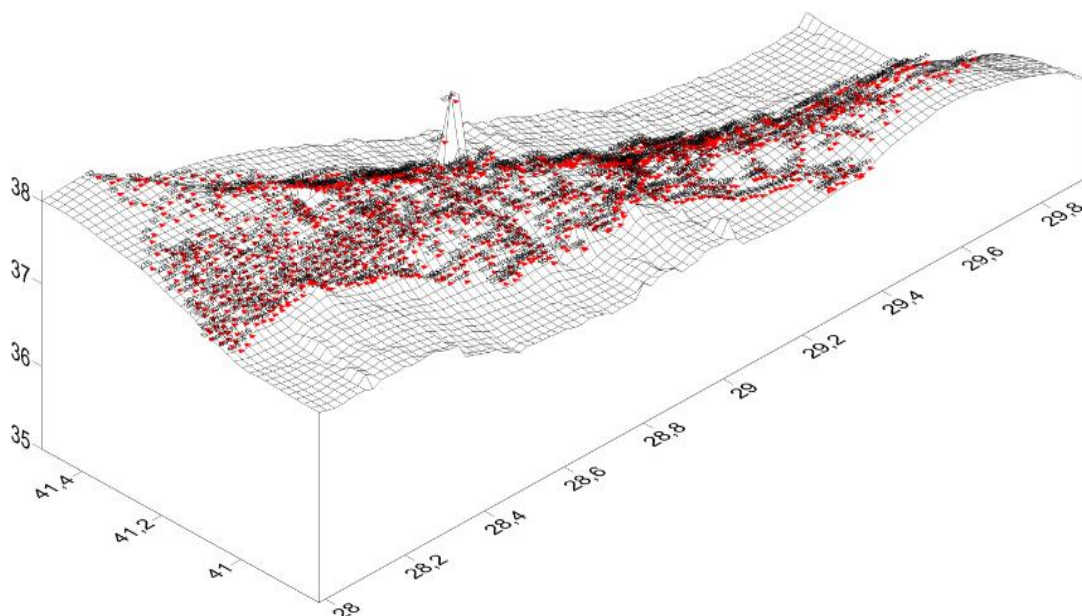


**Figure 4.3:** Istanbul GPS/leveling surface with blundered benchmarks.

Considering Figure 4.3 above; a sharp bounce (point no: 624) on GPS/leveling data can be seen visually. The figure compared with the topography in Istanbul, and the point with number of 624, which causes that sharp bounce, is determined as a blunder and omitted from the data set. The map belongs to overlaid wireframe and postmap without blunder can be seen in Figure 4.4 following.

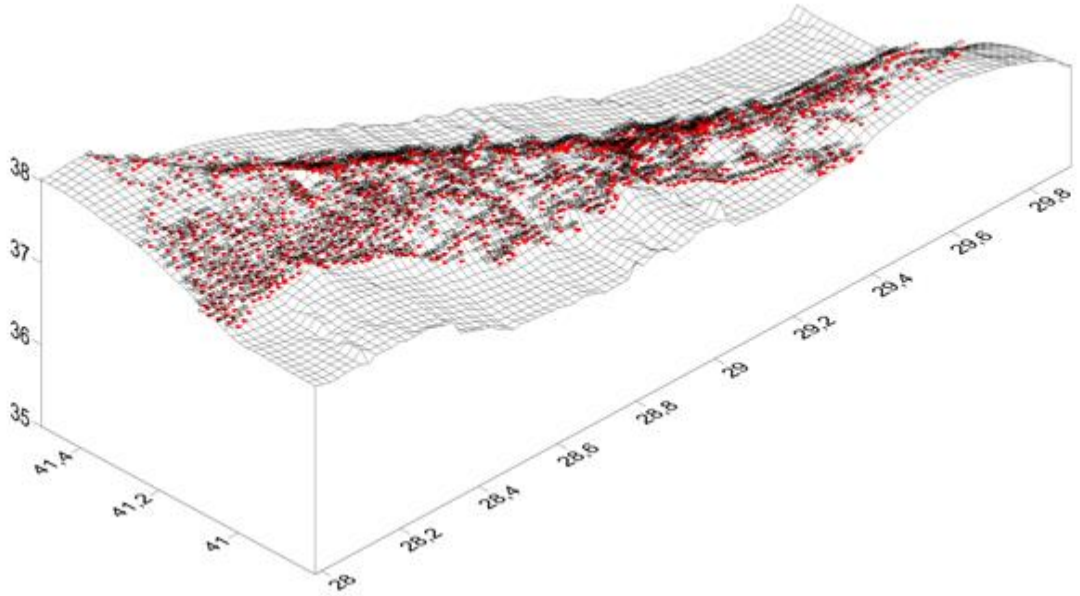


**Figure 4.4:** Istanbul GPS/leveling surface after removing the blundered benchmarks.

This can be seen when looking at Figure 4.4 above that the sudden change on the topography of Istanbul is eliminated and a smooth geoid surface is obtained. Since the determined models do not reveal reasonable residuals at benchmarks 96 and 1060, these two points are decided as blunder as well, and omitted from the data set.

Testing local geoid with model points, which are used to evaluate the performance of local geoid models, give an optimistic results and cannot examine the performance of the model objectively. Therefore, in order to test the performance of local geoid model; test points, which are approximately 5% of the entire GPS/leveling data (equal to 50 points), are identified. These 50 test points are distributed homogenously and represent the topography well. While selecting the test points, it is also considered not to harm the distribution of reference benchmarks that contributes to calculation of grid models. The rest of the points after choosing test points are referred as geoid reference points (1151 points). The Istanbul GPS/leveling surface, the distribution of geoid reference points and test points are shown in Figures 4.5, 4.6 and 4.7 respectively.

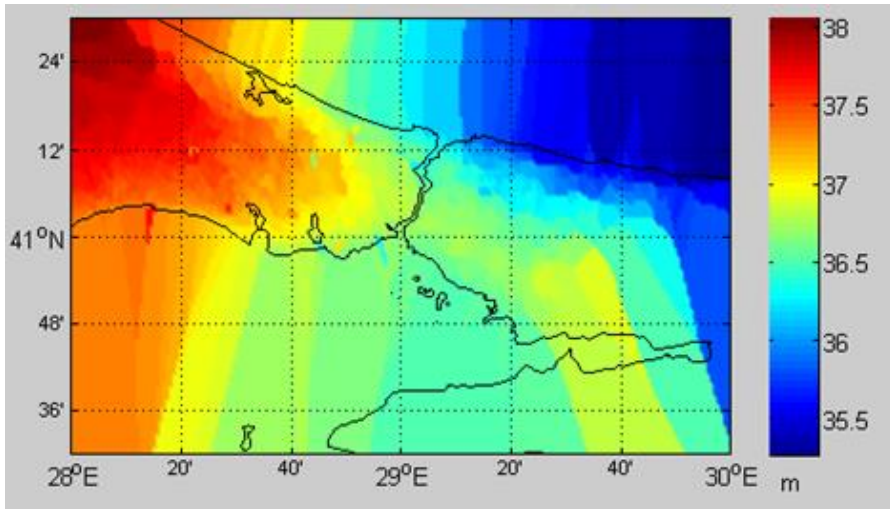


**Figure 4.5:** Istanbul GPS/leveling surface.

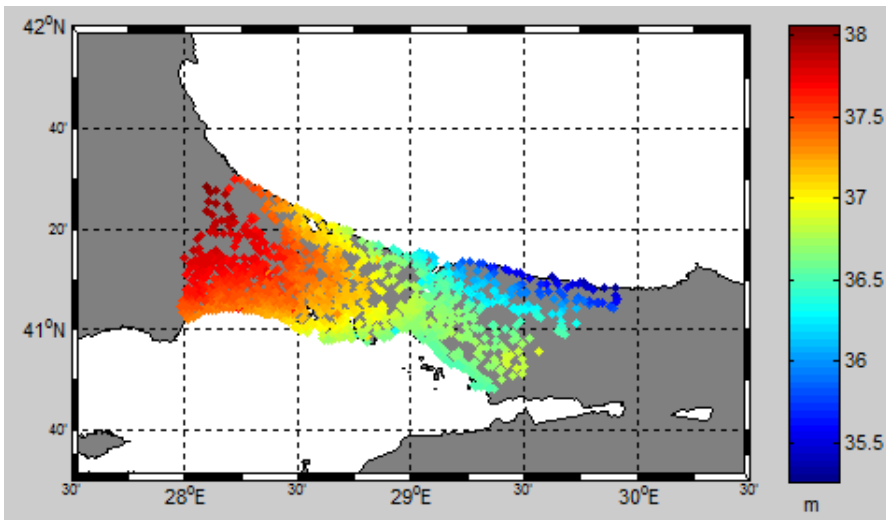


**Figure 4.6:** Distribution of 1151 geoid reference points.

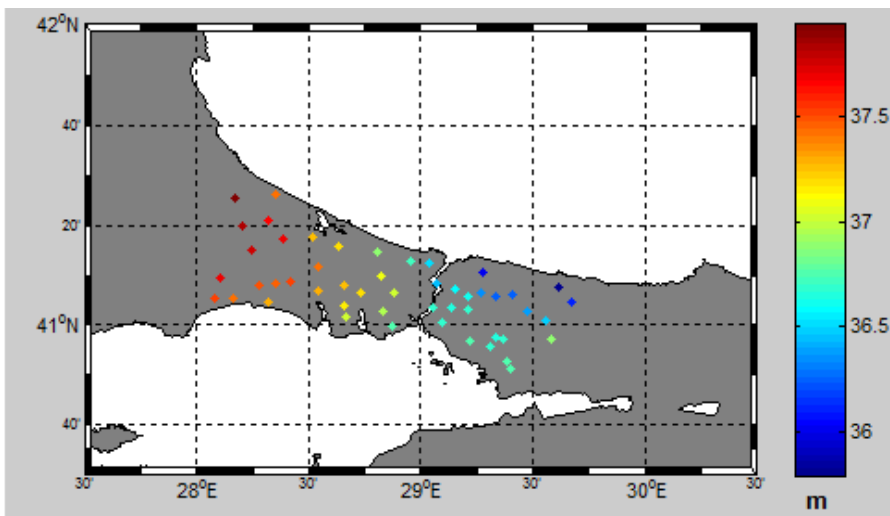


**Figure 4.7:** Distribution of 50 test points.

The distribution of the geoid reference points and test points on SRTM3 topographic data ( $\pm 16$  cm reported accuracy) are also given in following Figure 4.8.

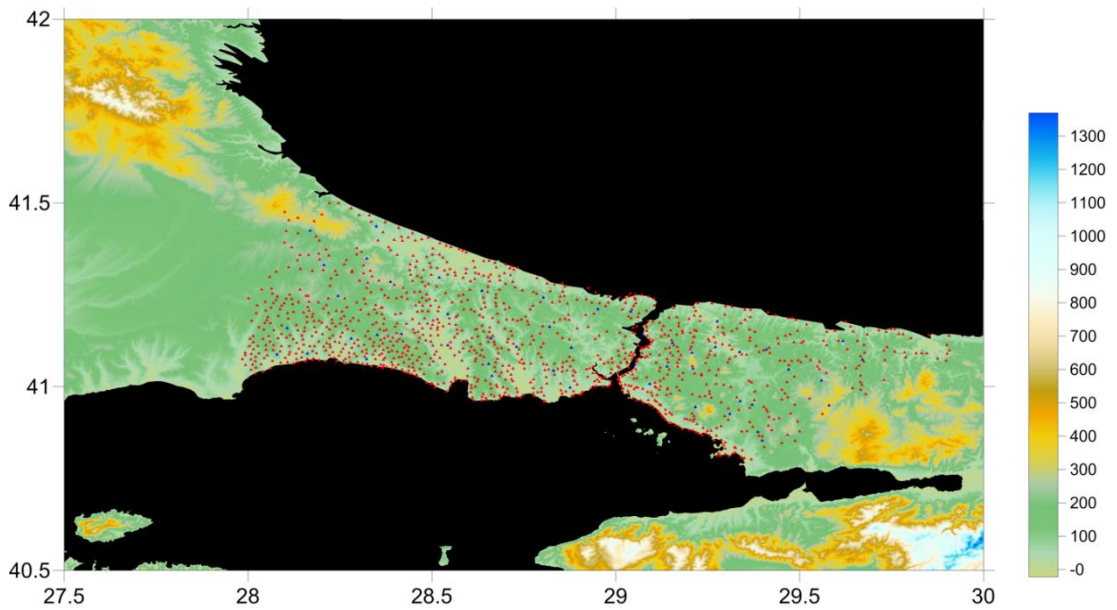
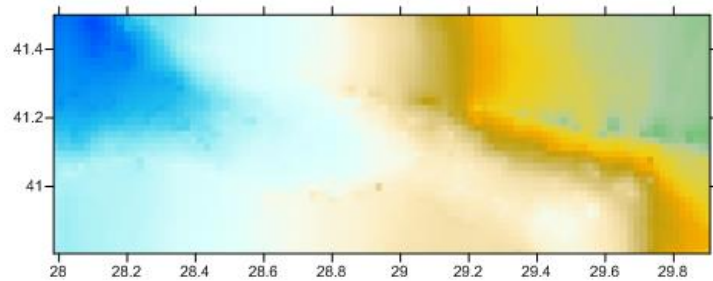


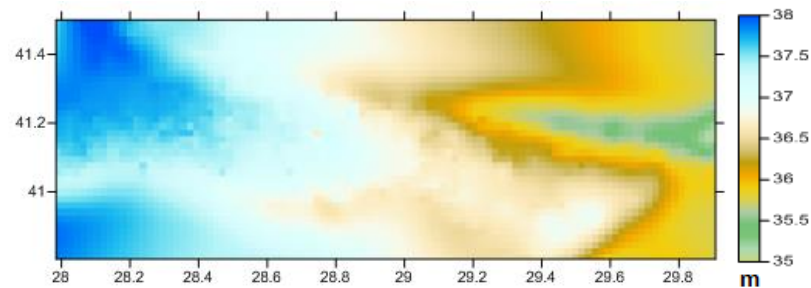
**Figure 4.8:** Geoid reference points and test points on SRTM3 data (URL-9).

### 4.3 Data Gridding and Interpolation Results

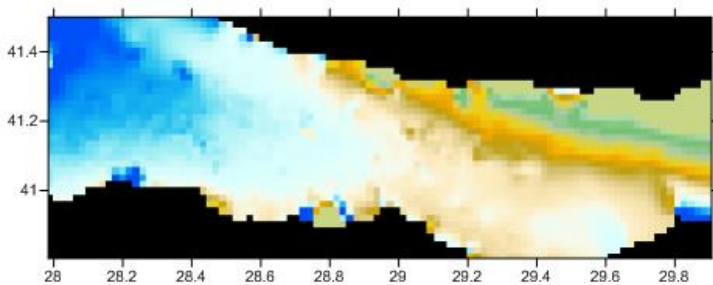
By using 12 different gridding methods (please see Figure 4.1) and 1151 geoid reference points, the grid geoid models are calculated. The surfaces of local geoid models, visualized relying on the calculated grid data from the each interpolation method are provided in Figure 4.9.



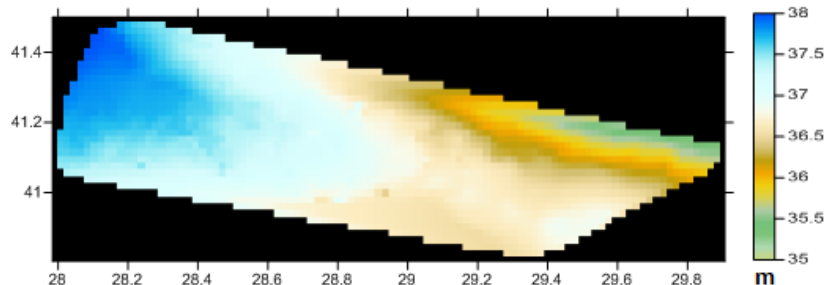
(a) Inverse Distance to a Power



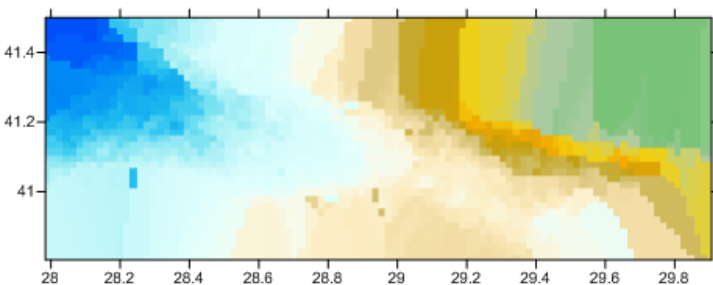
(b) Minimum Curvature



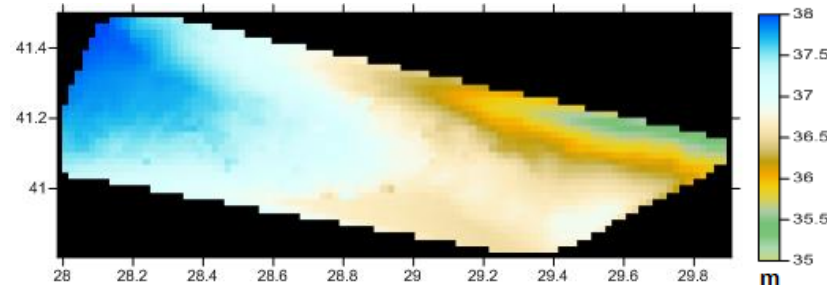
(c) Modified Shepard's Method



(d) Natural Neighbor

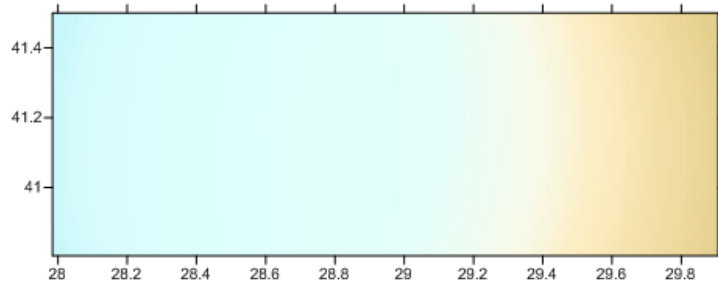


(e) Nearest Neighbor

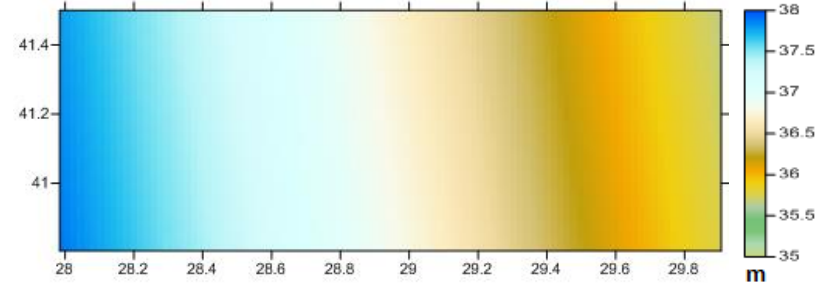


(f) Triangulation with Linear Interpolation

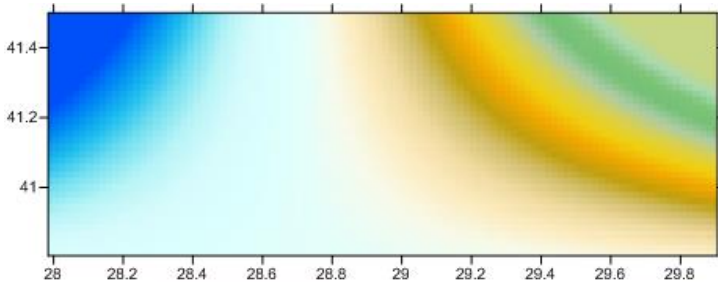
**Figure 4.9:** The contour maps of Istanbul GPS/leveling geoid based on various gridding methods.



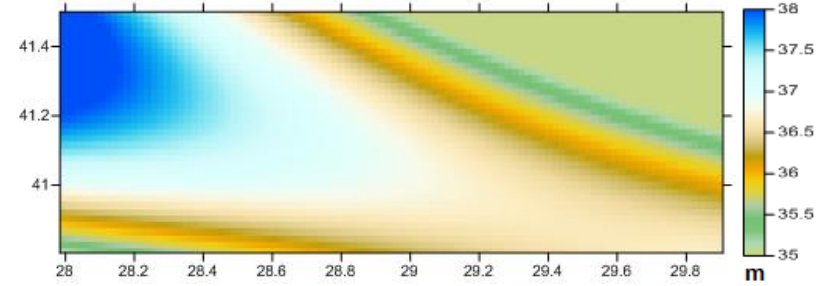
(g) Moving Average



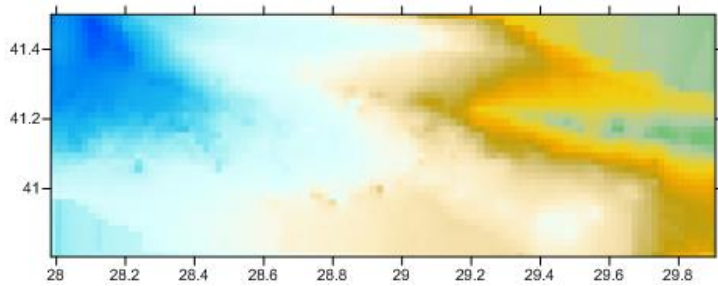
(h.1) Polynomial Regression - Simple Planar Surface



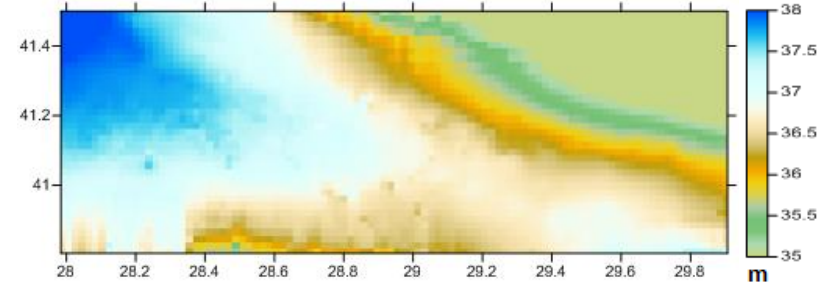
(h.2) Polynomial Regression - Bilinear Saddle



(h.3) Polynomial Regression - Quadratic Surface

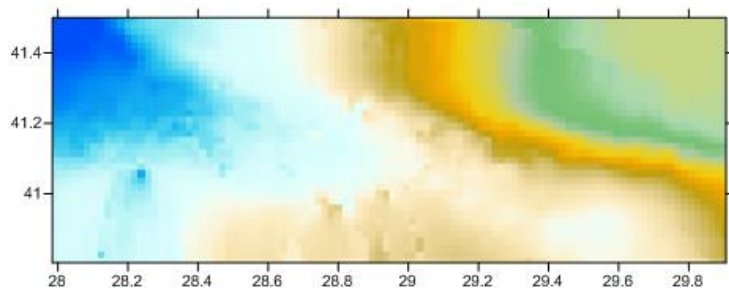


(i.1) Radial Basis Function - Inverse Multiquadric

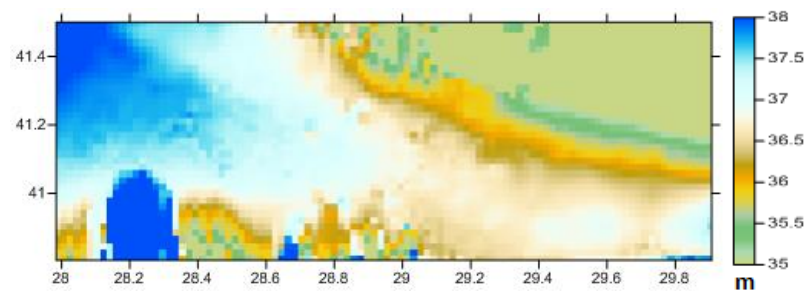


(i.2) Radial Basis Function - Multilog

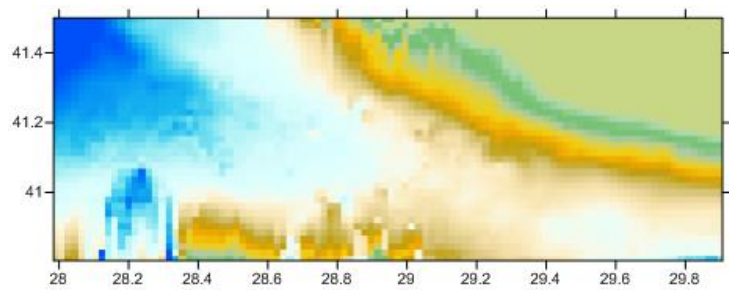
**Figure 4.9 (continued):** The contour maps of Istanbul GPS/leveling geoid based on various gridding methods.



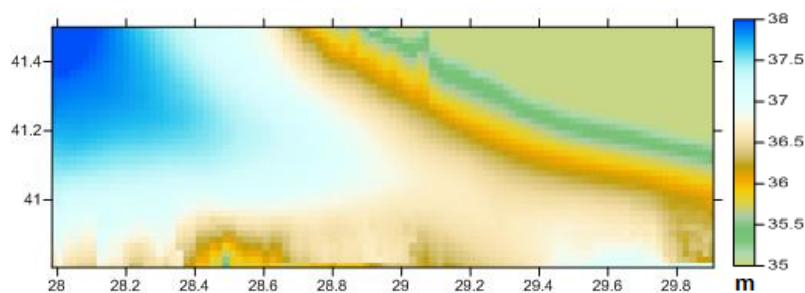
**(i.3)** Radial Basis Function – Multiquadratic



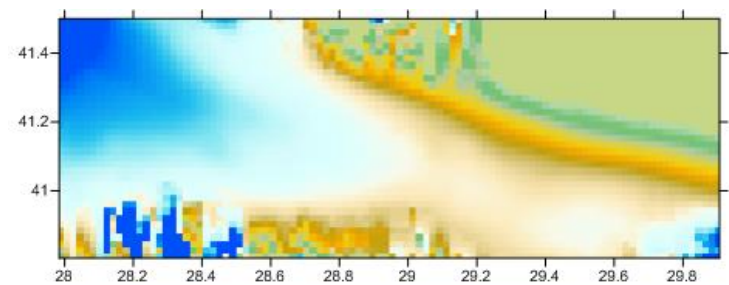
**(i.4)** Radial Basis Function – Natural Cubic Spline



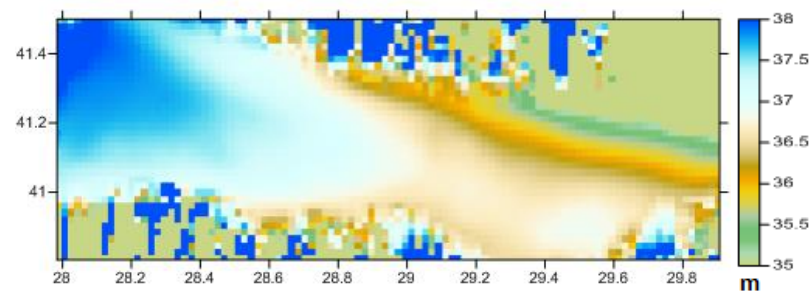
**(i.5)** Radial Basis Function – Thin Plate Spline



**(j.1)** Local Polynomial - First Order



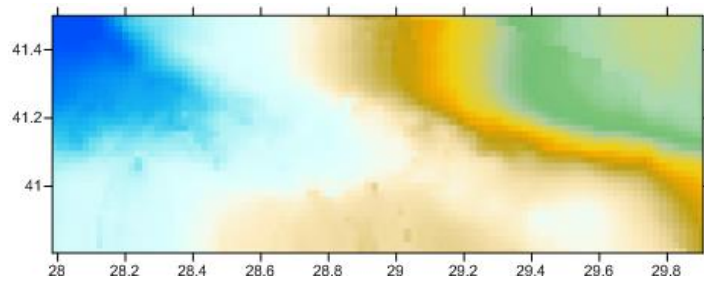
**(j.2)** Local Polynomial - Second Order



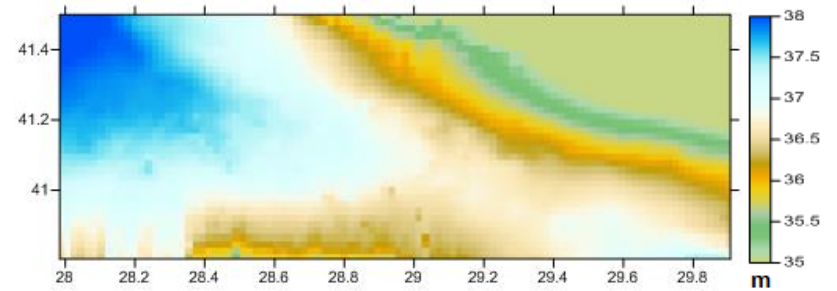
**(j.3)** Local Polynomial - Third Order

**Figure 4.9 (continued):** The contour maps of Istanbul GPS/leveling geoid based on various gridding methods.

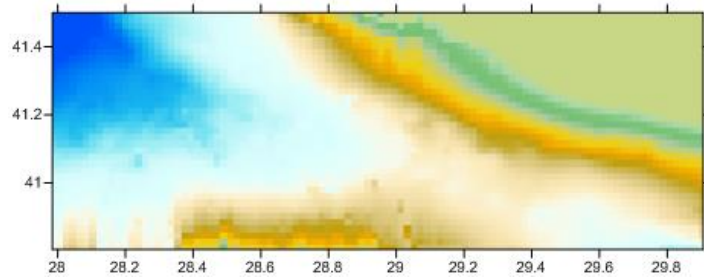




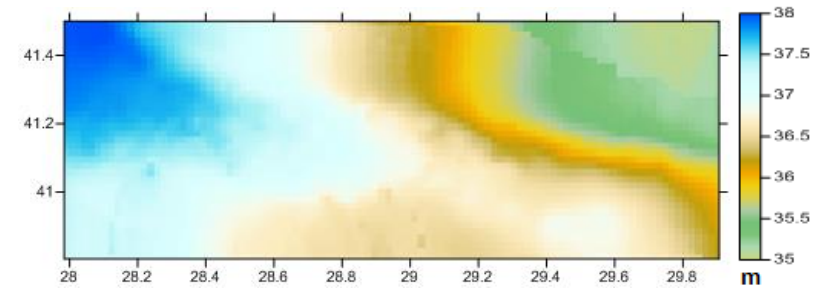
**(k.1)** Point Kriging - No Drift



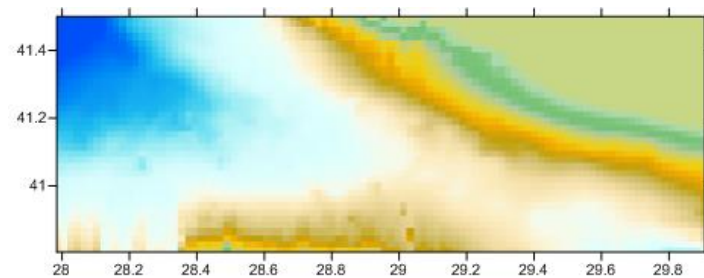
**(k.2)** Point Kriging- Linear Drift



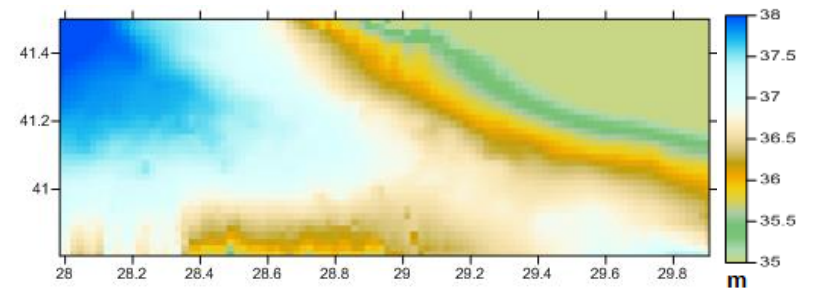
**(k.3)** Point Kriging- Quadratic Drift



**(k.4)** Block Kriging – No Drift



**(k.5)** Block Kriging – Linear Drift



**(k.6)** Block Kriging – Quadratic Drift

**Figure 4.9 (continued):** The contour maps of Istanbul GPS/leveling geoid based on various gridding methods.

In order to evaluate the gridding method performances, two methods are used:

- a) Cross validation methods are performed in Surfer and statistics belong to residual (N) values are obtained.
- b) After gridding process with 1151 geoid reference points, these points are interpolated by using four different interpolation methods (Linear, Nearest, Cubic and Spline interpolations), and minimum, maximum, mean, standard deviation and root mean square error values are considered.

The applied cross validation methodology is a statistical evaluation procedure for model performance. In this method, the initial point is described as the ‘new point’ and model parameters are estimated by using the rest of the points. By using the model, the residual at new point is estimated and this estimated value is compared with an error of closure belongs to known height at the same point. This operation is repeated with each of the new point till the end of the evaluation considering each point as new in data set. The root mean square error (RMSE) of the cross validation is calculated by using following equation (Harvey, 1991).

$$m_{aver.} = \frac{1}{n} \sum_{i=1}^n \sqrt{\mu_i^2 + \sigma_i^2} \quad (4.1)$$

where the average RMSE is referred as  $m_{aver.}$ ,  $n$  is the iteration number,  $\sigma$  is the standard deviation and  $\mu_i$  is the mean value of the evaluated residuals. To sum up, cross validation algorithm, which removes sample points and interpolates to the removed location, is an effective way to compare interpolation methods (Mitas and Mitasova, 1999).

In order to assess model accuracy objectively, gridded data with 1151 points are interpolated with linear, nearest, cubic and spline interpolation by using 50 test points. The interpolation results on gridded data are evaluated and illustrated in Appendix (see Tables A.2-A.5). In the process of gridding the geoid reference points with polynomial regression – cubic surface method, the error “The system of regression equations is singular” is occurred. Therefore, geoid reference points and test points are both required to be normalized.

Linear, nearest and cubic interpolation methods are applied to gridded data, which is performed with triangulation with linear interpolation, by using both Surfer and

Matlab codes, respectively. This can be seen on the Table A.2 belongs to linear interpolation that there is 1.2 cm difference on the result of standard deviation at reference points while this result is 0.2 cm at test points. These differences at test points are 1.0 cm for nearest interpolation and 18.5 cm for cubic interpolation. The different triangulation geometry and using different reference points for estimation may cause that standard deviation differences. As a last; linear, nearest, cubic and spline interpolation plots are given in Appendix (see Figures B.1-B.4).

According to linear interpolation results given in Table A.2, the gridded data performed by biharmonic spline interpolation gives the most accurate results. Geoid undulation residuals at reference benchmarks vary between -10.8 cm and 10.3 cm, and standard deviation is 1.2 cm. The values at test benchmarks vary between -6.4 cm and 9.1 cm, and standard deviation at these benchmarks is 3.2 cm. On the other hand, moving average method whose RMSE value at reference and test benchmarks are 41.3 cm and 38.7 cm respectively, gives the worst result.

When considering nearest interpolation results in Table A.3, triangulation with linear interpolation gridding method (in matlab) gives the most accurate results. Geoid undulation residuals at test benchmarks vary between -6.8 cm and 9.5 cm, and standard deviation is 3.2 cm.

This can be seen on Table A.4 that, the gridded data performed by triangulation with linear interpolation in Matlab gives the most accurate result for cubic interpolation. Geoid undulation residuals at test benchmarks vary between -5.6 cm and 9.7 cm, and standard deviation is 3.0 cm.

According to Table A.5, point Kriging (linear drift) and point Kriging (quadratic drift) gridding methods give the best results for spline interpolation. Geoid undulation residuals at test benchmarks vary between -6.1 cm and 8.8 cm, and standard deviation is 3.1 cm for both methods.

The worst results for the models belong to moving average method for all interpolation techniques with 38.7 cm RMSE error at test benchmarks.



## 5. CONCLUSION

In this study, different interpolation algorithms are used to estimate GPS/leveling surface in Istanbul Metropolitan area. Due to the fact that there is no regional geoid within cm accuracy in Turkey, local GPS/leveling geoids are determined and performed in limited areas by using more dense data in transformation of GNSS ellipsoidal heights into orthometric heights in regional vertical datum. In order to determine local GPS/leveling geoid; the density, distribution and quality of the reference data are described in Large Scale Map and Spatial Data Production Regulation (2005, article 42). In addition to property of geoid reference points, interpolation method also has significant role in the accuracy of the determined model.

Spatial interpolation methods are not only used for geoid modelling applications in geodesy, but also used for most of the geoscience applications. Therefore, the research study for theoretical and numerical comparison of interpolation methods in literature, contributes the activities about this topic cardinally.

Within this study, different interpolation methods in literature are examined for local geoid determination and the drawn conclusions follow:

- In consideration of the statistics in Table A.1, cross-validation results of 12 interpolation methods, geoid undulation differences obtained from examination at reference and test points provide consistent results in general. The cross-validation statistics given in Table A.1, demonstrate the consistence of computed grid values within themselves. In the light of cross-validation results, this can be said that all of the methods except minimum curvature, polynomial regression (simple planar surface, bilinear saddle, quadratic surface) and moving average have standard deviation value approximately between the ranges of 5.5 cm – 9.0 cm.
- The performances of grid models, which have 1 arc minute resolution, obtained from different interpolation methods are evaluated at reference and

test points, respectively. The spatial resolution of the determined grid is chosen 1 arc minute considering the density of the geoid reference points as 4.5 km, which approximately corresponds to 1 arc second. In the process of these evaluations; linear, nearest, cubic and spline interpolation algorithms are applied on gridded data, which has 1' resolution, and obtained values are compared with observation values at the benchmarks. The interpolation methods, which are used to estimate grid values, are exact interpolator (more details about exact interpolator can be found in previous chapters).

- In consequence of assessments for linear interpolation at reference and test points, **biharmonic spline interpolation** gives the most accurate result. According to the statistics obtained with this method, geoid undulation residuals at reference benchmarks vary between -10.8 cm and 10.3 cm, and standard deviation is 1.2 cm. The geoid undulation residuals at test benchmarks vary between -6.4 cm and 9.1 cm, and standard deviation at these benchmarks is 3.2 cm. When considering statistics belong to biharmonic spline interpolation method, this is clear that the generated model can be used for 3<sup>rd</sup> order vertical control purposes in engineering projects that require height information better than 5 cm accuracy.
- The worst result according to statistics belongs to the model points that are estimated via **moving average method**. The accuracies (RMSE) of this grid model at reference and test benchmarks are 41.3 cm and 39.1 cm, respectively. The reason for this result is that the moving average method does not include the weighting procedure base on the distance among the data and interpolation point, and it assumes all the reference benchmark contribution as equally weighted. However, the geoid phenomenon is strongly correlated with distributions of the masses hence the geoid undulation of an interpolation point is strongly related with the data in the nearest territory. Therefore, un-weighted interpolation algorithms and the method that consider the entire computation area as a whole are not appropriate for geoid modelling.
- **Triangulation with linear interpolation (in Matlab)** gives the most accurate results for nearest interpolation at test points. According to the statistics obtained with this method, geoid undulation residuals at test

benchmarks vary between -6.8 cm and 9.5 cm, and standard deviation is 3.2 cm. When considering the statistics, as expected, the worst result belongs to the model that is estimated via moving average method. The accuracy (RMSE) of this grid model at test benchmarks is 39.1 cm. Hence the natural neighbor method reveals an almost 99% of improvement in terms of standard deviation comparing the **moving average method**.

- In the evaluation of cubic interpolation results at test points, this can be said that **triangulation with linear interpolation**, which is applied by Matlab codes, gives the most accurate result. According to the statistics obtained with this method, geoid undulation residuals at test benchmarks vary between -5.6 cm and 9.7 cm, and standard deviation is 3.0 cm. The worst result according to statistics belongs to the model that is estimated via **moving average method**. The accuracy (RMSE) of this grid model at test benchmarks is again 39.1 cm.
- According to the spline interpolation results at test points, **point Kriging (linear drift) and point Kriging (quadratic drift)** give the best results. Geoid undulation residuals at test benchmarks vary between -6.1 cm and 8.8 cm, and standard deviation is 3.1 cm for both methods. On the other hand, the worst method is **moving average** with 39.1 cm RMSE value.
- The development of this research study with finite element and soft computing methods, which are available in the literature and getting popular day by day in geodetic applications, and the use of different data sets except geoid are planned as the future work.
- When considering from the viewpoint of geodesy discipline, the highly accurate geoid model is an essential part of geodetic infrastructure. The local GPS/leveling geoids provide short-term and limited solution for the problem in height transformation. Therefore; regional geoid, whose accuracy is within cm, have to be performed across the country. In future years, this is planned to contribute to studies for computing regional geoid model.





## BIBLIOGRAPHY

- Ayan, T., Deniz, R., Arslan, E., Çelik, R. N., Denli, H. H., Akylmaz, O., Özşamlı, C., Özlüdemir, M. T., Erol, S., Erol, B., Acar, M., Mercan, H., Tekdal, E.** (2006). Istanbul GPS Nirengi Ağı (İGNA) 2005-2006 Yenileme Ölçü ve Değerlendirmesi. Istanbul Technical University Report, Volume 1, Istanbul. (In Turkish)
- Ayar, A.** (2009). Non Sibson Enterpolasyon Yöntemiyle Yerel Geoit Belirlenmesi, MSc Thesis, Istanbul Technical University, Turkey.
- Ayhan, M. E., Bank, E., Lenk, O. and Şeker, H.A.** (1987). South Western Anatolia (Agean Region) Doppler Geoid. *Bulletino di Geoid. E Sc. Affini Anno XLVI*, 4, 293-308.
- Chang, K. –T.** (2008). *Introductiim to Geographic Information System* (4th ed.). McGraw-Hill, Boston.
- Deniz, R. and Ayan, T.** (2002). *Physical Geodesy Lecture Notes*. Istanbul Technical University, Istanbul.
- Deniz, R., Çelik, R. N. (Eds.),** (2005). *Açıklamalı ve Örneklemeli Büyük Ölçekli Harita ve Harita Bilgileri Üretim Yönetmeliği*. HKMO Yayınları, Ankara, pp 86.
- de Smith, M. J., Goodchild, M. F. and Longley, P.A.** (2015). *A comprehensive Guide to Principles, Technqiues and Software Tools. Geospatial Analysis* (5th ed.), The Winchelsea Press, Winchelsea, UK.
- Direnç, A., Simav, M., Türkezzer, A., Kurt, A. İ., Kurt, M.** (2012). Türkiye’de Jeoit Belirleme Çalışmaları, Turkish National Geodesy Comission, TUYS Modernization Workshop, Zonguldak, March 28-30.
- Dressler, M.** (2009). *Art of Surface Interpolation*, Kunštát. Retrieved from <http://m.dressler.sweb.cz/AOSIM.pdf>, (March, 2016)
- Erol, B.** (2007). *Investigations on Local Geoids for Geodetic Applications*, PhD Thesis, Istanbul Technical University, Turkey.
- Erol, B.** (2016). Personal Interview, 27.04.2016, Istanbul Technical University.
- Ghanem, E. and Jiancheng, L.** (2000). Discussion on Some FFT Problems to Determine The Geoid, *Geo-Spatial Information Science*, 3:2, 53-57.
- Harvey, B. R.,** (1991). *Practical Least Squares and Statistics for Surveyors*, The School of Surveying, University of New South Wales, Kensington, N. S. W.
- Heiskanen, W. A., Moritz, H.** (1967). *Physical Geodesy*. Institute of Physical Geodesy, Technical University. Graz, Austria.
- Hofmann-Wellenhof, B. and Moritz, H.** (2005). *Physical Geodesy*. Springer-Verlag, Wien.

- Ince, E. S.** (2011). Geoid Investigations for the New Vertical Datum in Canada, MSc Thesis, University of Calgary, Canada. Retrieved from <http://www.geomatics.ucalgary.ca/graduatetheses>, (February, 2016).
- Isaaks, E. H. and Srivastava, R. M.,** (1989). An Introduction to Applied Geostatistics. Oxford University Press, Oxford.
- Jekeli, C.** (2000). Heights, the Geopotential, and Vertical Datums. 459, Ohio State University Reports, Geodetic Science and Surveying, Department of Civil and Environmental Engineering and Geodetic Science, Columbus, Ohio.
- Kavzoglu, T. and Saka, M. H.** (2005). Modelling Local GPS/Leveling Geoid Undulations Using Artificial Neural Networks. *Journal of Geodesy*, 78, 520-527.
- Li, J. And Heap, A. D. (2008).** A Review of Spatial Interpolation Methods for Environmental Scientists. *Geoscience Australia, Record 2008/23*, 137 pp.
- Mitas, L. and Mitasova, H.** (1999). Spatial Interpolation. In *Geographical Information Systems: Principles, Techniques, Management and Applications*, edited by Longley, P., Goodchild, M. F. And Rhind, D. W, Volume 1, 481-492.
- Olea, R. A.** (1999). *Geostatistics for Engineers and Earth Scientists*, Kluwer Academic Publishers.
- Robeson, S. M.** (1997). Spherical Methods for Spatial Interpolation: Review and Evaluation. *Cartography and Geographic Information Systems*, 24, 3-20.
- Roman, D. N.** (2007). Datums, Heights and Geodesy, Central Chapter of the Professional Land Surveyors of Colorado 2007 Annual Meeting
- Sandwell, D. T.** (1987). Biharmonic Spline Interpolation of Geos-3 and Seasat Altimeter Data. *Geophysical Research Letters*, 14: 2, 139-142.
- Sen, A. and Srivastava, R. M.** (1990). *Regression Analysis: Theory, Methods and Applications*. Springer Texts in Statistics, Springer, New York.
- Siu, N. and Lam N.** (1983). Spatial Interpolation Methods: A Review. *The American Cartographer*, 10: 2, 129-149 pp.
- Skiena, S. S.** (2008). *The Algorithm Design Manual* (2nd ed.), Springer-Verlag, London.
- Soycan, M. and Soycan, A.** (2003). Surface Modeling for GPS/Leveling Geoid Determination. *International Geoid Service*, 1:1, 41-51.
- Sutton, T., Dassau, O. And Sutton, M.** (2009). A Gentle Introduction to GIS. Chief Directorate: Spatial Planning & Information, Department of Land Affairs, Eastern Cape, South Africa.
- Thacker, W. I., Zhang, J., Watson, L. T., Birch, J. B., Iyer, M. A. and Berry, M. W.** (2009). Algorithm XXX: SHEPPACK: Modified Shepard Algorithm for Interpolation of Scattered Multivariate Data, Association for Computing Machinery.
- Torge, W.** (2001). *Geodesy* (3rd ed.). Walter de Gruyter, Berlin New York.
- Türkezer, A., Simav, M., Sezen, E., Direnç, A., Kurt, M., Lenk, O.** (2011).

Türkiye Yükseklik Sisteminin Modernizasyonu. UCTEA Chamber of Survey and Cadastre Engineers, 13. Turkish Scientific and Technical Mapping Symposium, Ankara, Turkey. April 18-22. (in Turkish)

- Yang, C. S., Kao, S. P., Lee, F. B. and Hung, P. S.** (2012). Twelve Different Interpolation Methods: A Case Study of Surfer 8.0. International Society for Photogrammetry and Remote Sensing (ISPRS) Congress, Volume XXXV.
- Yıldız, H.** (2012). Height Modernization Approach: An Evaluation For Turkey. Mapping Journal, 147. (in Turkish)
- Yılmaz, M. and Arslan, E.** (2005). Geoit Belirleme Yöntemleri. UCTEA Chamber of Survey and Cadastre Engineers, 10. Turkish Scientific and Technical Mapping Symposium, Ankara, Turkey, March 28-April 1. (in Turkish)
- Yılmaz, M. and Arslan, E.** (2006). Istanbul Metropolitan Alanında Geoit Araştırması. ITU Journal, 5: 3, 107-114. in Turkish
- URL1-** Turkish Hybrid Geoid. General Command of Mapping. Retrieved from <http://www.hgk.msb.gov.tr/english/p-6-turkish-geoid.html>, (February, 2016).
- URL 2-** Spatial Interpolation Techniques. National University of Ireland, Maynooth. Retrieved from <http://www.nuim.ie/staff/dpringle/gis/gis09.pdf>, (February, 2016).
- URL3-** An Introduction to Interpolation Methods. Retrieved from <http://pro.arcgis.com/en/pro-app/help/analysis/geostatistical-analyst/an-introduction-to-interpolation-methods.htm>, (February, 2015)
- URL4-** Delaunay Triangulations. Retrieved from <http://www.computational-cad.com/help/NetHelp/default.htm?url=Documents%2Ftheory.htm>, (March, 2016).
- URL5-** A Basic Understanding of Surfer Gridding Methods. Golden Software Newsletter. Retrieved from <http://www.goldensoftware.com/newsletter/issue71-surfer-gridding-methods-part1>, (March, 2016).
- URL6-** Time Series Methods. Retrieved from <http://www.prenhall.com/divisions/bp/app/russellcd/PROTECT/CHAPTERS/CHAP10/HEAD03.HTM>, (April, 2016).
- URL7-** Geostatistics in Hydrology: Kriging Interpolation. Retrieved from <http://www.dmsa.unipd.it/~berga/Teaching/STAM/stat.pdf>, (March, 2016).
- URL8-** How Kriging Works. Retrieved from [http://desktop.arcgis.com/en/arcmap/10.3/tools/3d-analyst-toolbox/how-kriging-works.htm#ESRI\\_SECTION1\\_E112B7FAED26453D8DA4B9AEC3E4E9BE](http://desktop.arcgis.com/en/arcmap/10.3/tools/3d-analyst-toolbox/how-kriging-works.htm#ESRI_SECTION1_E112B7FAED26453D8DA4B9AEC3E4E9BE), (April, 2016).
- URL9-** Sandwel, D. T. Scripps Institution of Oceanography University, University of California. <ftp://topex.ucsd.edu/pub/>, (February, 2016).



## **APPENDICES**

- APPENDIX A:** The cross validation statistics and the results of linear, nearest, cubic and spline interpolation on gridded data
- APPENDIX A.1:** The cross validation statistics
- APPENDIX A.2:** Linear interpolation results belong to different gridding methods
- APPENDIX A.3:** Nearest interpolation results belong to different gridding methods
- APPENDIX A.4:** Cubic interpolation results belong to different gridding methods
- APPENDIX A.5:** Spline interpolation results belong to different gridding methods
- APPENDIX B:** Linear, nearest, cubic and spline interpolation plots
- APPENDIX B1:** Nearest interpolation plots on gridded data
- APPENDIX B2:** Nearest interpolation plots on gridded data
- APPENDIX B3:** Cubic interpolation plots on gridded data
- APPENDIX B4:** Spline interpolation plots on gridded data

## APPENDIX A

**Table A.1:** The cross validation statistics

	<b>Min</b>	<b>Max</b>	<b>Mean</b>	<b>Std</b>	<b>Rmse</b>
<b>INVERSE DISTANCE to a POWER</b>	-34.8	49.7	0.0	6.1	6.1
<b>POINT KRIGING No Drift</b>	-34.8	50.9	0.0	4.9	4.9
<b>POINT KRIGING Linear Drift</b>	-36.5	50.9	0.0	4.8	4.8
<b>POINT KRIGING Quadratic Drift</b>	-36.5	50.9	0.0	4.8	4.8
<b>BLOCK KRIGING No Drift</b>	-36.0	50.9	0.0	4.9	4.9
<b>BLOCK KRIGING Linear Drift</b>	-36.5	50.9	0.0	4.8	4.8
<b>BLOCK KRIGING Quadratic Drift</b>	-36.5	50.9	0.0	4.8	4.8
<b>MINIMUM CURVATURE</b>	-44.4	205.9	0.3	9.1	9.1
<b>MODIFIED SHEPARD'S METHOD</b>	-35.6	50.1	-0.1	4.8	4.8
<b>NATURAL NEIGHBOR</b>	-38.3	50.6	-0.2	4.9	4.9
<b>NEAREST NEIGHBOR</b>	-52.1	50.3	0.1	7.1	7.1
<b>POLYNOMIAL REGRESSION Simple Planar Surface</b>	-75.9	66.3	0.0	20.8	20.8
<b>POLYNOMIAL REGRESSION Bi-linear Saddle</b>	-41.8	49.5	0.0	15.6	15.6
<b>POLYNOMIAL REGRESSION Quadratic Surface</b>	-43.7	48.7	0.0	9.8	9.8
<b>POLYNOMIAL REGRESSION Cubic Surface</b>	-39.4	43.5	0.0	6.8	6.8
<b>RADIAL BASIS FUNCTION Inverse Multiquadratic</b>	-37.2	50.7	0.1	5.7	5.7

**Table A.1 (continued):** The cross validation statistics

<b>RADIAL BASIS FUNCTION</b>	<b>Min</b>	<b>Max</b>	<b>Mean</b>	<b>Std</b>	<b>Rmse</b>
Multilog	-39.2	51.2	-0.1	5.4	5.4
<b>RADIAL BASIS FUNCTION</b> Multiquadratic	-45.5	51.3	0.0	5.9	5.9
<b>RADIAL BASIS FUNCTION</b> Natural Cubic Spline	-55.7	62.9	0.0	6.8	6.8
<b>RADIAL BASIS FUNCTION</b> Thin Plate Spline	-50.9	57.2	0.0	6.3	6.3
<b>TRIANGULATION WITH LINEAR INTERPOLATION</b>	-39.4	50.6	-0.2	4.9	4.9
<b>MOVING AVERAGE</b>	-80.9	126.4	0.7	41.3	41.3
<b>LOCAL POLYNOMIAL</b> 1. Order	-38.2	45.8	-2.0	5.7	6.1
<b>LOCAL POLYNOMIAL</b> 2. Order	-37.4	51.3	0.0	4.8	4.8
<b>LOCAL POLYNOMIAL</b> 3. Order	-37.7	51.7	0.0	4.7	4.7

**Table A.2:** Linear interpolation results belong to different gridding methods.

	(cm)	Min	Max	Mean	Std	Rmse
<b>INVERSE DISTANCE to a POWER</b>	Ref. Points	-42.0	28.7	0.0	3.9	3.9
	Test Points	-8.5	24.7	1.7	5.2	5.4
<b>POINT KRIGING No Drift</b>	Ref. Points	-37.8	28.7	0.0	2.9	2.9
	Test Points	-6.8	9.5	0.2	3.1	3.1
<b>POINT KRIGING Linear Drift</b>	Ref. Points	-37.8	21.2	0.1	2.9	2.9
	Test Points	-6.8	9.0	0.2	3.1	3.1
<b>POINT KRIGING Quadratic Drift</b>	Ref. Points	-37.8	21.1	0.1	2.9	2.9
	Test Points	-6.8	9.0	0.2	3.1	3.1
<b>BLOCK KRIGING No Drift</b>	Ref. Points	-37.4	23.8	0.3	3.2	3.2
	Test Points	-6.2	11.1	0.8	3.2	3.3
<b>BLOCK KRIGING Linear Drift</b>	Ref. Points	-37.5	23.8	0.5	3.1	3.2
	Test Points	-6.2	11.1	0.8	3.2	3.3
<b>BLOCK KRIGING Quadratic Drift</b>	Ref. Points	-37.5	23.8	0.5	3.1	3.2
	Test Points	-6.2	11.1	0.8	3.2	3.3
<b>MINIMUM CURVATURE</b>	Ref. Points	-29.7	22.6	0.0	3.1	3.1
	Test Points	-6.7	10.9	0.4	3.3	3.3
<b>MODIFIED SHEPARD'S METHOD</b>	Ref. Points	-31.3	20.0	0.0	2.5	2.5
	Test Points	-9.6	6.6	0.0	3.1	3.1
<b>NATURAL NEIGHBOR</b>	Ref. Points	-26.8	24.9	0.1	3.1	3.1
	Test Points	-6.4	10.7	0.4	3.2	3.2
<b>NEAREST NEIGHBOR</b>	Ref. Points	-50.8	32.6	-0.1	3.3	3.3
	Test Points	-7.8	7.3	0.2	3.3	3.3
<b>POLYNOMIAL REGRESSION Simple Planar Surface</b>	Ref. Points	-66.3	75.9	0.0	20.8	20.8
	Test Points	-39.2	76.5	9.1	20.9	22.7
<b>POLYNOMIAL REGRESSION Bi-linear Saddle</b>	Ref. Points	-49.5	41.8	0.0	15.6	15.6
	Test Points	-26.0	46.9	6.3	13.3	14.7
<b>POLYNOMIAL REGRESSION Quadratic Surface</b>	Ref. Points	-48.7	43.8	0.1	9.8	9.8
	Test Points	-18.0	36.2	2.8	9.1	9.5
<b>POLYNOMIAL REGRESSION Cubic Surface</b>	Ref. Points	-43.5	39.4	0.0	6.8	6.8
	Test Points	-27.8	18.4	-7.4	10.4	12.7



**Table A.2 (continued):** Linear interpolation results belong to different gridding methods.

<b>RADIAL BASIS FUNCTION</b>	(cm)	<b>Min</b>	<b>Max</b>	<b>Mean</b>	<b>Std</b>	<b>Rmse</b>
Inverse Multiquadratic	Ref. Points	-38.8	19.7	0.0	3.0	3.0
	Test Points	-6.3	23.4	0.9	4.5	4.5
<b>RADIAL BASIS FUNCTION</b> Multilog	Ref. Points	-37.4	18.7	0.0	2.7	2.7
	Test Points	-7.8	11.5	0.3	3.4	3.4
<b>RADIAL BASIS FUNCTION</b> Multiquadratic	Ref. Points	-35.9	18.2	0.0	2.6	2.6
	Test Points	-9.9	8.1	0.1	3.3	3.3
<b>RADIAL BASIS FUNCTION</b> Natural Cubic Spline	Ref. Points	-32.5	17.8	0.0	2.5	2.5
	Test Points	-7.1	10.0	0.1	3.3	3.3
<b>RADIAL BASIS FUNCTION</b> Thin Plate Spline	Ref. Points	-34.2	17.9	0.0	2.5	2.5
	Test Points	-6.6	8.8	0.1	3.1	3.1
<b>TRIANGULATION WITH LINEAR INTERPOLATION</b>	Ref. Points	-26.0	23.5	0.1	3.0	3.0
	Test Points	-6.6	10.0	0.4	3.1	3.1
<b>MOVING AVERAGE</b>	Ref. Points	-126.0	80.9	-0.1	41.3	41.3
	Test Points	-85.0	74.5	-0.6	39.1	39.1
<b>LOCAL POLYNOMIAL</b> 1. Order	Ref. Points	-45.2	37.6	2.0	5.5	5.9
	Test Points	-10.9	25.4	3.9	5.8	6.9
<b>LOCAL POLYNOMIAL</b> 2. Order	Ref. Points	-47.4	35.0	0.0	4.5	4.5
	Test Points	-8.4	13.2	0.4	4.1	4.1
<b>LOCAL POLYNOMIAL</b> 3. Order	Ref. Points	47.7	34.8	0.0	4.3	4.3
	Test Points	-7.7	12.6	0.3	3.9	3.9
<b>BIHARMONIC SPLINE INTERPOLATION</b>	Ref. Points	-10.8	10.3	0.0	1.2	1.2
	Test Points	-6.4	9.1	-0.1	3.2	3.2
<b>TRIANGULATION WITH LINEAR INTERPOLATION (Matlab)</b>	Ref. Points	-18.2	13.3	0.1	1.8	1.8
	Test Points	-5.6	9.7	0.1	2.9	2.9

**Table A.3:** Nearest interpolation results belong to different gridding methods.

	(cm)	Min	Max	Mean	Std	Rmse
<b>INVERSE DISTANCE to a POWER</b>	Test Points	-12.3	28.6	1.7	6.1	6.3
<b>POINT KRIGING No Drift</b>	Test Points	-9.2	12.0	0.2	4.2	4.2
<b>POINT KRIGING Linear Drift</b>	Test Points	-9.2	11.8	0.1	4.2	4.2
<b>POINT KRIGING Quadratic Drift</b>	Test Points	-9.2	11.8	0.1	4.2	4.2
<b>BLOCK KRIGING No Drift</b>	Test Points	-8.8	13.7	0.8	4.2	4.3
<b>BLOCK KRIGING Linear Drift</b>	Test Points	-8.8	13.7	0.8	4.2	4.3
<b>BLOCK KRIGING Quadratic Drift</b>	Test Points	-8.8	13.7	0.8	4.2	4.3
<b>MINIMUM CURVATURE</b>	Test Points	-9.5	11.1	0.2	4.3	4.3
<b>MODIFIED SHEPARD'S METHOD</b>	Test Points	-10.4	12.3	-0.1	4.5	4.5
<b>NATURAL NEIGHBOR</b>	Test Points	-8.6	13.5	0.4	4.2	4.2
<b>NEAREST NEIGHBOR</b>	Test Points	-15.8	10.1	0.1	5.1	5.1
<b>POLYNOMIAL REGRESSION Simple Planar Surface</b>	Test Points	-40.4	76.3	9.0	21.0	22.8
<b>POLYNOMIAL REGRESSION Bi-linear Saddle</b>	Test Points	-25.7	48.7	6.3	13.5	14.8
<b>POLYNOMIAL REGRESSION Quadratic Surface</b>	Test Points	-20.7	37.6	2.7	9.7	10.0
<b>RADIAL BASIS FUNCTION Inverse Multiquadratic</b>	Test Points	-9.0	26.2	0.8	5.4	5.4

**Table A.3 (continued):** Nearest interpolation results belong to different gridding methods.

<b>RADIAL BASIS FUNCTION</b>	(cm)	<b>Min</b>	<b>Max</b>	<b>Mean</b>	<b>Std</b>	<b>Rmse</b>
Multilog	Test Points	8.3	14.5	0.2	4.4	4.4
<b>RADIAL BASIS FUNCTION</b> Multiquadratic	Test Points	-7.7	10.7	0.0	4.3	4.3
<b>RADIAL BASIS FUNCTION</b> Natural Cubic Spline	Test Points	-7.6	11.9	-0.2	4.5	4.5
<b>RADIAL BASIS FUNCTION</b> Thin Plate Spline	Test Points	-7.2	10.6	-0.1	4.3	4.3
<b>TRIANGULATION WITH LINEAR INTERPOLATION</b>	Test Points	-8.2	12.6	0.4	4.2	4.2
<b>MOVING AVERAGE</b>	Test Points	-85.6	75.0	-0.6	39.1	39.1
<b>LOCAL POLYNOMIAL</b> 1. Order	Test Points	-13.5	27.2	4.0	6.3	7.4
<b>LOCAL POLYNOMIAL</b> 2. Order	Test Points	-10.0	15.0	0.5	4.7	4.7
<b>LOCAL POLYNOMIAL</b> 3. Order	Test Points	-10.3	14.3	0.3	4.6	4.6
<b>BIHARMONIC SPLINE INTERPOLATION</b>	Test Points	-6.8	9.5	-0.3	3.5	3.5
<b>TRIANGULATION WITH LINEAR INTERPOLATION (Matlab)</b>	Test Points	-6.8	9.5	0.0	3.2	3.2

**Table A.4:** Cubic interpolation results belong to different gridding methods.

<b>INVERSE DISTANCE to a POWER</b>	(cm)	<b>Min</b>	<b>Max</b>	<b>Mean</b>	<b>Std</b>	<b>Rmse</b>
	Test Points	-8.3	24.5	1.6	5.2	5.4
<b>POINT KRIGING No Drift</b>	Test Points	-6.1	9.3	0.1	3.2	3.2
<b>POINT KRIGING Linear Drift</b>	Test Points	-6.1	8.8	0.1	3.1	3.1
<b>POINT KRIGING Quadratic Drift</b>	Test Points	-6.1	8.8	0.1	3.1	3.1
<b>BLOCK KRIGING No Drift</b>	Test Points	-6.3	11.0	0.7	3.2	3.2
<b>BLOCK KRIGING Linear Drift</b>	Test Points	-6.3	11.0	0.7	3.2	3.2
<b>BLOCK KRIGING Quadratic Drift</b>	Test Points	-6.3	10.9	0.7	3.2	3.2
<b>MINIMUM CURVATURE</b>	Test Points	-7.4	10.3	0.3	3.4	3.4
<b>MODIFIED SHEPARD'S METHOD</b>	Test Points	-13.7	7.2	-0.3	3.9	3.9
<b>NATURAL NEIGHBOR</b>	Test Points	-225.81	74.2	-1.3	35.7	35.7
<b>NEAREST NEIGHBOR</b>	Test Points	-9.8	8.0	-0.1	3.5	3.5
<b>POLYNOMIAL REGRESSION Simple Planar Surface</b>	Test Points	-39.2	76.5	9.1	20.9	22.7
<b>POLYNOMIAL REGRESSION Bi-linear Saddle</b>	Test Points	-26.0	46.9	6.3	13.3	14.6
<b>POLYNOMIAL REGRESSION Quadratic Surface</b>	Test Points	-18.1	36.1	2.7	9.1	9.4
<b>RADIAL BASIS FUNCTION Inverse Multiquadratic</b>	Test Points	-8.6	23.4	0.8	4.6	4.7

**Table A.4 (continued):** Cubic interpolation results belong to different gridding methods.

<b>RADIAL BASIS FUNCTION</b>	(cm)	<b>Min</b>	<b>Max</b>	<b>Mean</b>	<b>Std</b>	<b>Rmse</b>
Multilog	Test Points	-11.3	11.4	0.2	3.7	3.7
<b>RADIAL BASIS FUNCTION</b> Multiquadratic	Test Points	-14.3	9.4	-0.1	3.8	3.8
<b>RADIAL BASIS FUNCTION</b> Natural Cubic Spline	Test Points	-9.1	12.7	-0.1	3.9	3.9
<b>RADIAL BASIS FUNCTION</b> Thin Plate Spline	Test Points	-8.3	11.0	-0.1	3.6	3.6
<b>TRIANGULATION WITH LINEAR INTERPOLATION</b>	Test Points	-13.9	114.2	4.7	21.0	21.5
<b>MOVING AVERAGE</b>	Test Points	-85.0	74.4	-0.6	39.1	39.1
<b>LOCAL POLYNOMIAL</b> 1. Order	Test Points	-11.0	25.7	3.8	5.8	6.9
<b>LOCAL POLYNOMIAL</b> 2. Order	Test Points	-8.1	13.2	0.3	4.2	4.2
<b>LOCAL POLYNOMIAL</b> 3. Order	Test Points	-8.0	12.3	0.2	3.9	3.9
<b>BIHARMONIC SPLINE INTERPOLATION</b>	Test Points	-6.4	9.5	-0.1	3.3	3.3
<b>TRIANGULATION WITH LINEAR INTERPOLATION (Matlab)</b>	Test Points	-5.6	9.7	0.1	3.0	3.0

**Table A.5:** Spline interpolation results belong to different gridding methods.

<b>INVERSE DISTANCE to a POWER</b>	(cm)	<b>Min</b>	<b>Max</b>	<b>Mean</b>	<b>Std</b>	<b>Rmse</b>
	Test Points	-8.3	24.5	1.6	5.2	5.4
<b>POINT KRIGING No Drift</b>	Test Points	-6.1	9.3	0.1	3.2	3.2
<b>POINT KRIGING Linear Drift</b>	Test Points	-6.1	8.8	0.1	3.1	3.1
<b>POINT KRIGING Quadratic Drift</b>	Test Points	-6.1	8.8	0.1	3.1	3.1
<b>BLOCK KRIGING No Drift</b>	Test Points	-6.3	11.0	0.7	3.2	3.2
<b>BLOCK KRIGING Linear Drift</b>	Test Points	-6.3	11.0	0.7	3.2	3.2
<b>BLOCK KRIGING Quadratic Drift</b>	Test Points	-6.3	10.9	0.7	3.2	3.2
<b>MINIMUM CURVATURE</b>	Test Points	-7.4	10.3	0.3	3.4	3.4
<b>MODIFIED SHEPARD'S METHOD</b>	Test Points	-13.7	7.2	-0.3	3.9	3.9
<b>NATURAL NEIGHBOR</b>	Test Points	-225.81	74.2	-1.3	35.7	35.7
<b>NEAREST NEIGHBOR</b>	Test Points	-9.8	8.0	-0.1	3.9	3.9
<b>POLYNOMIAL REGRESSION Simple Planar Surface</b>	Test Points	-39.2	76.5	9.1	20.9	22.7
<b>POLYNOMIAL REGRESSION Bi-linear Saddle</b>	Test Points	-26.0	46.9	6.3	13.3	14.7
<b>POLYNOMIAL REGRESSION Quadratic Surface</b>	Test Points	-18.1	36.1	2.7	9.1	9.4
<b>RADIAL BASIS FUNCTION Inverse Multiquadratic</b>	Test Points	-8.6	23.4	0.8	4.6	4.7

**Table A.5 (continued):** Spline interpolation results belong to different gridding methods.

<b>RADIAL BASIS FUNCTION</b>	(cm)	<b>Min</b>	<b>Max</b>	<b>Mean</b>	<b>Std</b>	<b>Rmse</b>
Multilog	Test Points	-11.3	11.4	0.2	3.7	3.7
<b>RADIAL BASIS FUNCTION</b> Multiquadratic	Test Points	-14.3	9.4	-0.1	3.8	3.8
<b>RADIAL BASIS FUNCTION</b> Natural Cubic Spline	Test Points	-9.1	12.7	-0.1	3.9	3.9
<b>RADIAL BASIS FUNCTION</b> Thin Plate Spline	Test Points	-8.3	11.0	-0.1	3.6	3.6
<b>TRIANGULATION WITH LINEAR INTERPOLATION</b>	Test Points	-13.9	114.2	4.7	21.0	21.5
<b>MOVING AVERAGE</b>	Test Points	-85.0	74.4	-0.6	39.1	39.1
<b>LOCAL POLYNOMIAL</b> 1. Order	Test Points	-11.0	25.7	3.8	5.8	6.9
<b>LOCAL POLYNOMIAL</b> 2. Order	Test Points	-8.1	13.2	0.3	4.2	4.2
<b>LOCAL POLYNOMIAL</b> 3. Order	Test Points	-8.0	12.3	0.2	3.9	3.9
<b>BIHARMONIC SPLINE INTERPOLATION</b>	Test Points	-6.4	9.8	0.0	3.3	3.3

## APPENDIX B

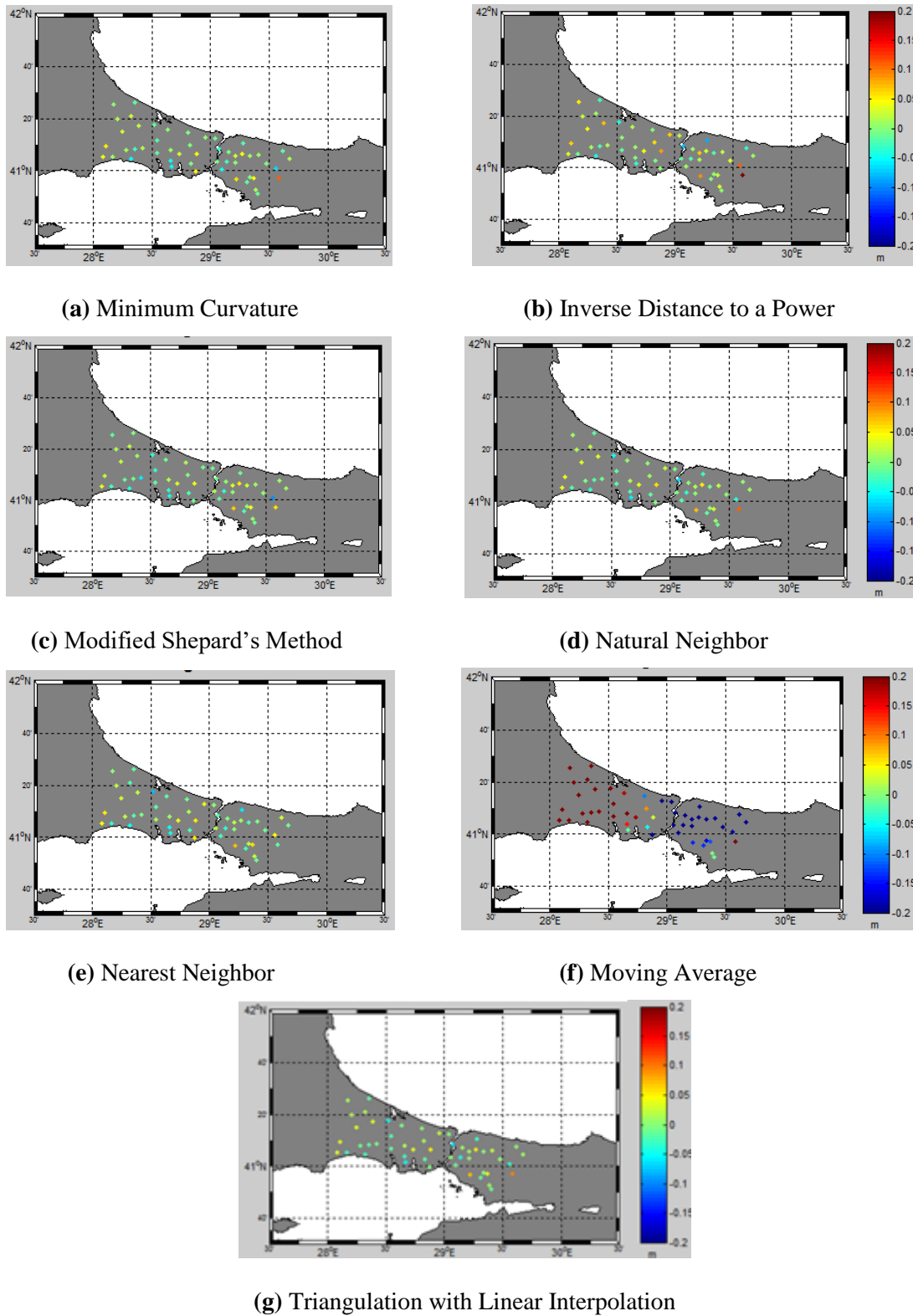
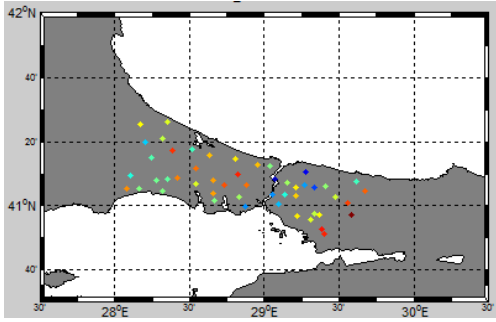
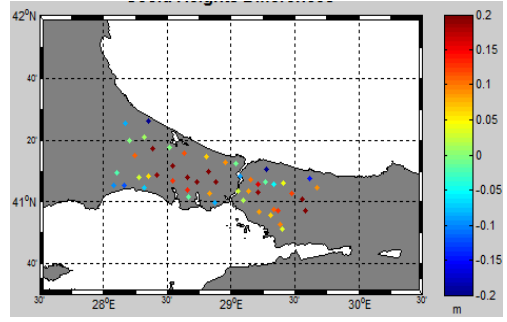


**Figure B.1:** The distribution of geoid undulation residuals at the test benchmarks depending on Linear Interpolation Algorithm.

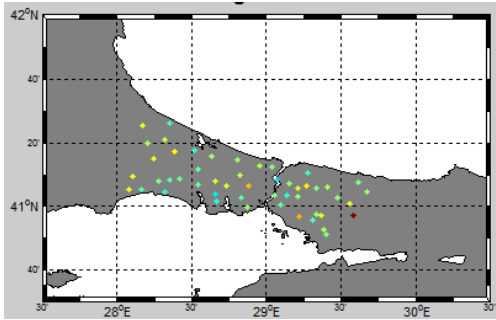




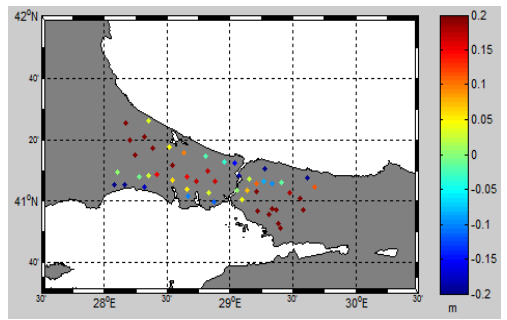
**(h.1)** Polynomial Regression- Quadratic  
Surface



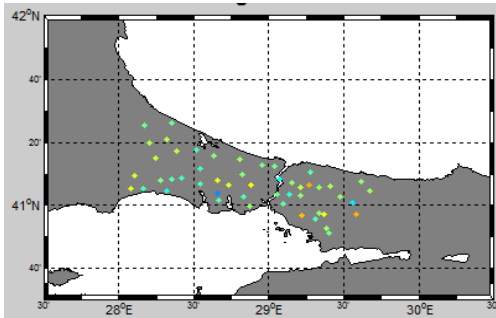
**(h.2)** Polynomial Regression- Bilinear  
Saddle



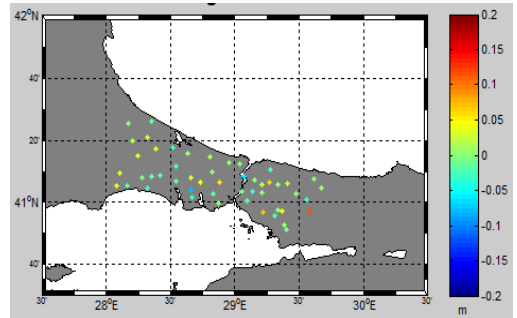
**(h.3)** Radial Basis-  
Inverse Multiquadric



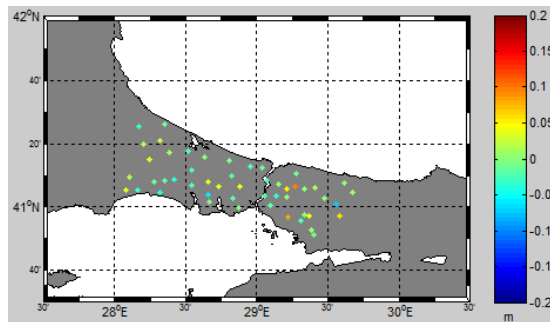
**(i.1)** Polynomial Regression-Simple  
Planar Surface



**(i.2)** Radial Basis- Multiquadric

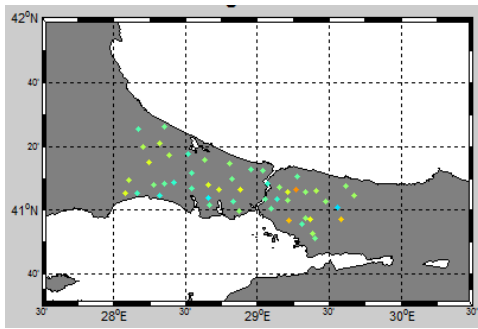


**(i.3)** Radial Basis- Multilog

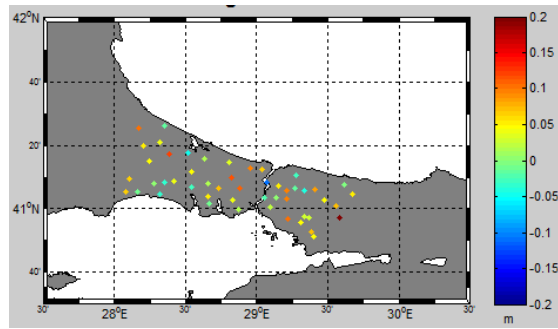


**(i.4)** Radial Basis- Natural Cubic Spline

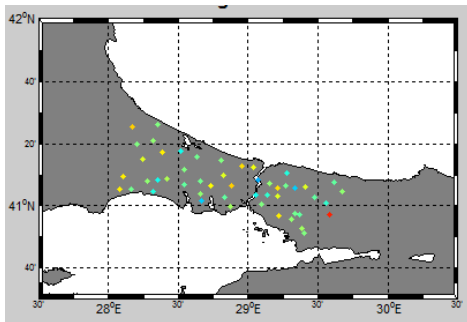
**Figure B.1 (continued):** The distribution of geoid undulation residuals at the test benchmarks depending on Linear Interpolation Algorithm.



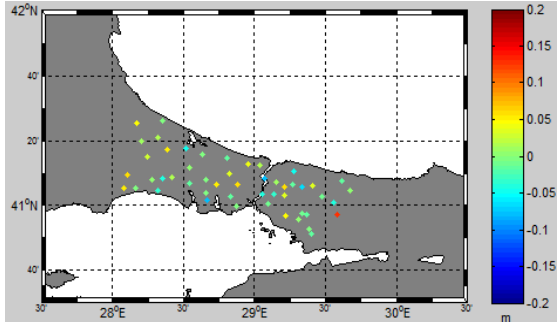
**(i.5)** Radial Basis- Thin Plate Spline



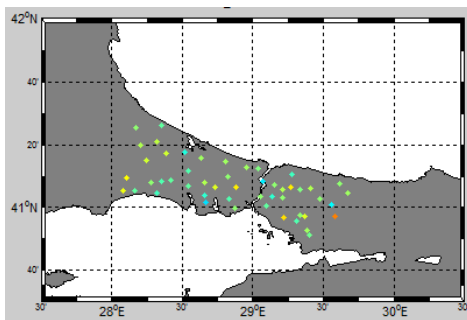
**(j.1)** Local Polynomial- 1.order



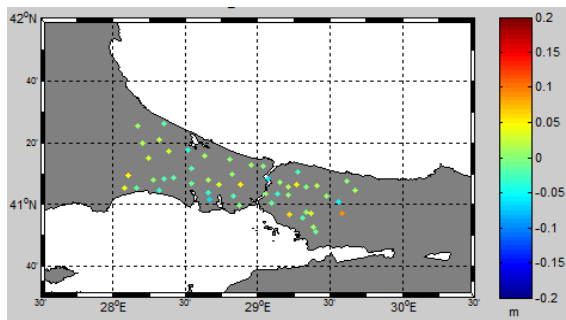
**(j.2)** Local Polynomial- 2.order



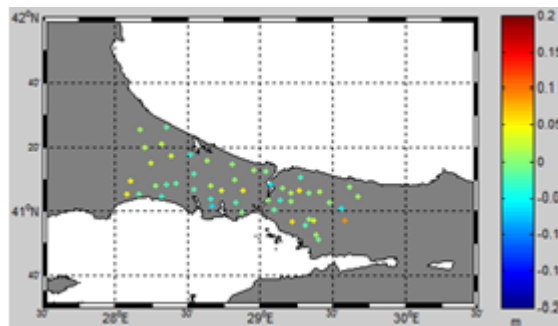
**(j.3)** Local Polynomial- 3.order



**(k.1)** Point Kriging- No Drift

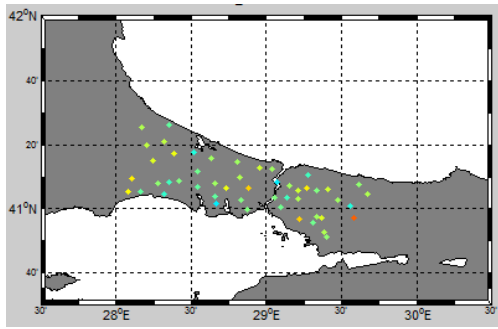


**(k.2)** Point Kriging- Linear Drift

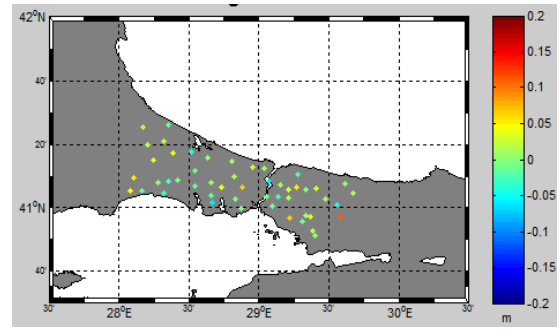


**(k.3)** Point Kriging- Quadratic Drift

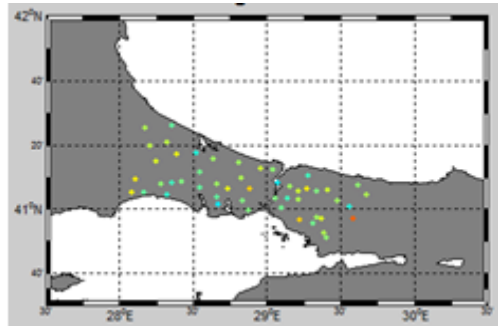
**Figure B.1 (continued):** The distribution of geoid undulation residuals at the test benchmarks depending on Linear Interpolation Algorithm.



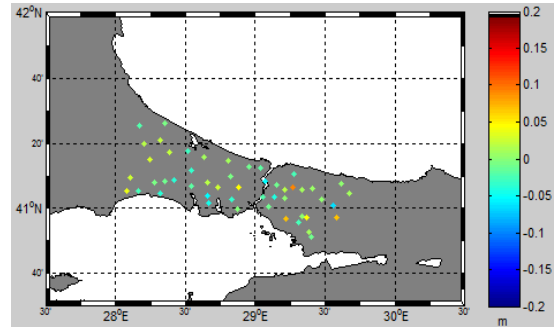
**(k.4)** Block Kriging- Linear Drift



**(k.5)** Block Kriging- No Drift

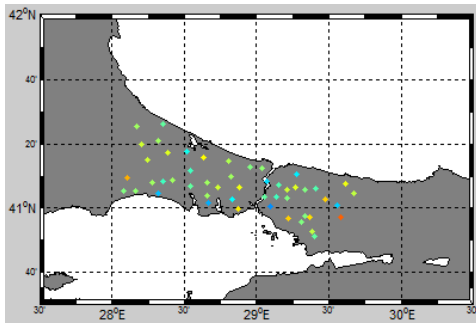


**(k.6)** Block Kriging- Quadratic Drift

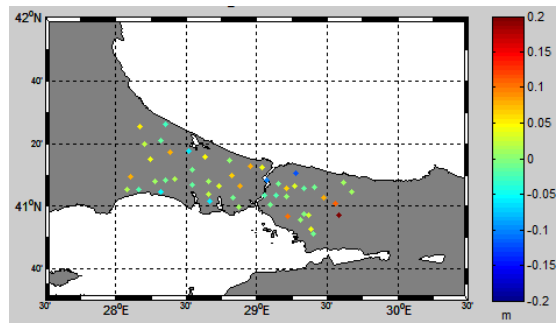


**(I)** Biharmonic Spline Interpolation

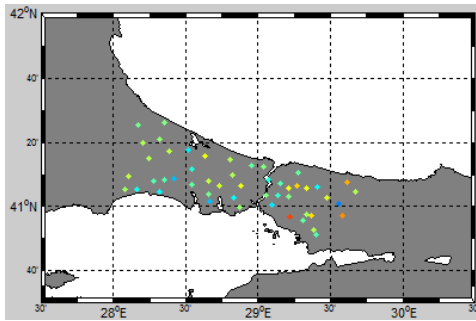
**Figure B.1 (continued):** The distribution of geoid undulation residuals at the test benchmarks depending on Linear Interpolation Algorithm.



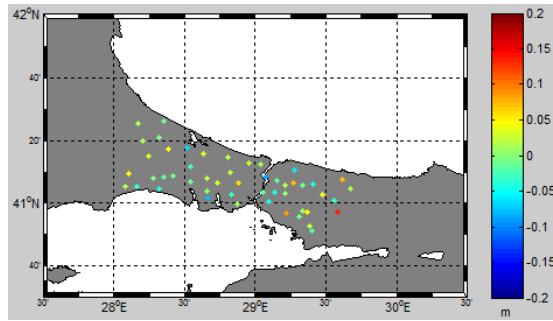
(a) Minimum Curvature



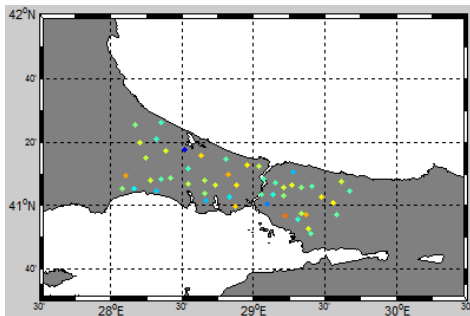
(b) Inverse Distance to a Power



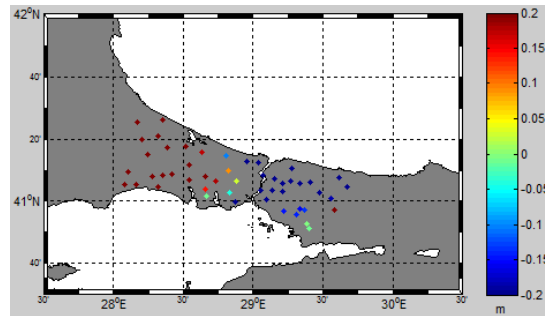
(c) Modified Shepard's Method



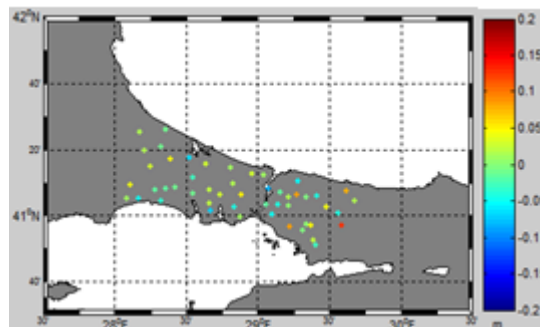
(d) Natural Neighbor



(e) Nearest Neighbor

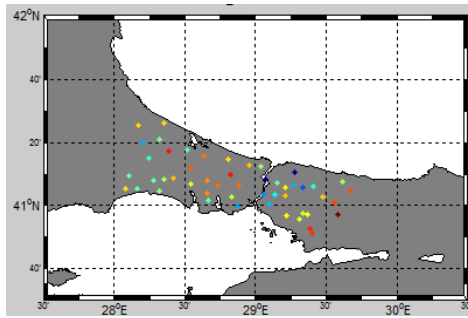


(f) Moving Average

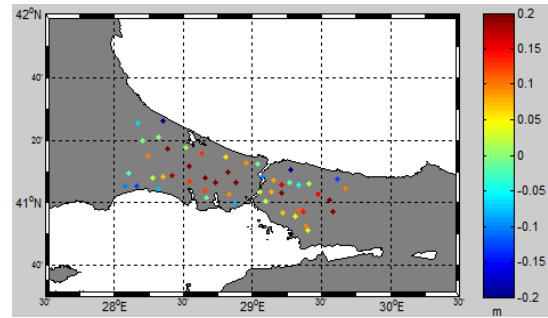


(g) Triangulation with Linear  
Interpolation

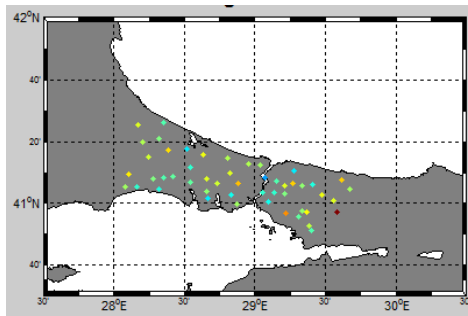
**Figure B.2:** The distribution of geoid undulation residuals at the test benchmarks depending on Nearest Neighbor Interpolation Algorithm.



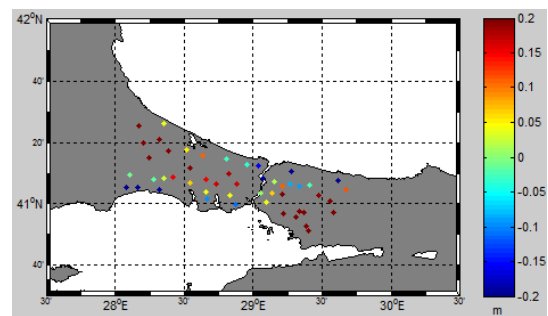
**(h.1)** Polynomial Regression-  
Quadratic Surface



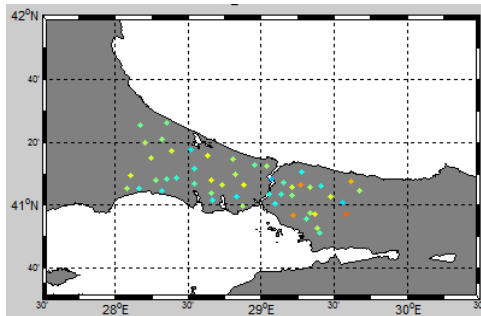
**(h.2)** Polynomial Regression- Bilinear  
Saddle



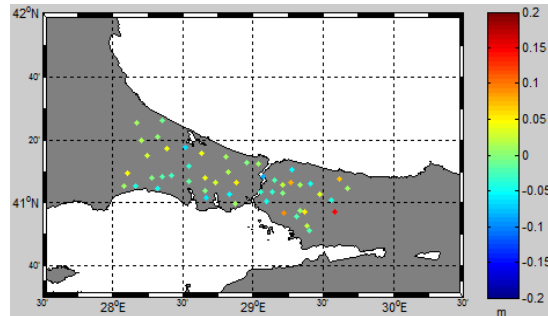
**(h.3)** Radial Basis-  
Inverse Multiquadric



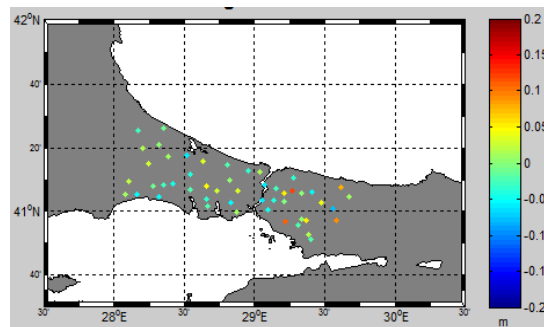
**(i.1)** Polynomial Regression-  
Simple Planar Surface



**(i.2)** Radial Basis- Multiquadric

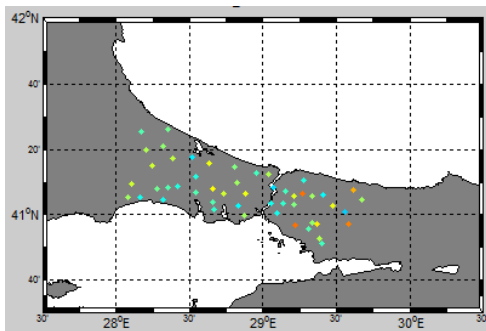


**(i.3)** Radial Basis- Multilog

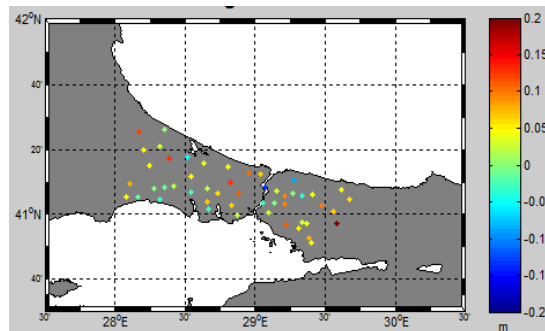


**(i.4)** Radial Basis- Natural Cubic Spline

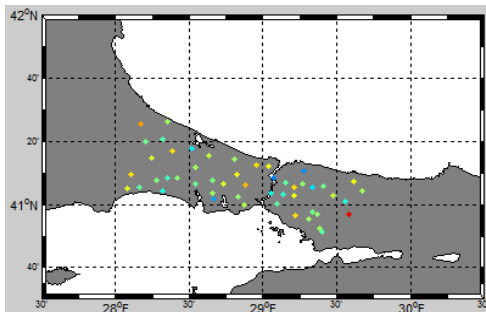
**Figure B.2 (continued):** The distribution of geoid undulation residuals at the test benchmarks depending on Nearest Neighbor Interpolation Algorithm.



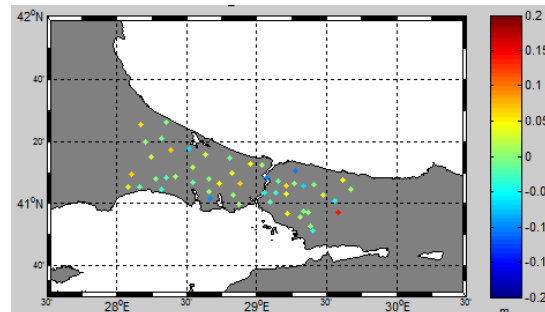
**(i.5)** Radial Basis- Thin Plate Spline



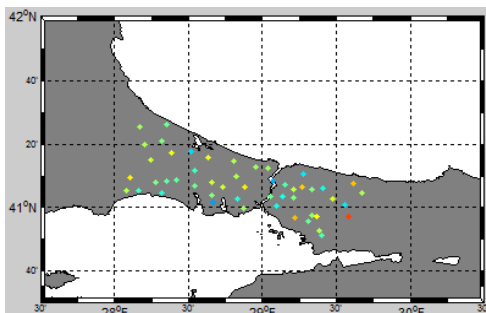
**(j.1)** Local Polynomial-1.order



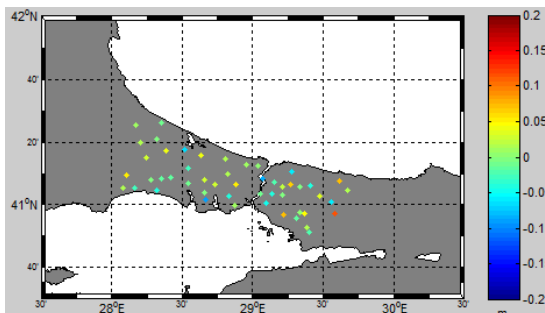
**(j.2)** Local Polynomial- 2.order



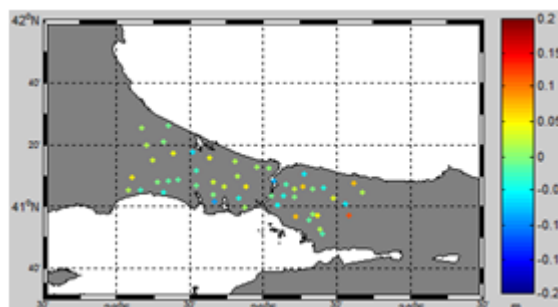
**(j.3)** Local Polynomial- 3.order



**(k.1)** Point Kriging- No Drift

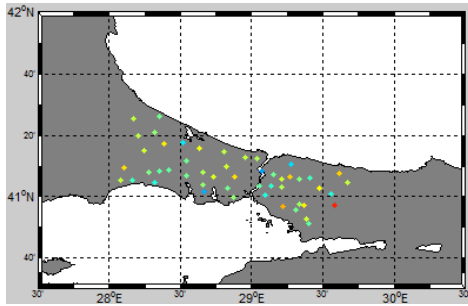


**(k.2)** Point Kriging- Linear Drift

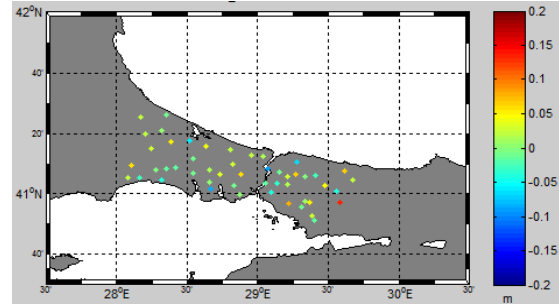


**(k.3)** Point Kriging- Quadratic Drift

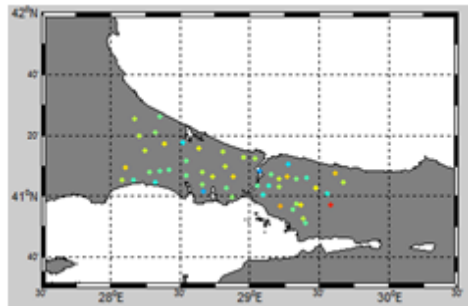
**Figure B.2 (continued):** The distribution of geoid undulation residuals at the test benchmarks depending on Nearest Neighbor Interpolation Algorithm.



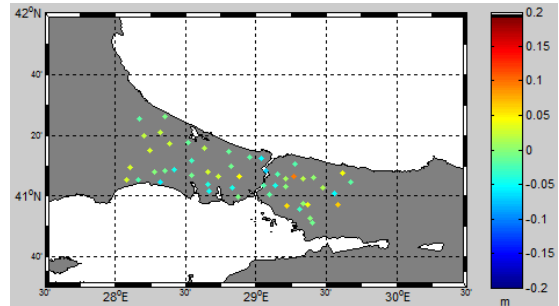
(k.5) Block Kriging- Linear Drift



(k.4) Block Kriging- No Drift

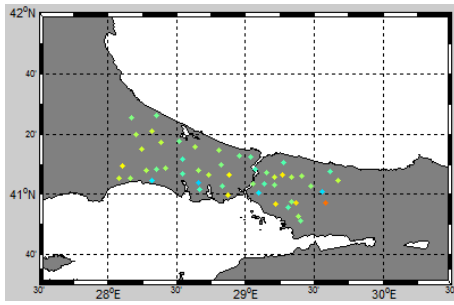


(k.6) Block Kriging- Quadratic Drift

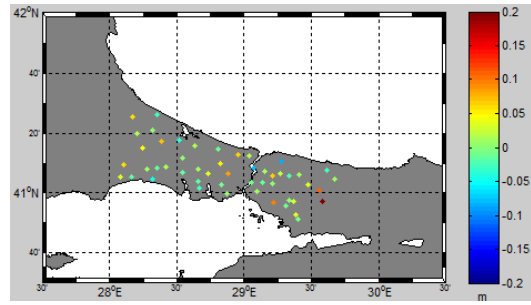


(l) Biharmonic Spline Interpolation

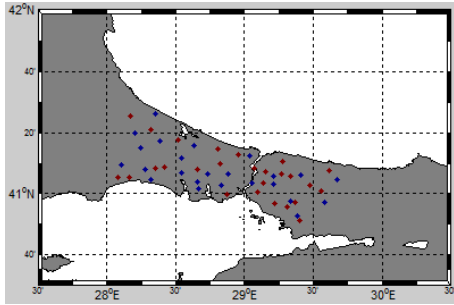
**Figure B.2 (continued):** The distribution of geoid undulation residuals at the test benchmarks depending on Nearest Neighbor Interpolation Algorithm.



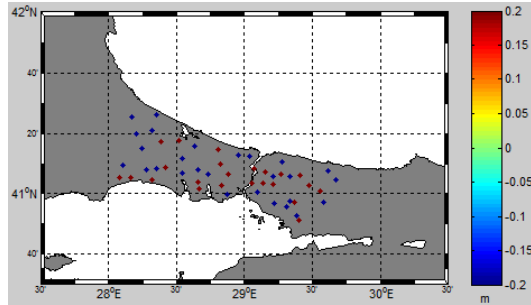
(a) Minimum Curvature



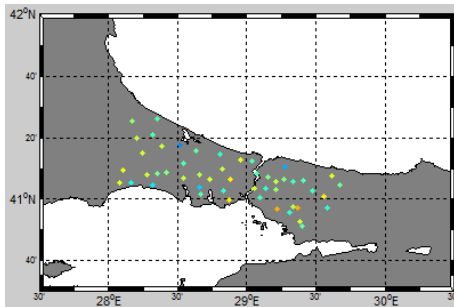
(b) Inverse Distance to a Power



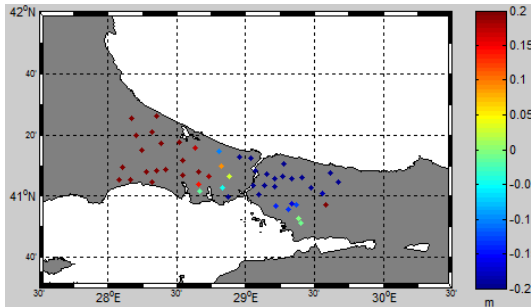
(c) Modified Shepard's Method



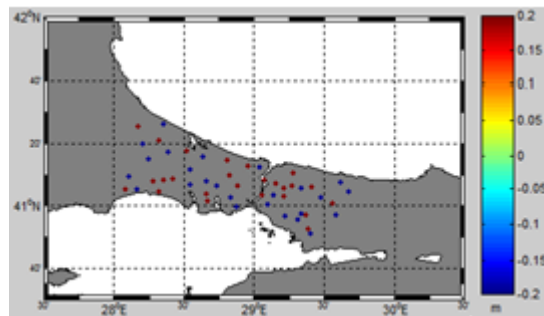
(d) Natural Neighbor



(e) Nearest Neighbor



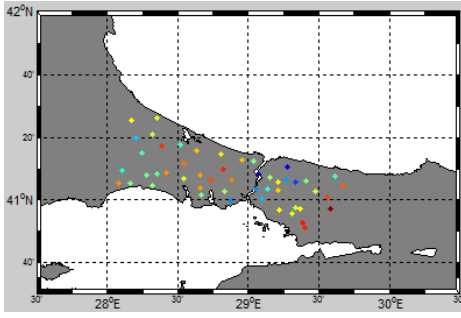
(f) Moving Average



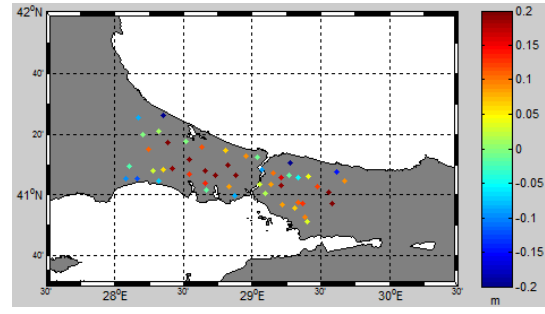
(g) Triangulation with Linear Interpolation

**Figure B.3:** The distribution of geoid undulation residuals at the test benchmarks depending on Cubic Interpolation Algorithm.

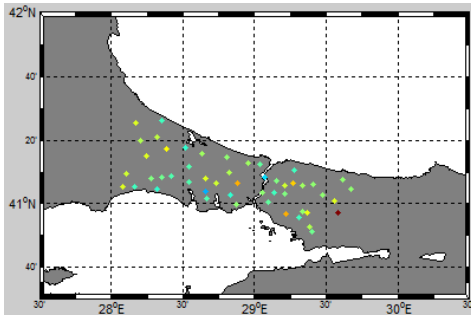




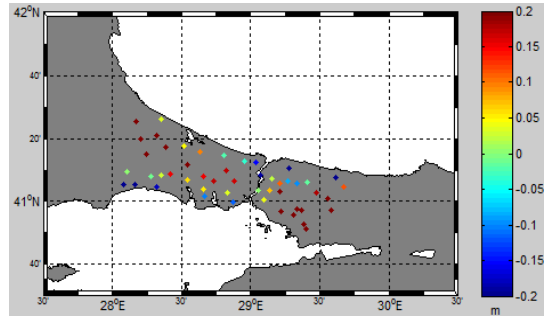
**(h.1)** Polynomial Regression-  
Quadratic Surface



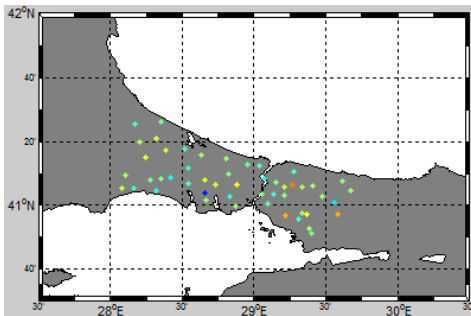
**(h.2)** Polynomial Regression- Bilinear  
Saddle



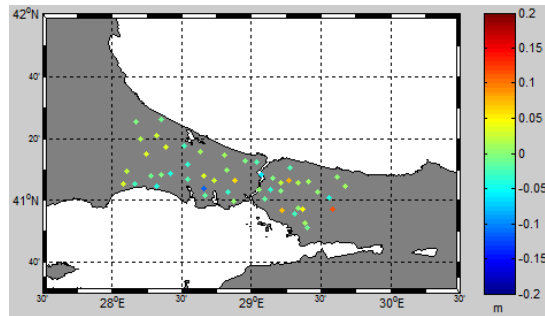
**(h.3)** Radial Basis-  
Inverse Multiquadric



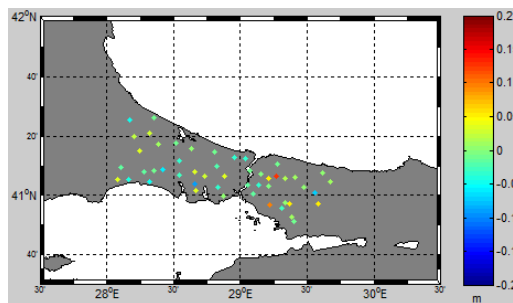
**(i.1)** Polynomial Regression-  
Simple Planar Surface



**(i.2)** Radial Basis- Multiquadric

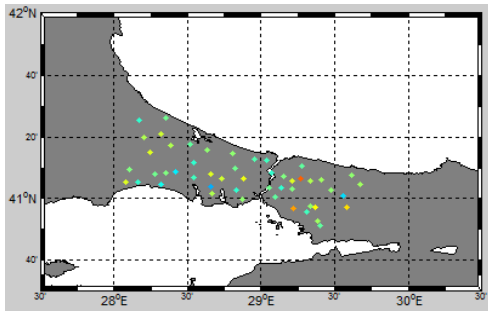


**(i.3)** Radial Basis- Multilog

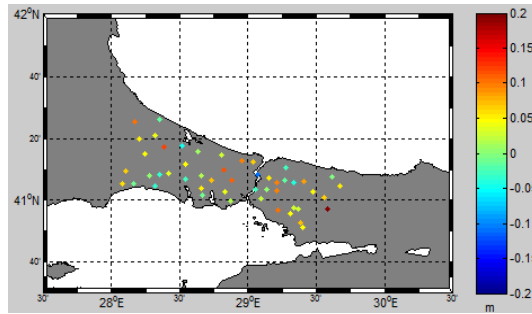


**(i.4)** Radial Basis- Natural Cubic Spline

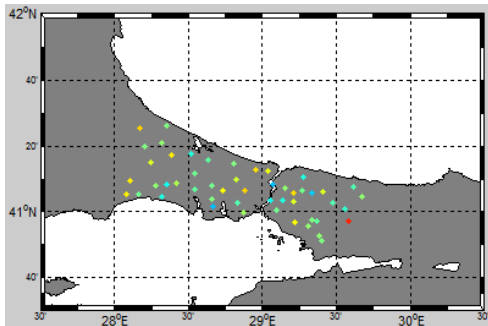
**Figure B.3 (continued):** The distribution of geoid undulation residuals at the test benchmarks depending on Cubic Interpolation Algorithm.



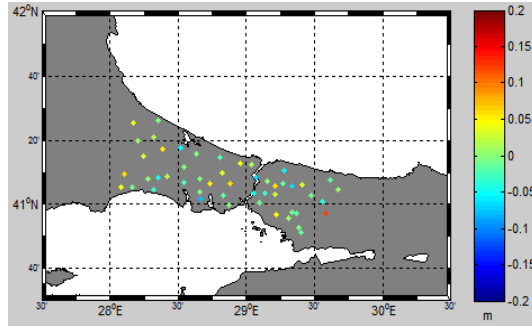
**(i.5)** Radial Basis- Thin Plate Spline



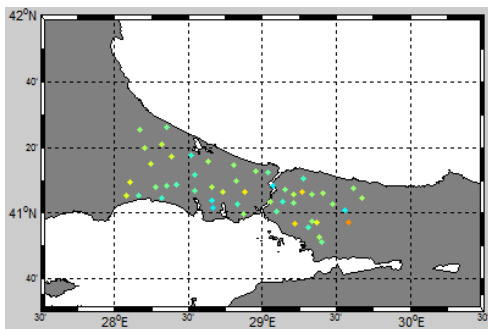
**(j.1)** Local Polynomial- 1.order



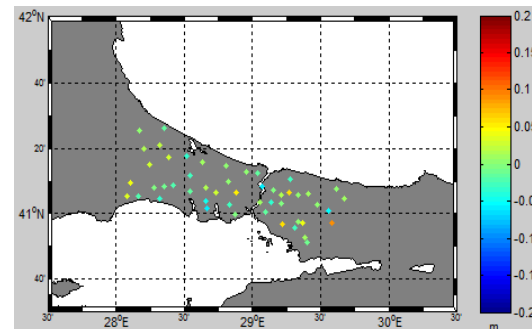
**(j.2)** Local Polynomial- 2.order



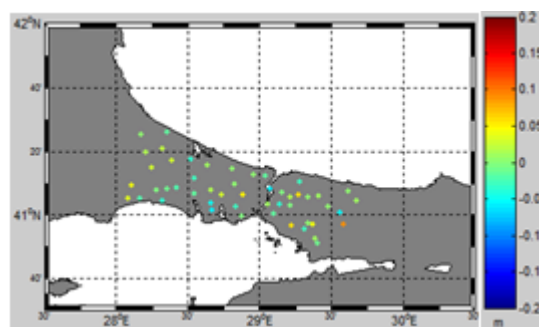
**(j.3)** Local Polynomial- 3.order



**(k.1)** Point Kriging- No Drift

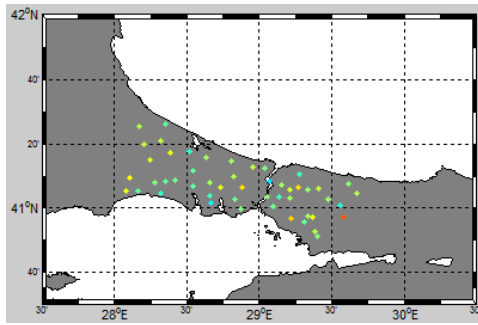


**(k.2)** Point Kriging- Linear Drift

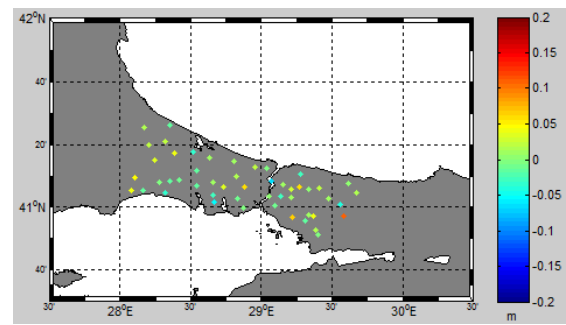


**(k.3)** Point Kriging- Quadratic Drift

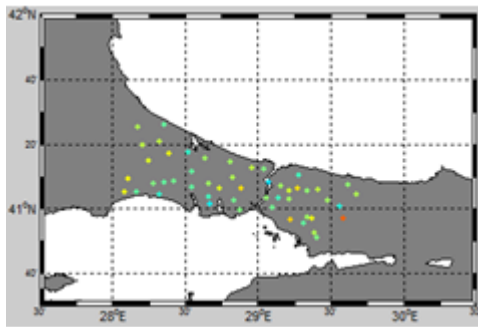
**Figure B.3 (continued):** The distribution of geoid undulation residuals at the test benchmarks depending on Cubic Interpolation Algorithm.



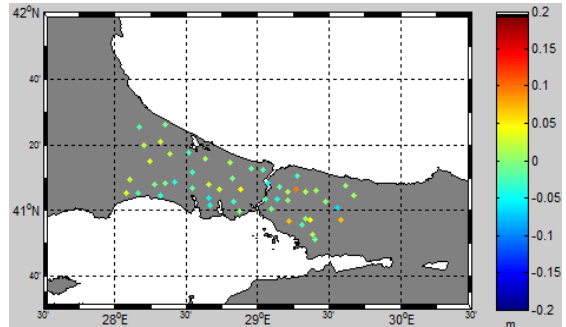
(k.4) Block Kriging- Linear Drift



(k.5) Block Kriging- No Drift

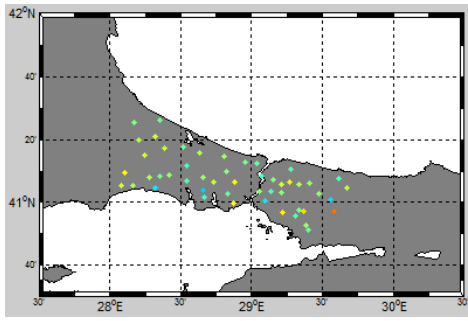


(k.6) Block Kriging- Quadratic Drift

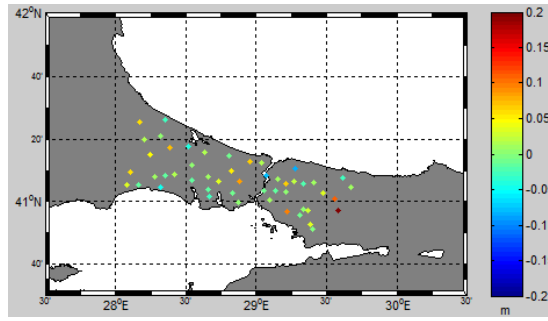


(l) Biharmonic Spline Interpolation

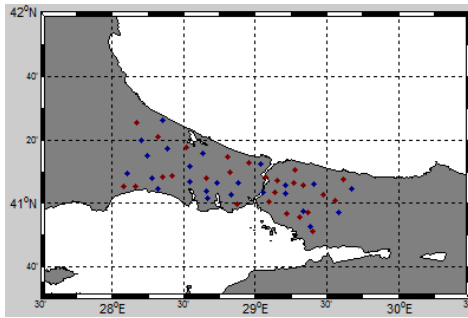
**Figure B.3 (continued):** The distribution of geoid undulation residuals at the test benchmarks depending on Cubic Interpolation Algorithm.



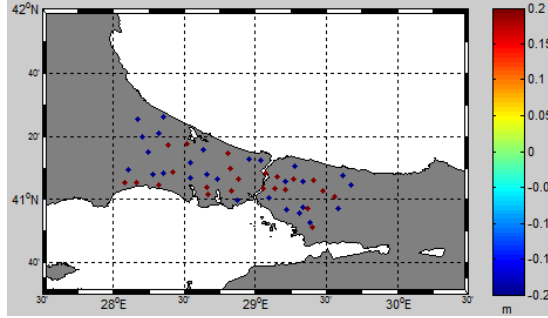
(a) Minimum Curvature



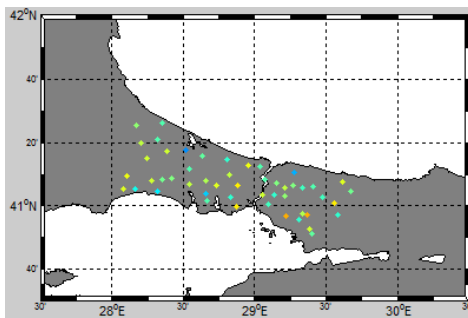
(b) Inverse Distance to a Power



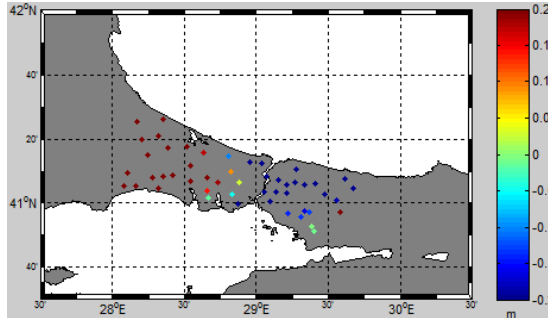
(c) Modified Shepard's Method



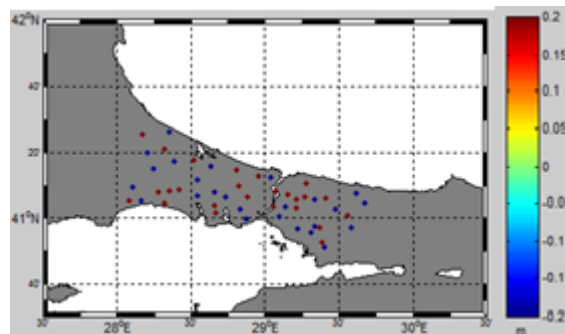
(d) Natural Neighbor



(e) Nearest Neighbor

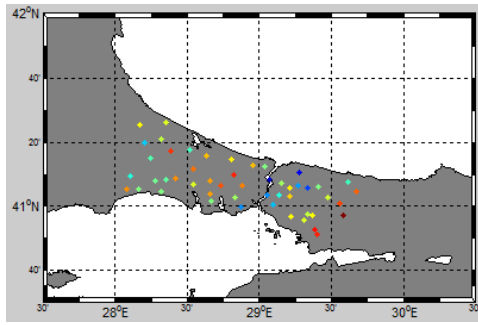


(f) Moving Average

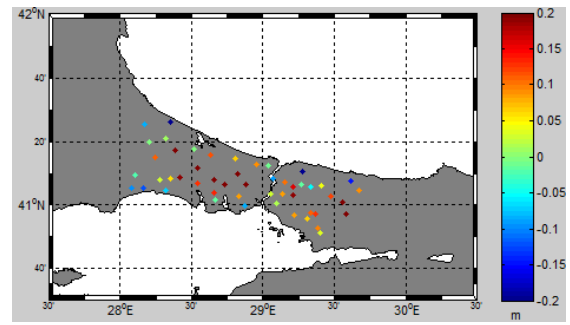


(g) Triangulation with Linear Interpolation

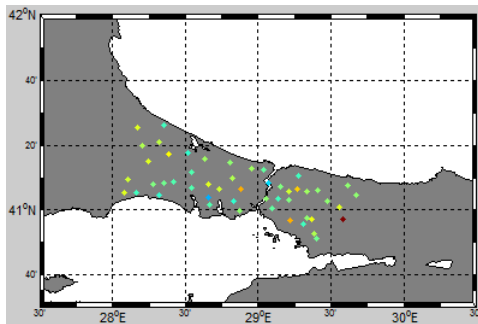
**Figure B.4:** The distribution of geoid undulation residuals at the test benchmarks depending on Spline Interpolation Algorithm.



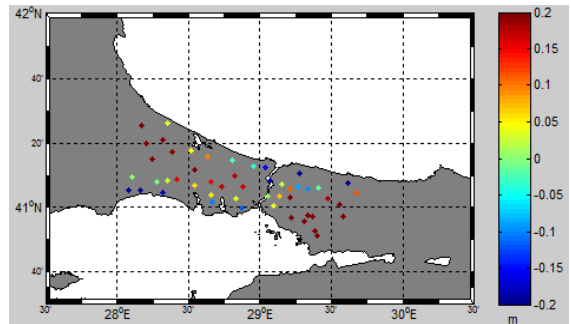
**(h.1)** Polynomial Regression-  
Quadratic Surface



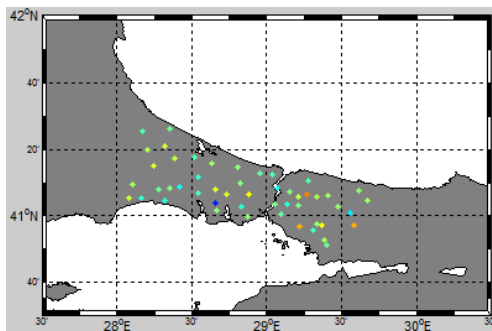
**(h.2)** Polynomial Regression- Bilinear  
Saddle



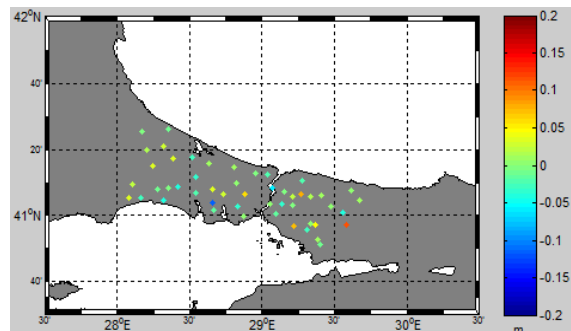
**(h.3)** Radial Basis-  
Inverse Multiquadric



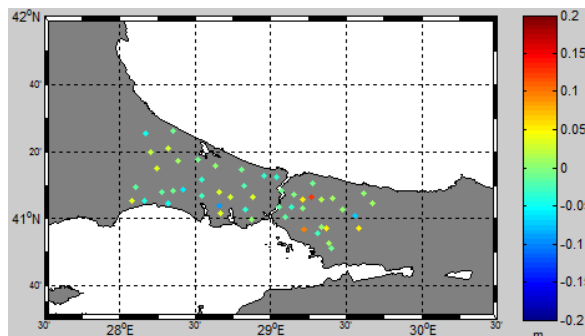
**(i.1)** Polynomial Regression-  
Simple Planar Surface



**(i.2)** Radial Basis- Multiquadric

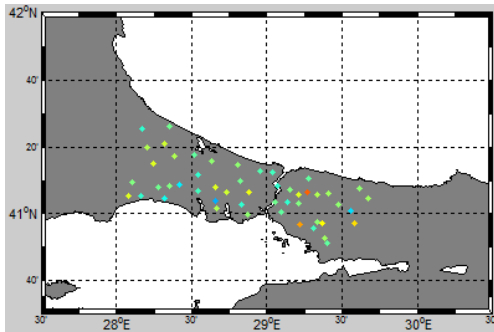


**(i.3)** Radial Basis- Multilog

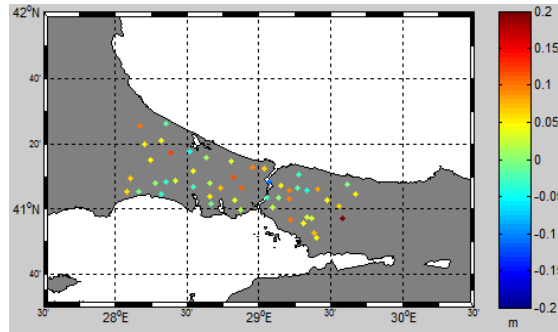


**(i.4)** Radial Basis- Natural Cubic Spline

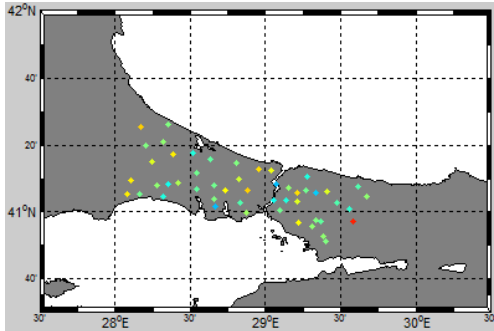
**Figure B.4 (continued):** The distribution of geoid undulation residuals at the test benchmarks depending on Spline Interpolation Algorithm.



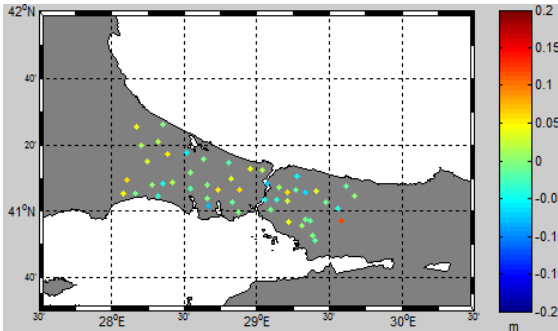
**(i.5)** Radial Basis- Thin Plate Spline



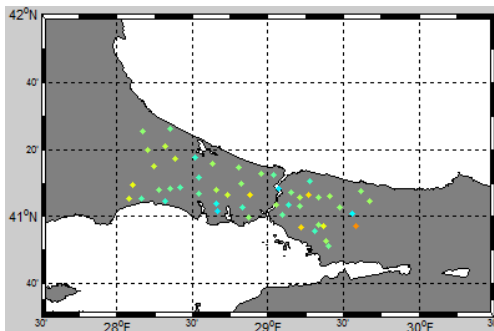
**(j.1)** Local Polynomial- 1.order



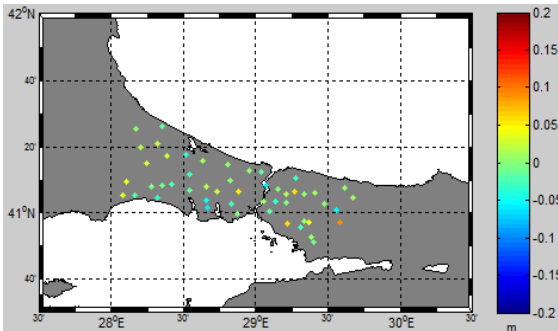
**(j.2)** Local Polynomial- 2.order



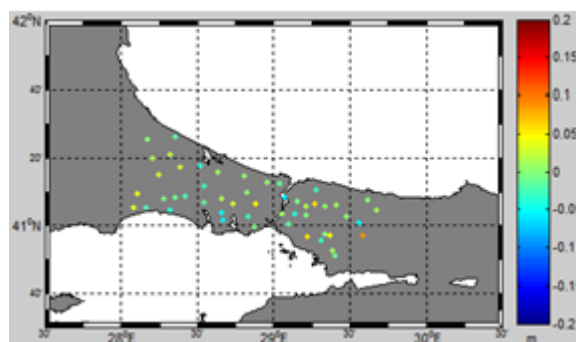
**(j.3)** Local Polynomial- 3.order



**(k.1)** Point Kriging- No Drift

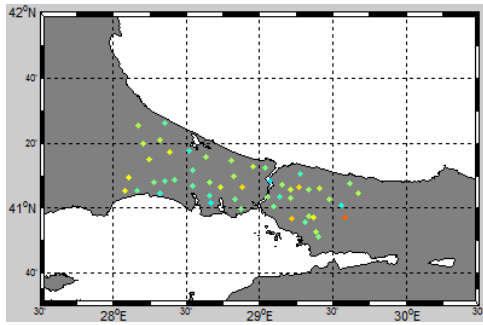


**(k.2)** Point Kriging- Linear Drift

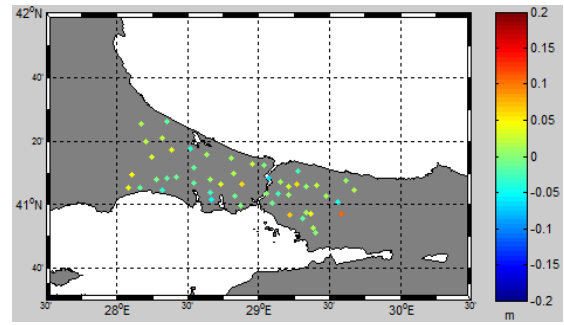


**(k.3)** Point Kriging- Quadratic Drift

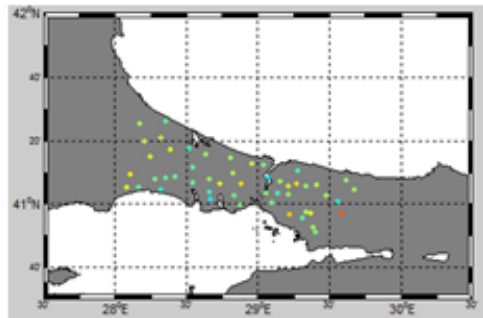
**Figure B.4 (continued):** The distribution of geoid undulation residuals at the test benchmarks depending on Spline Interpolation Algorithm.



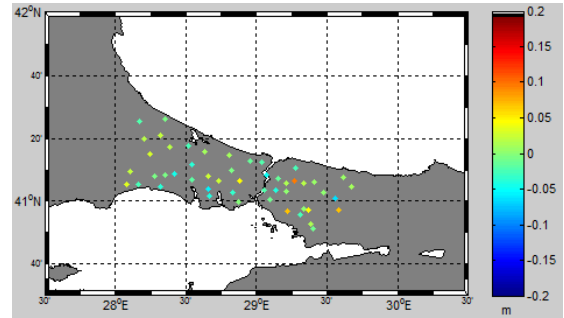
**(k.4)** Block Kriging- Linear Drift



**(k.5)** Block Kriging- No Drift



**(k.6)** Block Kriging- Quadratic Drift



**(l)** Biharmonic Spline Interpolation

**Figure B.4 (continued):** The distribution of geoid undulation residuals at the test benchmarks depending on Spline Interpolation Algorithm.





## CURRICULUM VITAE



**Name Surname** : Onur KARACA

**Place and Date of Birth** : Istanbul / 1990

**E-Mail** : [karacaonu@itu.edu.tr](mailto:karacaonu@itu.edu.tr)  
[onurkaraca\\_1903@hotmail.com](mailto:onurkaraca_1903@hotmail.com)

### EDUCATION

- **B.Sc.** : 2014, Istanbul Technical University, Civil Engineering Faculty, Geomatics Department

### PROFESSIONAL EXPERIENCE AND AWARDS:

- July, 2012 – August, 2012 Internship at Sistem Computer & Technical Services Industry INC. Leica Geosystems AG, Amberg Technologies, which is DTM and Nestle accredited agent in Turkey.
- 18 - 24, May, 2013 The representation of Istanbul Technical University in International Geodetic Students Meeting (IGSM) at Wroclaw University of Environmental and Life Sciences, Poland.
- July, 2013 – August, 2013 Internship at EMI Group Information Technologies, Istanbul, Turkey.
- 25, June - 1, July, 2014 The president of sponsorship committee in IGSM at Istanbul Technical University, Turkey.
- March, 2015 – April, 2015 Work experience at Mescioğlu Engineering, Turkey.
- 1 - 6, June, 2014 The representation of Istanbul Technical University in International Geodetic Students Meeting (IGSM) at Aalto University, Finland.
- October. 2016 – February, 2016 Thesis research study as an Erasmus student with grant at Aristotle University of Thessaloniki at School of Rural and Surveying Engineering Department.

### PUBLICATIONS, PRESENTATIONS AND PATENTS:

- Karaca, O. (2014). Detection of Changes in Land Cover After Mine Construction in Çukuralan Village, Bachelor thesis, Istanbul Technical University, Turkey.